Aus dem Physiologischen Institut, Lehrstuhl: Physiologische Genomik
im Biomedizinischen Zentrum (BMC)
Institut der Ludwig-Maximilians-Universität München
Vorstand: Prof. Dr. Magdalena Götz

Using gRNA Multiplexing for Epigenetic and Transcriptional Engineering

Dissertation
zum Erwerb des Doktorgrades der Naturwissenschaften
an der Medizinischen Fakultät der
Ludwig- Maximilians-Universität zu München

---

vorgelegt von

Christopher T. Breunig
aus
Pegnitz
2019

Mit Genehmigung der Medizinischen Fakultät
der Universität München

Betreuerin: Prof. Dr. rer. nat. Magdalena Götz

Zweitgutachter: Prof. Dr. rer. nat. Peter B. Becker

Dekan: Prof. Dr. med. dent. Reinhard Hickel

Tag der mündlichen Prüfung: 15.06.2020

Table of Contents

Abstract

The introduction of CRISPR/Cas9 simplified genetic, genomic, transcriptional, and epigenomic engineering approaches. CRISPR is a bipartite system, which means that while the molecular effect is defined by the utilized Cas9 variant, its targeting is determined by small RNAs molecules, the guide RNAs. Because of the bipartite nature, CRISPR enables to target multiple sites in single cells at once, which is however dependent on gRNA multiplexing. Here I applied CRISPR in three different projects.

Firstly, I created STAgR (String Assembly gRNA cloning), a single step method, which allows the generation of multiplexed gRNA vectors in a time- and cost- efficient manner.

Secondly, I aimed to combine this technique with novel dCas9-based methyltransferation tools to manipulate chromatin marks identified by epigenome-wide association studies, which occur in Alzheimer's disease patients. I discovered, however, that all tested cell and tissue types, are already hypermethylated on these sites indicating no causal relationship.

Thirdly, I deployed the STAgR method to manipulate multiple transcription factors aiming to induce transcriptional programs of certain subtype specific neurons using dCas9-based transcriptional activator tools. Current approaches of reprogramming remain insufficient, likely, because they are based on the activation of a limited number of cell identity factors. I was able to confirm the induction of various transcription factors following my strategy while the reprogramming *in vivo* analysis of cell identity reprogramming is still ongoing.

Zusammenfassung

CRISPR/Cas9 bietet zum ersten Mal eine einfache Möglichkeit zur genetischen, genomischen, transkriptionellen und epigenomischen Manipulation. Das CRISPR System besteht aus zwei verschiedenen Komponenten. Während der molekulare Effekt durch die verwendete Cas9-Variante definiert ist, wird der Ort des Effekts durch kleine RNA Moleküle, die sogenannten guideRNAs, bestimmt. Im Rahmen dieser Arbeit wurden drei verschiedene Projekte bearbeitet. Zum einen, entwickelte ich STAgR (String Assembly gRNA cloning), eine Methode, welche es ermöglicht, in einem einzigen Schritt multiplexe gRNA Vektoren kosten- und zeiteffizient zu generieren.

Zum anderen sollte diese Methode in Kombination mit neuartigen dCas9-basierten Methyltransferasewerkzeugen benutzt werden um gezielt bestimmte DNA Methylierung zu manipulieren. Diese Modifikationen wurden durch epigenomweite Assoziationsstudien identifiziert, da eine signifikante Veränderung in Alzheimer Patienten berichtet wurde. Jedoch tragen alle getesteten Zell- und Gewebetypen an diesen Stellen bereits hohe Methylierungslevel, weswegen ein kausaler Zusammenhang unwahrscheinlich ist.

In dem letzten Teil dieser Arbeit wurde die STAgR- Methode benutzt um gleichzeitig die Expression von mehreren Transkriptionsfaktoren zu manipulieren Aktuelle experimentelle Reprogrammierungsansätze basieren auf der Überexpression von Zellidentitätsfaktoren. Dies führt zwar zu einer Transdifferenzierung zum gewünschten Zelltyp, jedoch bleibt eine Spezifizierung aus. Da dies wahrscheinlich auf einer begrenzten Anzahl von Identitätsfaktoren basiert, soll mit Hilfe von dCas9- basierten Transkriptionsaktivatoren ganze Transkriptionsprogramme manipuliert werden, welche einen neuronalen Subtyp spezifizieren. Ich konnte die Expression verschiedener Transkriptionsfaktoren induzieren, die Reprogrammierung von sutypspezifischen Neuronen *in vivo* ist jedoch noch nicht abgeschlossen.

A. Introduction

1. Cell states and identity

The concept that all organisms are assembled from similar units of organization is now more than 180 years old. In 1838, Theodor Schwann and Matthias Schleiden postulated their theory of cells being the building blocks and basic units for structure, physiology, and organization in every living being. This theory has foreshadowed some of the greatest paradigms of modern biology, such as Darwin's theory of evolution or Mendel's laws of inheritance. Today, we know that those building blocks are not only structural units providing frameworks for the organs, the cells are rather the minimal physiological unit of the body (Harris 1999). Each of the individual cells in a human body (and there are more than 10^{13} (Bianconi et al. 2013)) can adopt a specialized physiological state which is important and necessary for the individual cellular functions. Until now, these different cell types are mostly classified by their appearance, their functional role in the system or their capability to give rise to other, different cell types. The fact that each body contains various different cellular types creates one of the most interesting scientific conundrums (Vickaryous and Hall 2006). All cells in a human body originate from a single cell, the zygote (Mitalipov and Wolf 2009). This means that all cells (with few exceptions) contain the same genetic material and therefore the information to be in any of the cellular states. How the phenotypic and functional diversity of cells in a body is formed out of the same genome is still being investigated. Nearly 80 years ago, Conrad Hal Waddington contributed a concept which helps to understand how this might be established. In his publication in 1957 he writes that "we certainly need to remember that between genotype and phenotype, and connecting them to each other, there lies a whole complex of developmental processes" (Waddington 1957), suggesting a layer of information beyond genetics. He continues: "It is convenient to have a name for this complex: 'epigenotype' seems suitable", defining the beginning of epigenetic research. He visualized this idea in his so called "epigenetic landscape" (Fig. 1A) (Waddington 2012). The development and differentiation of the zygote is portrayed as a marble rolling down a hill. The marble has different paths to choose from and the further the marble progresses down the hill, the more committed the cell is to a terminally differentiated state. The landscape shaping components are cell fate-determining factors - transcription factors - which initiate specific transcriptional programs. These programs define the path of the marble and therefore predetermine which fate the stem cell, once it is committed, pursues (Fig. 1A). Once a cell

commits to a certain fate it undergoes a lasting and non- reversible epigenetic change; the cell remains in this committed state even if the initial trigger is no longer present.

1.1 Master transcription factors, cell identity and reprogramming

By now it is known that the "landscapers" Waddington was describing are a class of genes, known as transcription factors. These factors are proteins which recognize 5 to 15 bp long DNA motifs often located at gene promoters or cis- regulatory elements such as enhancers (Whyte et al. 2013). Through this interaction and the binding of other co- activators as well as co- repressors, transcription factors regulate the expression of specific genes by recruiting the transcriptional machinery to a gene promoter (Spitz and Furlong 2012). If a single transcription factor orchestrates a whole cellular fate by activating either other transcription factors or regulating a number of fate determining targets, it is considered a master transcription factor. As these factors possess a potency to force an entire specific cellular fate their expression pattern can be highly specific (Vaquerizas et al. 2009). Moreover single factors or a combination are seen to determine and protect cell identities and lineage choices (Morris and Daley 2013). Some of these factors are even potent enough to influence the identity of a terminally differentiated cell (Fig. 1B). The first factor which was shown to possess such reprogramming capacity was the basic helix loop helix transcription factor MYOD. In 1987, it was shown that when overexpressed in terminally differentiated fibroblasts MYOD pushed the cells beyond their natural potency and out of their "dead- end valley" in the epigenetic landscape to reprogram them into contracting myocytes, a muscle identity (Davis, Weintraub, and Lassar 1987). Yet it is not only possible to push a cell from one dead- end valley to another, but to directly reverse the path the marble took down the epigenetic landscape (Fig. 1C). Yamanaka and colleagues reversed differentiation to induce a pluripotent cell by the overexpression of four different transcription factors, OCT4, KLF4, SOX2 and cMYC in embryonic as well as adult fibroblasts (Takahashi and Yamanaka 2006). These experiments lead to a large series of transcription factor mediated reprogramming. Through overexpression of master transcription factors, it is possible to generate a large number of different cellular identities out of various somatic cells. Like this, e.g. cardiomyocytes (Ieda et al. 2010), beta cells (Q. Zhou et al. 2008) or even neurons (Berninger et al. 2007; Masserdotti, Gascon, and Götz 2016; Vierbuchen et al. 2010) were generated, using different starting cells. Even if this kind of reprogramming is based on overexpression of artificial transgenes, these transcription factors induce a new permanent epigenetic and transcriptional state which is maintained even after removal or silencing of said transgenes (Woltjen et al. 2009). Amongst master transcription factors there are certain subclasses in

reprogramming potency. There are factors which enable a reversion of differentiation, factors which can induce alternative options for differentiation and factors which enable a “dead- end valley” to “dead- end valley” transition in a process called direct reprogramming (Fig. 1C).

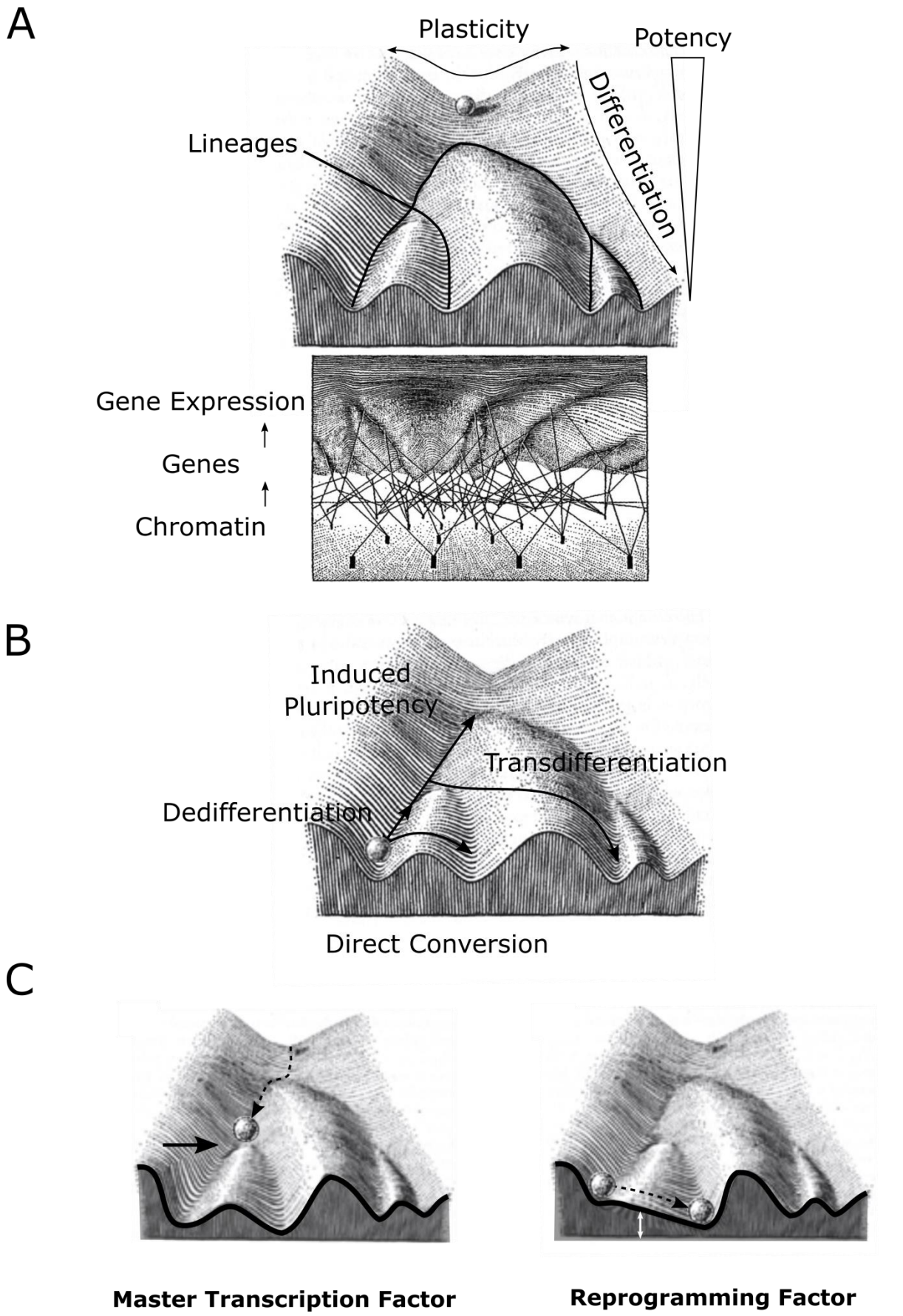

Fig. 1 | The Waddington Epigenetic Landscape. A Overview over the Waddington Landscape. Waddington described important terms like plasticity, potency, lineages in form of narrowing valleys. The different slopes are

created by underlying factors: chromatin regulates genes, genes regulate gene expression and this gene expression defines the valleys. **B** Visualization of induced pluripotency, dedifferentiation, transdifferentiation, and direct conversion of cells. **C** Visual description of the theory what a master transcription factor or a reprogramming factor does to the Waddington Landscape. Modified after License date: Nov. 14, 2019; License number: 4707660543298.

1.2 Cortex development and neuronal subtype specification

The mammalian neocortex is a complex structure, which can be subdivided into six different layers. These cortical layers are composed of three distinct mature cell types: neurons, astroglia and oligodendroglia (Peters and Jones 1984). Each of those layers harbor different subtypes of these main cellular classes. Neurons can be further subdivided into two main classes. These are inhibitory GABAergic interneurons which connect locally to surrounding targets and excitatory glutamatergic projection neurons whose axonal extensions extend intracortically, subcortically or even sub-cerebrally (Molyneaux et al. 2007). Neurons can be also classified based on the laminar position of their cellular bodies, morphology of soma or dendrites, and their axonal connectivity (Jabaudon 2017; Lodato, Shetty, and Arlotta 2015). This immense heterogeneity already begins to emerge early during development. After the expansion of the dorsolateral wall of the rostral neural tube, the ventricular zone forms above the ventricle and later the subventricular zone. Progenitor cells, which emerge from these structures, then give rise to the numerous subtypes of projection neurons of the different neocortical layers. This happens during embryonic days E11.5 until E17.5 in a spatially and temporally tightly controlled process (Caviness and Takahashi 1995). The six-layered neocortex is generated in an “inside- out fashion” as later born neurons of the superficial layers have to migrate past earlier- born deep- layer neurons (Fame, MacDonald, and Macklis 2011). These superficial layers mostly consist of neurons derived from basal progenitors from the subventricular zone (Tarabykin et al. 2001). Overall, the mammalian neocortex shows a substantial neuronal diversity, also within, but especially between the different layers. One of these cellular subtypes is the one of callosal projection neurons (CPN), a class of neurons, which can be further subdivided into deep layer CPN or CPN of the superficial layer. While deep layer CPN show long- distance dual projection axons, their counterpart of the superficial layers participates in the local circuitry within cortical columns (Fame, MacDonald, and Macklis 2011). There is a number of factors which define the development of upper layer neurons and more specifically CPN. So for example, SATB2 (Special AT- rich sequence-binding protein 2), was shown to be critical as a molecular regulator during CPN specification (Alcamo et al. 2008; Britanova et al. 2008). This DNA binding transcription factor acts as an

anchor for chromatin remodelers and modifiers like HDAC1 (Baranek et al. 2012; Britanova et al. 2008). Like this, it supports repression of CTIP2 and actively suppresses the subcortical projection neuron fate by indirectly controlling axonal outgrowth and fasciculation (Arlotta et al. 2005; Baranek et al. 2012; Britanova et al. 2008). CUX2 (Cut- like homebox 2) is a member of the Cut family of transcription factors and was shown to take part in regulation of dendrite branching, spine development and synapse formation in layer II to III neurons in the cerebral cortex (Cubelos et al. 2010). MEF2C, short for Myocyte enhancer factor- 2C, is a transcription factor which was found to positively regulate transcriptional activities of bHLH factors during neurogenic differentiation (B. L. Black et al. 1996; Mao and Nadal-Ginard 1996). Through temporal and spatial expression patterns during neuronal differentiation it was postulated that this transcription factor could be important for development of cortical architecture and neuronal maturation (Heidenreich and Linseman 2004; Leifer et al. 1993) and was also found to be essential for axonal outgrowth of subcerebral projection neurons (MacDonough 2016). CUX1 was shown to be complementary to CUX2 and as well an intrinsic regulator of dendrite branching, spine development, and synapse formation in layer II to III (Cubelos et al. 2010; Nieto et al. 2004). TLE2 (Transducin- like enhancer protein 2) is an interaction partner of FoxG1 and was shown to specify telencephalon development (Roth et al. 2010). LHX2 (LIM homebox 2) was shown to have crucial roles in progenitor specification, which then give rise to neocortical projection neurons (Molyneaux et al. 2007). It is also postulated that LHX2 may provide a balance of proliferation and differentiation in cortical progenitors (Chou and O'Leary 2013). BHLHB5 has been demonstrated to draw sharp areal boundaries in the developing cortex and to orchestrate projection neurons to gain specific phenotypic traits (Joshi et al. 2008). BRN2, a POU- domain transcriptional regulator, was found to be expressed in superficial cortical layers and essential for subtype specific differentiation into pyramidal neurons as well as proper cortical lamination and neuronal migration (McEvilly et al. 2002; Sugitani et al. 2002). NURR1 is a transcription factor which is linked to control of dopaminergic identity and was recently shown to be able to induce reprogrammed neurons with laminar specific hallmarks (Kadkhodaei et al. 2009, 1, 2013; Mattugini et al. 2019). Heterogeneity and subtype specificity present special challenges for neural replacement therapies. If neurons are lost by traumatic brain injury or neurodegenerative diseases, it is likely not sufficient to replace them with any neuronal cell (Heinrich, Spagnoli, and Berninger 2015; Kriks et al. 2011). Lost subtypes have to be replaced by subtypes, to be able to form lost neuronal circuits. Recent insights into the control of cell identity indicated that any cell might be compelled to become a neuron once specific

transcriptional programs have been triggered (Lu, Bradley, and Zhang 2014). The genetic introduction of exogenous copies of reprogramming factors engineered for constitutive expression through the addition of viral elements has proven to be a powerful approach to generate new neurons, both *in vitro* and *in vivo* (Gascón et al. 2015; Gohlke et al. 2008; Guo et al. 2014; Giacomo Masserdotti et al. 2015). Such a change in cell identity can be enforced through the expression of master cell-fate-determining regulators like Neurogenin, ASCL1, MYT1L, BRN1/2, NEUROD1/4 or PAX6 (Berninger et al. 2007; Heinrich et al. 2010; Vierbuchen et al. 2010; Heins et al. 2002). Nonetheless, established master reprogramming factors (like ASCL1, NGN2 and NEUROD1 and 4, MYT1L and BRN2) are potentially, even in combinations, insufficient to drive subtype- specific neuronal fates and ensure full cellular maturation. The set of master transcription factors (specifically NEUROD1 and NEUROD4) should therefore be extended and supplemented by factors which were thought to take influence on transcriptional programs which could define specific cellular subtypes. Nowadays tremendous amounts of sequencing data provide a basis for an idea which factors could play a role in subtype specific differentiation. Also, knockout studies conducted earlier give ideas about what factors play important roles for neuronal differentiation and subtype specification. As I aimed for trans-differentiation to callosal projection neurons, the following factors, which were chosen as candidates were SATB2, CUX2, MEF2C, CUX1, LHX2, BHLHB5, BRN2, NURR1, and TLE2.

2. Epigenetic gene regulation

In eukaryotes, chromatin exists of DNA which is wrapped around small proteins, the so called histones. There are a number of chromatin modifying enzymes, which add or remove small chemical residues from histone tails or directly from DNA bases (Tessarz and Kouzarides 2014). Some of these modifications have been shown to influence chromatin accessibility and therefore control transcription to a certain extent. However the correlation of changes in chromatin marks and the resulting change in gene expression patterns does not necessarily imply a causation (Bultmann and Stricker 2018). Even if various studies have shown that these modifications and resulting chromatin features can have influence on a transcriptomic level, it is still difficult to link these changes to a phenotypic outcome. Despite the fact that chromatin can be modified in at least 100 different ways, only of a few of these modifications are studied in respect to gene activation and silencing which will be introduced briefly in the following.

2.1 Chromatin Modifications

2.1.1 DNA Methylation

The simplest yet the most prominent chromatin modification is the methylation of the nucleobase cytosine to 5- methylcytosine (5mC) (Lister et al. 2009). The modification itself was already discovered in 1948 (Hotchkiss 1948), whereas the proposal that it is stably inherited, influences gene expression and therefore affects cellular differentiation took another 25 years (Holliday and Pugh 1975; Riggs 1975). In mammals nearly all of the present DNA methylation occurs in CpG dinucleotides, but still can exist in any context of the genome (Lister et al. 2009). The machinery which is in control of this modification is by now also known in detail. A combination of the DNA methyltransferases DNMT3A and DNMT3B is responsible for *de novo* methylation of unmodified cytosine residues to 5mC (Okano et al. 1999) whereas DNMT1 ensures that DNA methylation which was present before replication is inherited to both strands afterwards (E. Li, Bestor, and Jaenisch 1992). Methylation patterns of promoter regions are often associated with the alteration of chromatin density and therefore the accessibility for transcription factor binding, impairing expression of subsequent genes (Cedar and Bergman 2009). Early studies dating back to the beginning of the nineties showed that hypermethylation of CpG islands in X-chromosome inactivation (XCI) results in active silencing of a whole chromosome, to guarantee dosage compensation of X-encoded genes in female cells (Duncan et al. 2018; Lock et al. 1986; Singer-Sam et al. 1990). In contrast to these mechanistic properties of DNA methylation, it was shown that CpG islands in the promoter region of endoderm development master regulator FOXA2 are highly methylated in expressing tissues, suggesting the exact opposite (Bahar Halpern, Vana, and Walker 2014). This shows that in reality the property of epigenetic regulation of DNA methylation might be far more complex than previously thought.

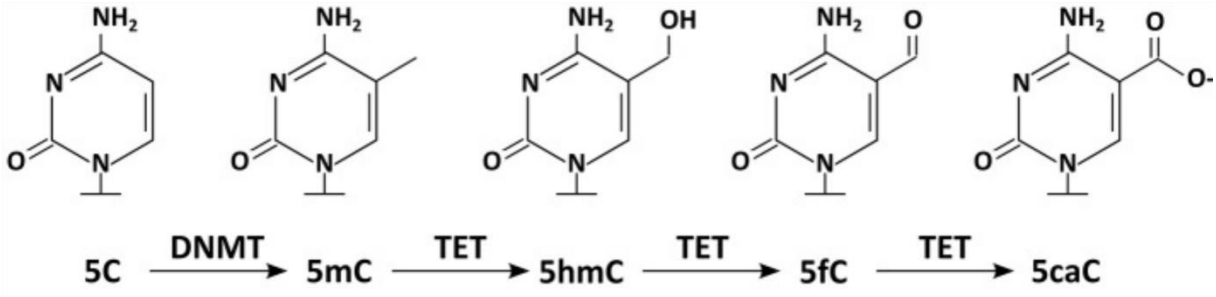

Fig. 2 | Overview of chemical species of DNA methylation. DNMT enzymes *de novo* methylate the 5C residue of cytosine which can then subsequently be de- methylated by TET enzymes. Species which are generated in the process are 5hmC, 5fC and 5caC. Modified after S. H. Stricker and Götz 2018.

While the term “DNA methylation” often mainly refers to 5mC, we today know that there are some more DNA modifications based on methylation and even de- methylation. In addition to cytosine, adenine can be a target for methylation as well to form N6- methyladenine (6mA) (T. P. Wu et al. 2016). The same cytosine residue as in 5mC can be similarly methylated at another position, to form N3- methylcytosine (3mC) (Sadakierska-Chudy, Kostrzewa, and Filip 2015). As de- methylation of 5mC occurs via three subsequent enzymatic reactions it brings forth three additional derivates (Fig. 2) (Booth, Raiber, and Balasubramanian 2015). The de- methylation machinery, to which the family of the ten- eleven translocation enzymes (TET1, TET2 and TET3) belongs, catalyzes the oxidation of 5mC to C5-hydroxymethylcytosine (5hmC). To fully demethylate the cytosine residue, there are two more steps necessary; C5-formylcytosine (5fC) and C5-carboxylcytosine (5caC) before thymine DNA glycosylase (TDG) actively removes the mark (He et al. 2011; Ito et al. 2011; Yu et al. 2015; G. Zhang et al. 2015). There is some evidence that these derivates are not only steps in between the removal of an epigenetic mark but rather can have regulatory functions too. So for example the transcription factor UHRF1 recognizes 5hmC and actively needs this modification to bind its motif (Arita et al. 2008; Fang et al. 2016; Frauer et al. 2011). This suggests a functional role for 5hmC as UHRF1 was shown to bear key roles in maintaining DNA methylation during an early onset of development and hence regulating later stages of neuronal differentiation (Ramesh et al. 2016). Even if the last two derivates of TET- mediated de- methylation occur very rarely in the genome, efforts have been made to investigate epigenetic readers of 5fC and 5aC (Ito et al. 2011). 5fC and 5caC, mainly appearing in early embryos, embryonic stem cells and neuronal tissues, was shown to enable binding of factors involved in transcription and chromatin regulation, more specifically forkhead box domain transcription factors and parts of the NuRD complex (Iurlaro et al. 2013; Spruijt et al. 2013).

2.1.2 Histone marks

The function and regulatory properties of chromatin is not only limited to direct DNA modifications, but is thought to hold an additional layer of information through the histone code. Here the main protein component of chromatin, the so called histones provide a far bigger basis for different chemical modifications, set or removed by numerous chromatin modifying enzymes (Tessarz and Kouzarides 2014). All histones, except the linker histone H1, are assembled into octamers containing two copies of the core units H2A, H2B, H3 and H4 which are entangled by exactly 147 bp of DNA, forming the so called nucleosomes (Richmond and Davey 2003). To date, 12 different modifications have been found at 130 different amino acid residues, mostly part of the N- terminal tail of histones (Tan et al. 2011; Tessarz and Kouzarides 2014) These chemical modifications, like acetylation, phosphorylation or methylation, are thought to influence virtually all processes involving chromatin, e.g. transcription, replication and DNA repair. This is thought to be done by directly influencing the accessibility of binding sites for regulatory factors on DNA through changes of the physical properties of chromatin or by forming a whole new layer of signal transduction (Strahl and Allis 2000). Even if there is still a need for elucidating specific roles and functions of distinct chromatin modifications, certain residues were shown to correlate with certain transcriptional states. Trimethylation of lysine 4 on histone H3 (H3K4me3) and acetylation of lysine residues K9 and K27 of the very same subunit tend to occur at the promoter region of genes which are actively transcribed (Fig. 3) (Bernstein et al. 2005; Heintzman et al. 2007; Kim et al. 2005; Santos-Rosa et al. 2002). Marks which are characteristic for active gene transcription can not only be found in promoter regions, but are also elevated in gene bodies as well as cis- regulatory elements, such as enhancers. So are active gene bodies marked with trimethylation of two different lysine residues, namely H3K79 and H3K36 and enhancers with high levels of H3K4 monomethylation and H3K27 acetylation (Barski et al. 2007; Heintzman et al. 2007, 2009). In contrast to these active marks, trimethylation of H3K27 and H3K9 was shown to be enriched in repressive chromatin states during development (Fig. 3) (Boyer et al. 2006).

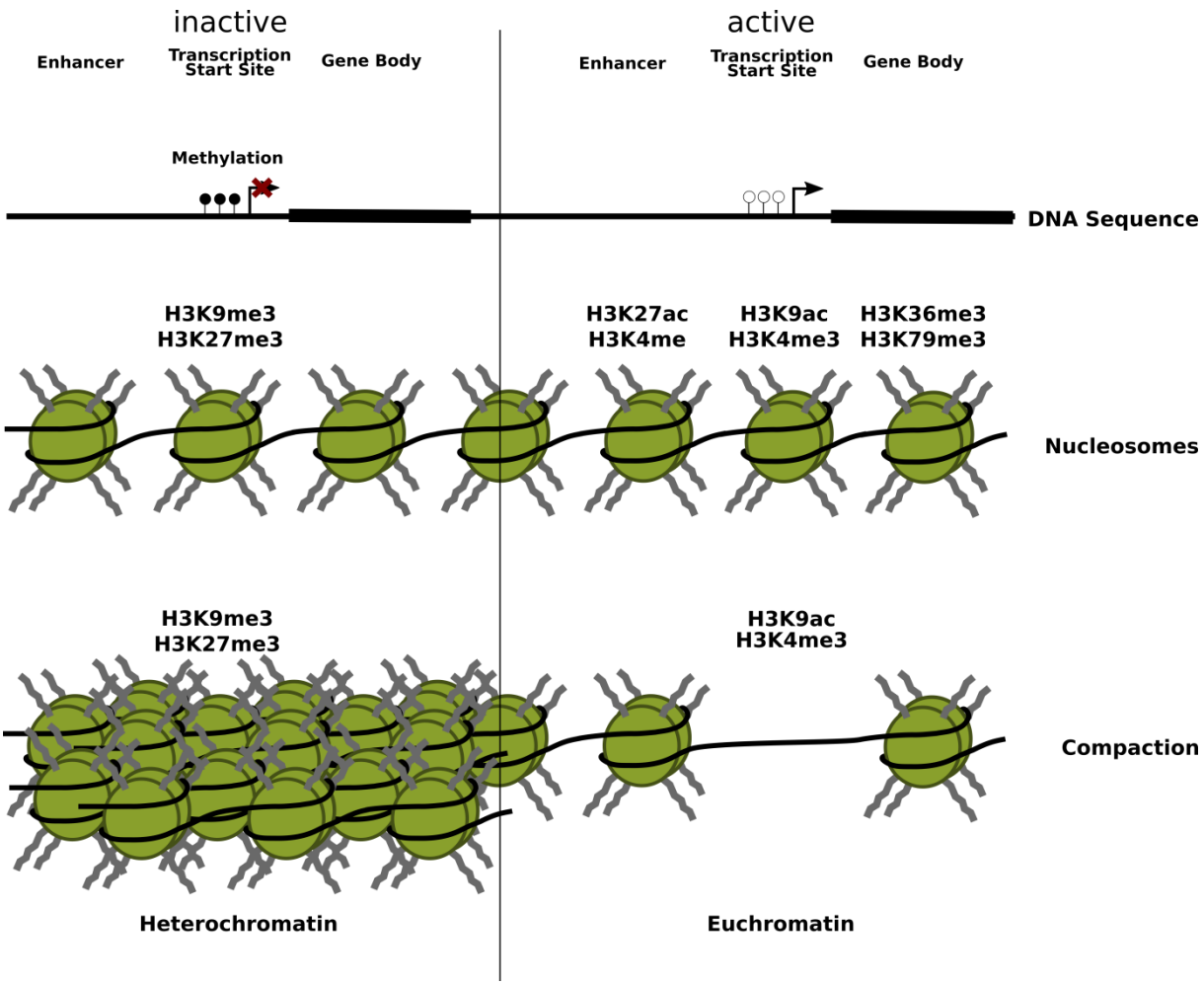

Fig. 3 | How chromatin marks may influence gene activity. Specific chromatin marks can potentially have influence on gene activity. Typical marks for an inactive state are DNA methylation, H2K9me3 and H3K27me3 at transcription start sites of genes. Chromatin compaction can also be an indicator for inactive gene regions. Markers for active genes can be H2K27ac or H3K4me at cis- regulatory elements such as enhancers or H3K9ac and H3K4me3 at transcription start sites. H3K26me3 and H3K79me3 can be found at gene bodies of active genes.

Nonetheless, even if the presence or absence of chromatin marks (DNA Methylation and histone modifications) can be associated with transcriptional activity, there is still a need to establish whether changes in chromatin marks only correlate with transcriptional changes or if there is a causal connection.

3. CRISPR/Cas9 – controllable transcription factor and chromatin modifier

Advances in "omics"-methods have characterized the epigenome and its potential influence on transcriptional programs based on correlations. Yet, it remained difficult to prove a causal connection between epigenetic features and transcriptional control. Early studies which aimed for proof of this connection did so by altering chromatin marks on a global basis. This was done by mutation of either chromatin modifying enzymes, robbing the cell of its modifying machinery (Boonsanay et al. 2016) or the histone residue itself, by making a modification impossible on a global scale (Funato et al. 2014). However, this cannot provide insight into distinct functions of individual chromatin marks at specific sites.

With the discovery of ZFNs (Zinc Finger Nucleases) and TALENs (Transcription Activator-like Effectors) it for the first time became possible to bind and modify specific parts of the genome as well as the epigenome with a high degree of specificity (Miller et al. 2011; Moscou and Bogdanove 2009; Urnov et al. 2005; F. Zhang et al. 2011). However, changing target sites required a complete re- design of these artificial transcription factors which is why they never were fully embraced by the scientific community (Adli 2018). With the dawn of the CRISPR/ Cas9 technology, this changed dramatically. CRISPR stands for clustered regularly interspaced short palindromic repeat and was first discovered in *Escherichia coli* in 1987 (Ishino et al. 1987). It was found to be part of a complex defense mechanism of the bacterial immune system (Makarova et al. 2006) and once the mechanistic functions of the separate parts were unraveled, CRISPR/Cas9 was engineered to become one of the most significant biotechnological tools for genome editing of the early 21st century (Gasiunas et al. 2012; Jinek et al. 2012). This bipartite system is based on an endonuclease (Cas9) which can be targeted to any specific part of the genome, by programming it with a short RNA, the so called guideRNA (gRNA). The gRNAs are composed of a 20 bp protospacer motif, which defines the targeting site by sequence complementarity, and a scaffold sequence, which forms a complex with the Cas9 protein. If the 20 bp targeting site is followed by a so- called protospacer adjacent motif (PAM- an NGG motif in case of *S. pyogenes* Cas9), stable Cas9 binding can be established and double strand breaks introduced, enabling various options for genome editing (Fig. 4A/B) (Anders et al. 2014; Sternberg et al. 2014).

The removal of the nuclease activity of the nuclease Cas9 by point mutations in the coding sequence resulted in a versatile and most flexible tool for epigenomic research, namely the catalytically inactive dead Cas9 (dCas9) (Qi et al. 2013). It is possible to target nearly every

part of the genome and use dCas9 as a shuttle for specific chromatin modifying enzymes or artificial transcription factors opening up numerous possibilities to manipulate the epigenome.

3.1 Transcriptional Engineering – targeted manipulation of gene expression

One very prominent way to exploit dCas9 is its use in manipulating expression of endogenous genes. As the rather big protein of dCas9 establishes a reliable interaction with DNA it can be used to spatially hinder the transcriptional machinery (such as transcription factors and RNA Polymerase II) to assemble at the transcription start site and therefore interfere with endogenous expression of a target gene (Qi et al. 2013). To exploit the shuttle function of dCas9 to its fullest one can fuse different effector domains to the N-terminus of the catalytically dead endonuclease. Like this, one can repress expression of target genes by targeting the transcription start sites with strong repressor complexes such as the Kruppel-associated Box (KRAB) (Gilbert et al. 2013).

However, dCas9 fusion constructs can not only be used to block transcription, but be exploited to do rather the opposite, as targeting the transcriptional start site of genes with strong transcriptional activators can result in robust gene induction. The first generation of these fusion constructs was based on viral or non- viral transcription factor domains, like the 16- amino- acid- long transactivator domain (VP16) derived from the Herpes simplex virus. Targeting this domain to the transcriptional start site of a gene can result in a solid gene induction. This is accomplished by utilizing the domains original function, namely the interaction with a variety of transcription factors and recruitment of key components of the transcriptional machinery, including RNA Pol II (Y. Liu et al. 1999). A multitude of different alterations of these artificial transcription factors have emerged over the years. As the number of VP16 repeats has been shown to correlate with transcriptional activator capacity (Sadowski et al. 1988; Seipel, Georgiev, and Schaffner 1992), potent multimers of the transactivator domain have been generated. This includes the most prominent version with four tandem repeats, VP64, and also the eight- (VP128) and twelve- copy (VP192) version (Balboa et al. 2015; Cheng et al. 2013; Maeder et al. 2013; Mali et al. 2013). An additional variation is the so called butterfly dCas9, which was designed to carry two copies of VP64 on both protein ends, further increasing its activator capability (J. B. Black et al. 2016; Chakraborty et al. 2014; Gao et al. 2014).

The field of transcriptional engineering is still evolving. Combinations of VP64 and other transactivator domains have been proven to be most potent. VPR, which is a tripartite transactivator complex, artificially pushes the levels of endogenous gene expression to nearly

physiological levels. It is composed of VP64 fused to two additional factors, namely P65 and Rta (Chavez et al. 2015). Like VP64, Rta is transactivator domain derived from a virus (Epstein- Bar virus), whereas P65 is a domain from the mammalian NF- κB transcription factor (Hardwick et al. 1992; Seipel, Georgiev, and Schaffner 1992). Direct fusion constructs are only one way to recruit transactivator domains to target sites: dCas9 has been equipped with protein tags, which then help to recruit multiple effector domains which are fused to the tag's counterpart. In that way, effector domains can be accumulated at e.g. transcriptional start sites to establish solid endogenous gene induction (Tanenbaum et al. 2014; H. Zhou et al. 2018). Additionally, the RNA scaffold of gRNAs has been engineered to harbor two recognition sites for the MCP protein, forming a stable protein RNA interaction. Once equipped with transactivator domains like P65 or HSF1, this can be used to accumulate effector domains at a Cas9 marked target site and results in highly efficient gene induction (Konermann et al. 2014a; Zalatan et al. 2015).

Utilizing this technique for targeting endogenous versions of e.g. transcription factors, harbors massive potential, even in cellular reprogramming. It was shown that targeted activation by dCas9'VPR of the two pro- neural factors NGN2 and NEUROD1 in iPSCs can trigger neural differentiation (Chavez et al. 2015). BRN2, ASCL1 and MYT1L, the so called BAM factors, were shown to yield a high capacity to direct reprogram mouse embryonic fibroblasts into neurons when overexpressed as transgenes (Vierbuchen et al. 2010). The same holds true for endogenous gene activation, as butterfly dCas9'VP64 shows direct conversion capability from MEFs to neurons when targeted to the BAM loci simultaneously (J. B. Black et al. 2016). Cells could not only be trans- differentiated, it was also shown that a solid de-differentiation can be achieved by targeting the endogenous loci of OCT4 and SOX2 with a dCas9SunTag enhanced system, to induce pluripotency (P. Liu et al. 2018). Neural progenitors already committed to a glial fate could also be dedifferentiated by targeted SOX1 activation, and got back a lost differentiation potential to a neuronal fate (Baumann et al. 2019).

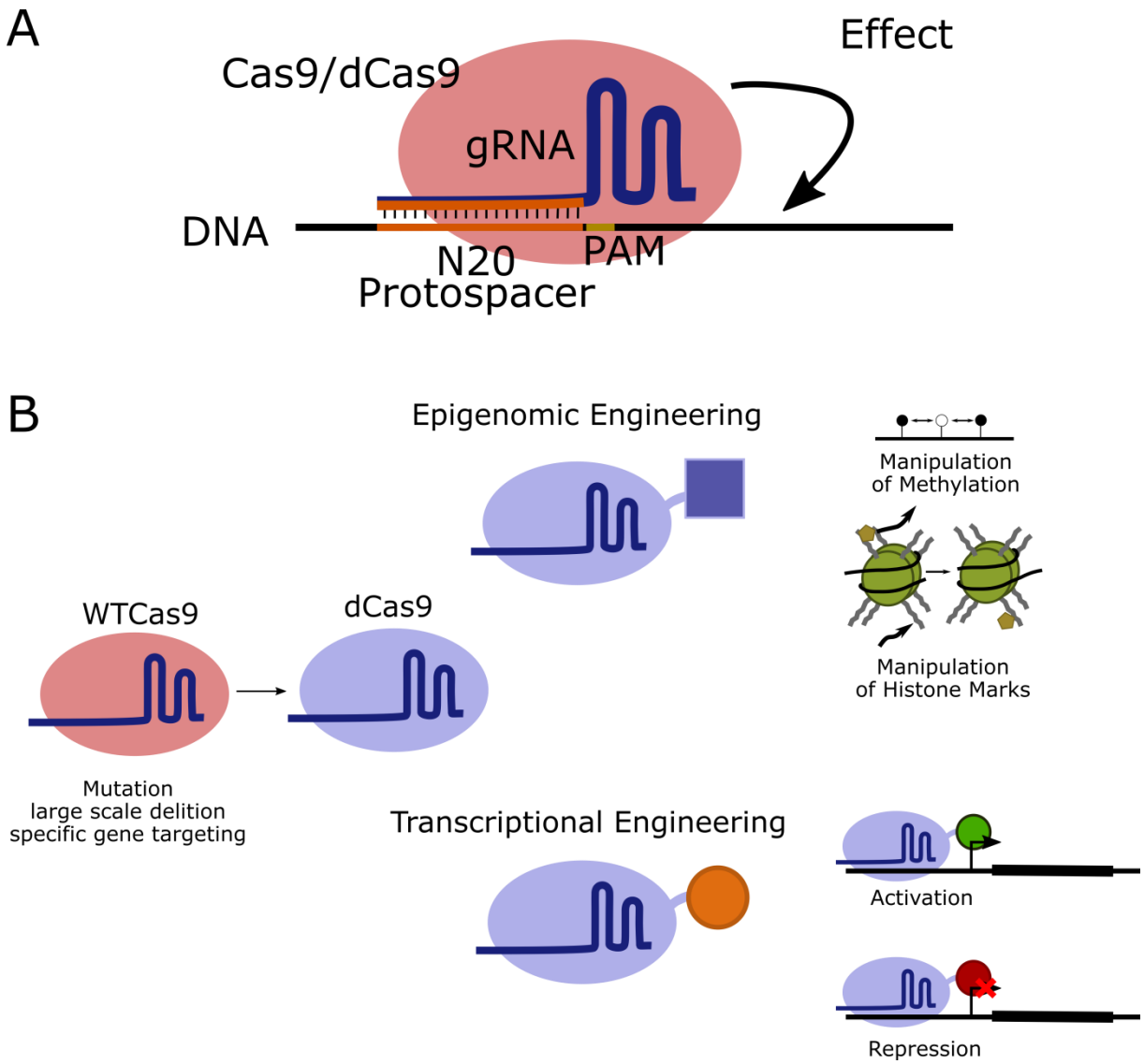

Fig. 4 | Possible utilizations of CRISPR. A The gRNA forms a complex with the Cas9 protein. This RNA protein complex then scans the genomic DNA for the complementary sequence of the N20 protospacer, followed by the for binding necessary Protospacer Adjacent Motif (PAM). **B** CRISPR based tools provide a tremendous amount of possibilities. WTCas9 can be used to induce base- specific mutations, large scale deletions or for specific gene targeting. Mutations of the enzymatic domain of Cas9 have generated a dead version of the protein. The options this tool can be used in, have been subdivided into two groups: Epigenomic engineering and transcriptional engineering. In Epigenomic engineering dCas9 is used to shuttle chromatin modifier to specific places in the genome to set or remove for example DNA methylation or specific chromatin marks. Transcriptional Engineering summarizes the manipulation of transcription of endogenous genes by targeting their promoter region with activators or repressors.

3.2 Epigenomic Engineering – targeted manipulation of chromatin marks

Trying to unravel the function of chromatin modifications does not necessarily answer the question of causality. The introduction of dCas9 opened up a tremendous amount of opportunities to directly target exactly this kind of questions. Tools generated for epigenomic engineering are based on dCas9 shuttles which enable a site- specific manipulation of chromatin marks by targeting loci with chromatin modifying enzymes or their catalytical domains. This has been done for a variety of complex chromatin modification but also for the simplest one, DNA methylation, providing first evidence of a potential direct effect of DNA methylation on transcriptional regulation. Various fusion constructs of dCas9 to DNMT enzymes, like the mammalian *de novo* methyltransferase DNMT3A (or its catalytical domain) or the prokaryotic CG methyltransferase M.SSSI/MQ1 have been reported to induce *de novo* methylation of unmethylated CpGs (Amabile et al. 2016; Lei et al. 2017a; Vojta et al. 2016a; Ziller et al. 2018). Higher methylation rates could be achieved by combining DNMT3A with its co- factor DNMT3L (Stepper et al. 2017a). *De novo* methylation capacity appears to be highly dependent on the target locus, as methylation efficiency varies from 2 to up 80% depending on the target gene (Huang et al. 2017; Jurkowski, Ravichandran, and Stepper 2015; Pflueger et al. 2018). These epigenomic engineering tools provide the possibility to draw a link between specific epigenomic- and transcriptional changes. This however requires a target- specificity as potential off- target effects of these systems won't allow unraveling the functional consequences of specific DNA methylation. As shown by Pflueger et al. many of the utilized dCas9 fusion methylation tools show high off- target DNA methylation, which could be improved by accumulating DNMT3A via a dCas9 Sun-tag system (Pflueger et al. 2018). Nonetheless, even a catalytically dead version of DNMT3A leads to some DNA methylation, suggesting that the endogenous DNMT machinery is recruited resulting in unwanted CpG modification. This clearly shows the importance to further develop more advanced methylation tools.

Nonetheless, engineered methylation resulted in subsequent transcriptional reduction of target genes, providing first evidence that chromatin modifications can potentially modulate transcription (Amabile et al. 2016; Huang et al. 2017; X. S. Liu et al. 2016a). Targeted methylation could counteract elevated levels of synuclein alpha protein (SNCA) in human iPSCs derived from dopaminergic neurons from Parkinson's disease patients (Kantor et al. 2018). In another example DNA methylation of multiple target sites in primary breast cells could prevent senescence and drive hyper- proliferation, a phenotype typically seen in breast

cancer development, suggesting DNA hypermethylation not only as a hallmark of cancer, but as a driving force (Saunderson et al. 2017).

Of course similar systems have been developed with de- methylation machinery (Anton and Bultmann 2017; Morita et al. 2016; Okada et al. 2017; Xu et al. 2016). Quite similar to the methylation studies, the effects are rather variable. The molecular consequences vary from 10% to full de- methylation (Baumann et al. 2019; Choudhury et al. 2016; Okada et al. 2017). The transcriptional consequences of de- methylation range from rather mild induction (Choudhury et al. 2016; Morita et al. 2016) to strong gene activation (X. S. Liu et al. 2016a; X. Shawn Liu et al. 2018). Different *in vitro* and *in vivo* studies could also link de-methylation of disease relevant genes to phenotypic changes. The de- methylation of tumor suppressor genes is for example sufficient to trigger proliferation phenotypes (Choudhury et al. 2016) or de- methylating of the FMR1 locus in affected neurons is able to rescue disease hallmarks of the fragile X syndrome (X. Shawn Liu et al. 2018).

These systems can even be applied for manipulation of the histone code. When deployed to promoter regions and distal enhancers, a dCas9 fusion construct with the histone acetyltransferase p300 for instance could activate transcription in MYOD and OCT4, to levels which were even higher than those achieved by transcriptional engineering (Hilton et al. 2015). Trimethylation of H3K4 could restore the expression levels of silenced genes in various cancerous cell types by targeting the promoter regions with histone methyltransferase PRDM9 (Cano-Rodriguez et al. 2016). In contrast to this dCas9’LSD1 helped to characterize and verify various enhancer regions, as de- methylation of target histones resulted in gene silencing (Kearns et al. 2015; Mendenhall et al. 2013).

In most cases of epigenomic engineering, modification of chromatin marks were followed by transcriptional changes. This however differs strongly between the distinct modifications, suggesting that not every single mark harbors the same regulatory potential. However, this is apparently also highly dependent on the target locus which means that specific marks could maybe only regulate a specific subset of sites.

3.3 gRNA multiplexing

A lot of different approaches in genomic, transcriptional and epigenomic engineering suggest that it is often not enough to target just a single site. As CRISPR is bipartite, the only limitation which is set in terms of multiple targeting is the number of gRNAs which are provided for the machinery. Of course, one could just simply mix a number of similar gRNA expression vectors prior to deployment, however this does not ensure that cells will (A) get all gRNAs simultaneously and (B) in stoichiometric amounts.

To overcome this bottleneck, different techniques have been developed to generate vectors which harbor more than one gRNA expression cassette, so called multiplexed gRNA vectors. Due to the small size of one single gRNA expression cassette it is possible to create vectors with up to 14 different expression cassettes in a row (Peterson et al. 2016). Generation of these vectors however is often based on large synthesized oligonucleotides. There therefore is a need for methods to generate these kinds of vectors faster and especially cheaper. Protocols which were introduced for generation of multiplexed gRNA vectors were based on classical cloning with restriction and ligation (Dow et al. 2015; J. F. Li et al. 2013; Yan et al. 2016), isocaudomer based cloning (C. Wang et al. 2015) or Golden Gate Cloning and variants (Kabadi et al. 2014; Sakuma et al. 2015a; Vazquez-Vilar et al. 2016). Other gRNA multiplexed systems rely on the transcription of a precursor RNA driven by one single promoter. The precursor transcript is then further processed to release single gRNAs. This can be achieved by different measures, but nearly all of the systems rely on ribonucleases which excise linker sequences or cut between gRNA sequences. These linkers can be tRNA sequences which are recognized and excised by endogenous RNases (K. Xie, Minkenberg, and Yang 2015) or small hairpin/micro RNA motifs which are cut by the ribonuclease DROSHA (C. Xie et al. 2017; Yan et al. 2016), releasing flanking gRNAs into the cell.

In the process of this PhD thesis, I established a novel gRNA multiplexing assembly protocol. String Assembly gRNA cloning (STAgR) is exploiting several aspects of Gibson cloning and based on generation of small building blocks by simple overhang PCRs. These are then subsequently assembled in one single overnight reaction. This technique provides an easy, cost-effective and efficient way to multiplex gRNA vectors and was unmatched in its flexibility and customizability. With the establishment of the STAgR technique, I found a solid basis for extending the transcriptional and epigenetic engineering tools.

4. Epigenetic regulation in Alzheimer's disease

Alzheimer is a neurodegenerative disease in which amongst other factors and physiological symptoms neuritic amyloid plaques and tangles of intracellular hyperphosphorylated tau can cause synaptic dysfunction and neuronal cell death which leads to a decrease of cerebral matter (Selkoe 2012). In Alzheimer's Disease there are many hints that there is an influence of environmental factors and therefore an epigenetic influence on disease development. The disease undoubtedly has a genetic component, but this component seems only rarely to be the cause of the burden. Genome wide association studies (GWAS) have identified genetic mutations which patients have in common and could therefore be a driving force of disease development. They unravelled mutations in genes like *APP* (Goate et al. 1991; P. H. St George-Hyslop et al. 1987), *PSEN1* (Sherrington et al. 1995; P. St George-Hyslop et al. 1992; Van Broeckhoven et al. 1992) and *PSEN2* (Sherrington et al. 1996) which can lead to an early onset of the disease (before 65 years). However this familiar inherited variant only seems to occur in a very small percentage (5%) of all Alzheimer's cases. The other 95% seem to be a sporadic form where aberrations in the gene of apolipoprotein E- ε4 (*APOE*) lead to a higher risk to develop this late-onset form (after 65 years) (Diniz et al. 2017; R. Zhao et al. 2017). Nonetheless only 25% of people having these mutations then really develop the disease, whereas another 50% don't even carry aberrant genetic information but develop it anyway (Van Cauwenberghe, Van Broeckhoven, and Sleegers 2016).

Epigenetic modifications, the chemical marks attached to the DNA or histones, are integrating environmental and intrinsic signals in the cell (Jaenisch and Bird 2003). Signalling pathways, environmental effects and cellular memories are all imprinted in the complex patterns of chromatin marks, which individually can potentially regulate expression of specific genes and taken together constitute the epigenome. Some of these chromatin mark patterns are transitory and change dynamically during development, described by Waddington in his epigenetic landscape. In contrast to this some states can be established stably and even be inherited. However, the described changes cannot only occur during development but there is also evidence that during various diseases an abnormal distribution of epigenetic signals can occur. Therefore an epigenetic influence on disease development seems likely. So for example leads the miss- regulation of the clearly epigenetic controlled mechanism of epithelial to mesenchymal transition to a hijacking of a normal cellular program to support cancer progression and metastasis (Acloque et al. 2009). Wrong cellular epigenetic signals can also lead to a false distribution up to an absence of for example T cells in the severe combined

immunodeficiency syndrome (R. H. Buckley 2004; Rebecca H. Buckley 2004). Lastly a large body of work has shown that in many diseases, including the neurodegenerative diseases Alzheimer's (AD) and Parkinson's (PD), abnormal chromatin marks do occur and therefore abnormal physiological cellular states can be adopted (Ammal Kaidery, Tarannum, and Thomas 2013; Mastroeni et al. 2011; Urdinguio, Sanchez-Mut, and Esteller 2009).

The exact mechanisms of Alzheimer's disease are still unknown and the disease burden cannot be solely explained by genetic factors. Therefore studies have been conducted to look into epigenetic differences which could be linked to disease development. Among the best profiled chromatin modifications in AD is DNA methylation, an especially stable epigenetic mark. The promoter region of the APP gene for instance was found to be hypermethylated in Alzheimer cases (Tohgi, Utsugisawa, Nagane, Yoshimura, Genda, et al. 1999; Tohgi, Utsugisawa, Nagane, Yoshimura, Ukitsu, et al. 1999). A neuron specific methylome analysis of post mortem brain samples revealed a hypomethylation of the promoter of the gene *BRCA1* which was consistent with a significant overexpression of the same gene (Mano et al. 2017). Overexpressed and mislocalized BRCA1 seems to contribute to a decline of genomic integrity under the burden of accumulated amyloid ß (a characteristic for Alzheimer's pathology) in several mouse models. This phenomenon goes hand in hand with promoter hypomethylation, suggesting (A) a contribution of BRCA1 to AD pathogenesis and (B) an underlying epigenetic mechanism based on promoter methylation which misregulated BRCA1 expression (Mano et al. 2017). Recently, studies have revealed that some differentially methylated positions seem to be potent biomarkers for AD progression. CpG islands of the *APOE* gene seem to be hypomethylated in AD cases in the frontal lobe more specific in the non- neuronal cells of post mortem patient samples (Foraker et al. 2015; Tulloch et al. 2018). Furthermore it has been suggested that an increase of methylation of the gene of Phosphatidylinositol binding clathrin assembly protein (*PICALM*) is connected to cognitive decline during AD progression (Mercorio et al. 2018). Numerous studies have tried to link distinct methylation patterns to Alzheimer's disease. Overall, it appears that there is a global decrease in 5mC in post-mortem AD brain samples, be it in cortical neurons or more generally in the hippocampus, entorhinal cortex and cerebellum (Chouliaras et al. 2013; Condliffe et al. 2014; Mastroeni et al. 2010).

Two independent epigenome-wide association studies (EWAS) have recently used large cohorts of pre-symptomatic AD patients and control groups to collect brain samples and to determine DNA methylation changes (De Jager et al. 2014; Lunnon et al. 2014). Importantly, both studies revealed identical disease associated DNA methylation marks (close to the genes

RHBDF2, RPL13, C10orf54– CDH23 and *ANK1*) (Fig. 5). Moreover, those epigenetic marks emerge early during pathogenesis, correlate to a loss of gene expression, and occur so frequently that a role in the disease, either by spontaneous occurrence (as epimutations) or as an epigenetic memory of environmental factors, seems plausible. However, our knowledge about the effects of disease associated chromatin marks is very limited. So far, functional insights could be exclusively obtained by indirect approaches (e.g. by genetic manipulation) and was largely limited to developmental marks and animal models (like for example in genomic imprinting (Latos et al. 2009; Stefan H Stricker et al. 2008). As direct manipulation of individual chromatin marks (in human cells) remained impossible until very recently, it is still enigmatic to which extend disease associated chromatin marks contribute to the disease, how they operate and how they could be counteracted.

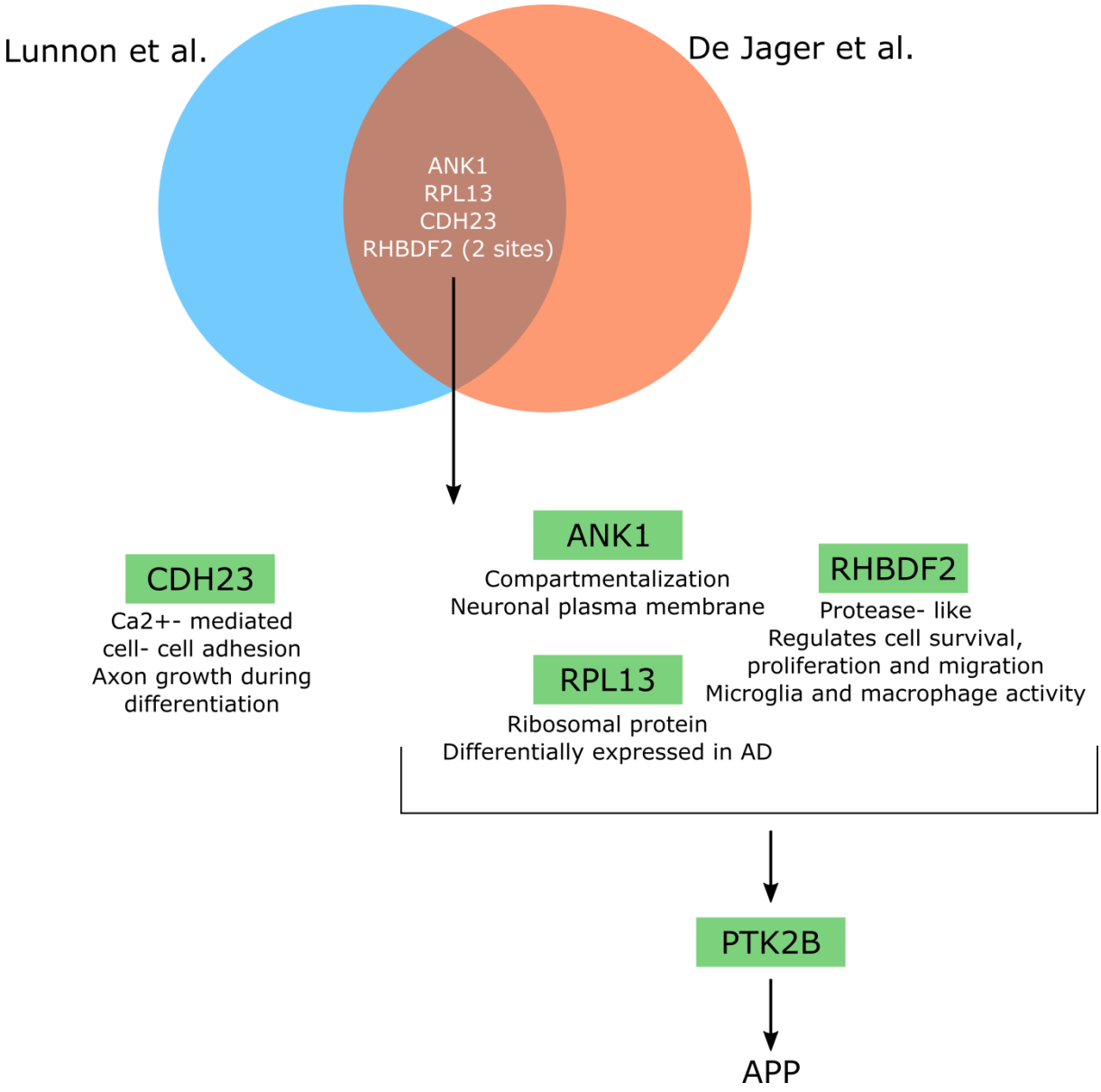

Fig. 5 | Highly methylated loci identified in two independent EWAS. 5 single CpGs sites were identified in two independent EWA studies and were found to be highly methylated in Alzheimer's Disease patients, compared to control groups. ANK1, RPL13, and RHBDF2 are known to be linked to PTK2B, a gene already identified to be AD- associated. Modified after Lord and Cruchaga 2014.

5. Scientific aims

Utilizing CRISPR/Cas9 in transcriptional as well as epigenomic engineering opens up a tremendous amount of scientific avenues. The aims of my studies concentrate mostly on tool generation for the fast progressing CRISPR field and biological questions which are simplified by the generated tools. CRISPR/Cas9 also helps to tackle more classical scientific approaches from a different point of view. Direct neuronal reprogramming is possible through transgenic introduction of constitutively active master transcription factor genes. The spectacular success of direct reprogramming approaches should, however, not obscure the fact that these methods are currently far from perfect. Direct neuronal reprogramming is at present, rather inefficient, as only a fraction of cells appropriately switches cell identity while others remain undifferentiated or stuck in intermediate stages (Coutts and Keirstead 2008); toxic, as a significant proportion of cells die after virus- mediated expression of cell fate determining transcription factors, both *in vitro* and vivo approaches (Gascón et al. 2016) and incomplete, as cells do not fully differentiate into mature and adequate neuronal subtypes (Gascón et al. 2016). By activating the endogenous gene copies of master regulators by transcriptional engineering, I aim to overcome certain difficulties and limitations the reprogramming field is facing. One huge limitation is the number of master regulator genes that can be introduced at once. This could potentially be the reason for insufficient and incomplete maturation during artificial trans-differentiation. Toxicities connected to unphysiological expression levels caused by viral promoters (especially *in vivo*) might also be a consequence of inadequate and immature cell states. By exploiting one of the biggest advantages of the CRISPR system, namely the possibility to target multiple genes simultaneously, I aimed to orchestrate the trans- differentiation process to gain neuronal subtype specificity of upper layer callosal projection neurons. Here cells should be primed by the neuronal pioneering factor NEUROD1 as it was shown that this factor can convert reactive astrocytes to glutamatergic neurons *in vitro* and *in vivo* (Guo et al. 2014). This should be uses as a basis to then further push the cells into a specific subtype, targeting multiple factors at once using dCas9 based activators.

One additional aim is to manipulate DNA methylation marks occurring in Alzheimer's patients by epigenomic engineering. Like this potential disease relevant marks should be recreated at five different loci, which had previously been shown to be associated with Alzheimer's disease (De Jager et al. 2014; Lunnon et al. 2014). With these manipulations, I set out to validate a contribution of pathological chromatin marks to the disease. Previous

studies have been shown that current methylation tools based on dCas9 still show off- target effects. Therefore I aim for deploying amongst the classical ones, novel methylation tools, generated during this study. I generated fusion constructs with viral (M.CVIPI from the Chlorella virus (Buryanov and Shevchuk 2005)) and plantal (DNA (cytosine-5)-methyltransferase 1A (DNM1A) and DNA (cytosine-5)- methyltransferase DRM2 (DRM2) methyltransferases which were optimized for human expression. Advantages gained could be better controllability, independence of host factor interactions, and depending on the type of methyltransferase, the investigation of effects of non-human methylation patterns.

All approaches in transcriptional as well as epigenomic engineering attempted during this thesis required a reliable gRNA multiplexing system. Therefore, I first set out to establish such a system.

B Results

1. Generating Multiplexed gRNA vectors with String Assembly gRNA Cloning (STAgR)

This chapter contains text and data that were published in:

Breunig CT, Durovic T, Neuner AM, Baumann V, Wiesbeck MF, Köferle A, Götz M, Ninkovic J, Stricker SH: **"One step generation of customizable gRNA vectors for multiplex CRISPR approaches through string assembly gRNA cloning (STAgR)". PLoS One** 13, e0196015 (2018).(C. T. Breunig et al. 2018a)

Breunig CT, Neuner AM, Giehrl-Schwab J, Wurst W, Götz M, Stricker SH: "**A Customizable Protocol for String Assembly gRNA Cloning (STAgR)"** *J. Vis. Exp.* (142), e58556, doi:10.3791/58556 (2018).(C. T. Breunig et al. 2018b)

CRISPR experiments are highly dependent on the target information provided by gRNAs. Some paradigms do not only require delivery of one but multiple gRNAs to one single cell reliably. An ideal protocol to generate multiplexed gRNA vectors would be simple, fast and cost-effective and could be conducted reliably while maintaining a high degree of customizability. In order to meet these requirements, I developed String assembly gRNA cloning (STAgR). STAgR makes use of the Gibson assembly method (Gibson et al. 2009). The Gibson method is based on a witty combination of three different enzymes. An exonuclease removes nucleotides from the 5'-end of double- stranded but linearized DNA. Complementary single stranded DNA regions can then anneal to each other. Phusion DNA polymerase fills then the gaps and TAQ DNA ligase covalently joins the annealed complementary DNA fragments, by removing the individual nicks. The STAgR method allows the assembly of multiple gRNA expression cassettes into an expression vector in a single overnight reaction by using the N20 gRNA sequences as complementary DNA sequences. PCR-amplified building blocks are generated from a short DNA template, the string, which is composed of a gRNA scaffold sequence of choice, a transcriptional stop signal (poly dT) and a Pol III promoter (Fig. 6). By including the gRNA targeting sequence (N20) as primer overhangs during the PCR amplification of the string sequence, the building blocks for Gibson assembly can be generated from one universal template. By exploiting this,

STAgR is not only simple, but remains highly customizable because various combinations of different strings and backbones are possible (Fig. 7B).

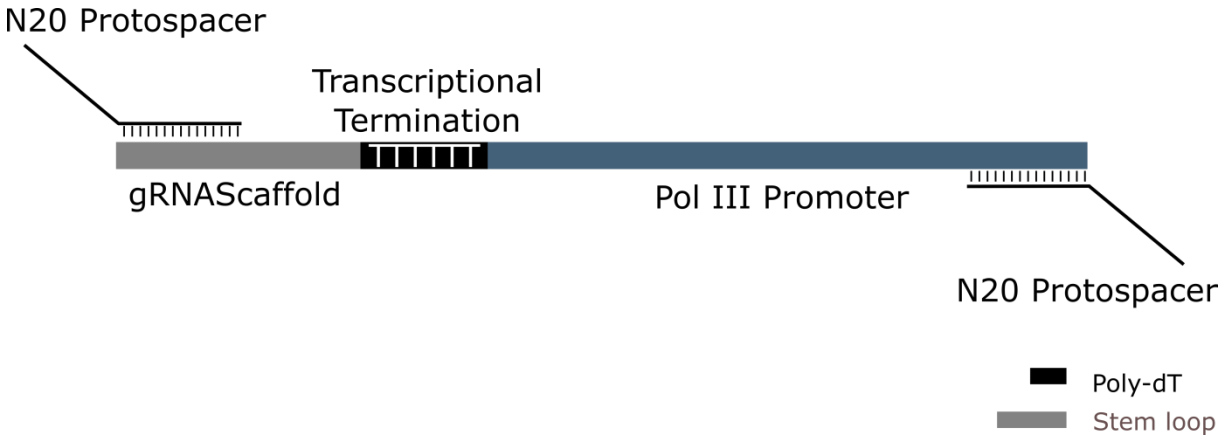

Fig. 6 | The STAgR string. To generate building blocks for multiplexed gRNA vectors the string has to be amplified with overhang primers, adding the N20 targeting information via PCR as a Gibson overhang. The string consists of a gRNA scaffold, a poly- T transcriptional stop and a Pol III promoter

1.1 Optimization of STAgR conditions

The protocol was tested by setting up a strategy for a gRNA expression plasmid with four different individual gRNAs, targeting the promoter region of the gene *Ascl1*. All expression cassettes were driven by the human U6 promoter, terminated by the classical spCas9 gRNA scaffold and a poly-T sequence. The individual PCR conditions for gRNA building blocks and vectors were determined by gradient PCR and can be found in the Materials and Methods section. Following successful PCR amplification of the strings as well as a vector using overhang primers (Fig. 8A/B), the DNA fragments were assembled in a Gibson reaction. This enzymatic assembly is sensitive to two different factors: the ratio of individual DNA fragments in the reaction mix and the incubation time. Both parameters where tested individually: Equimolar amounts of three gRNA string-based building blocks were added to the vector in either a three-fold or five-fold excess or the vector in a three-fold excess relative to the amount of used inserts (Fig. 8E). The Gibson assembly reaction was stopped after 20, 30, 40, and 60 minutes. Reactions were transformed into bacteria and colonies screened by colony PCR (Fig. 8C/D). This strategy was used to both rapidly screen bacterial clones for the desired assembly product and gauge the efficiencies of the assembly under the different conditions. Quantifications in Figure 8E show the percentage of different obtained gRNA subsets in dependence on the ratio of educts and reaction time. As expected, the nature of the assembly products varied with the ratio of the individual components and time. I found that gRNA building blocks as well as vectors should be combined in an equimolar ratio and

incubation times should not exceed 40 minutes at 50°C. Using these parameters, 34% of all clones contained the desired four gRNA cassettes. With these results, I could show that STAgR can efficiently assemble multiple gRNA expression cassettes under the optimized conditions (Fig. 8D/E). Hence, these parameters were used in all subsequent experiments (Fig. 8F). Sanger sequencing was used to confirm the seamless assembly of desired multiplexed gRNA expression vectors designed *in silico*. Colony PCR also revealed that STAgR clones which did not contain all gRNA expression cassettes showed bands which represented subsets of different gRNA expression cassette numbers. Sanger sequencing revealed that these clones indeed lack one or more gRNA expression cassettes without a further cloning scar, breakage points or sequence repetitions. Each STAgR reaction therefore not only spawns gRNA vectors with the intended number of gRNA cassettes, but additionally yields a subset of different combinations and number of gRNA expression units which can be used for additional experiments.

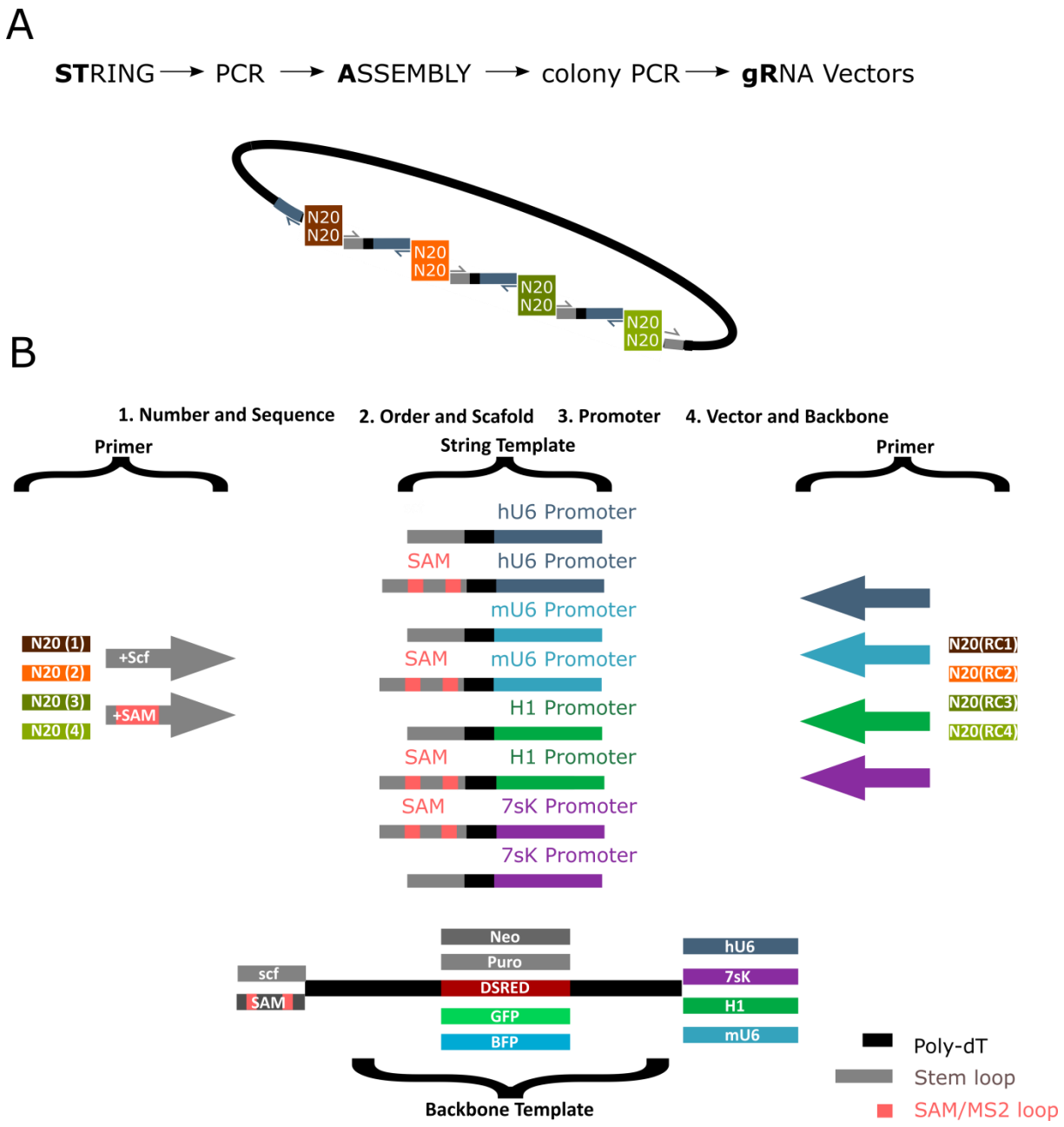

Fig. 7 | Overview of the STAgR method. A String Assembly gRNA cloning is a 3 step cloning method to generate multiplexed gRNA vectors. The overhangs which are implemented via PCR are not only the target information of the gRNAs but also serve as homology sequence for Gibson assembly. **B** STAgR was engineered to be highly customizable. The choice of string and backbone provide a wide variety of possibilities to form the perfect vector for any experiment. Parts of this figure were modified and taken from C. T. Breunig et al. 2018b.

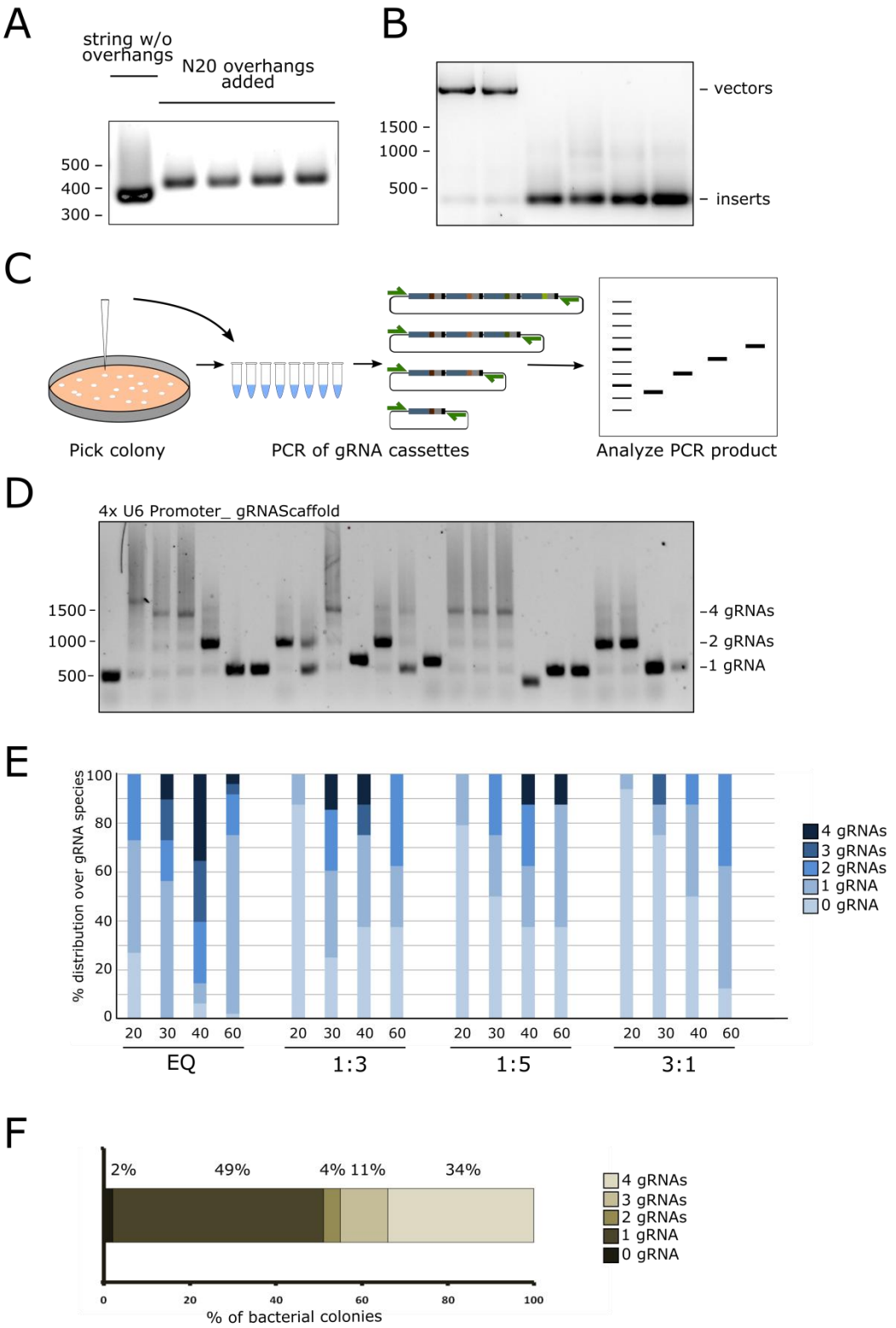

Fig. 8 | Establishment and optimization of STAgR. A PCR amplification of string with primers lacking overhangs (lane 1) and with overhangs and therefore the target information added (lanes 2- 4). PCR products were analyzed on a 1.5% agarose gel, stained with SYBR safe. **B** STAgR PCR of two vectors (lane 1 and 2) and

four insert building blocks with the N20 added (lane 3 to 6). PCR fragments were analyzed on a 1.5% agarose gel, stained with SYBR safe. **C** Overview of the colony PCR. Obtained clones are picked with a pipette tip and biological material is transferred to PCR tubes. The PCR mastermix is then evenly distributed over all PCR tubes. The primers amplify the gRNA cassette. The length of the amplicon corresponds to the number of gRNA cassettes present. **D** Analytical agarose gel of a 4xSTAgR cloning and colony PCR. **E** Statistics of the optimization process of STAgR cloning. The same set of building blocks was assembled in different ratios and the reaction was stopped at different timepoints. The timepoints were 20, 30, 40, and 60 min. The building blocks were combined in molar equality, 1:3, 1:5 and 3:1(vector to inserts) (n =48). **F** Quantification of cloning efficiencies from three different 4xSTAgR reactions using optimized conditions (molar equality and 40 min incubation time) (n =130). Parts of this figure were modified and taken from C. T. Breunig et al. 2018a.

1.2 STAgR gRNAs are expressed individually and functionally

Each gRNA within a STAgR vector is driven by its own promoter. Therefore, every single unit has to be expressed individually to form operational gRNA molecules. Unfortunately, quantification and verification of expression levels of individual gRNAs is still challenging by conventional methods.

In order to ascertain that STAgR vectors functionally express multiple gRNAs, I conducted a genetic assay using WTCas9. In this experiment, a multiplexed STAgR vector was directly compared to a gRNA vector only carrying one gRNA. This gRNA targets the open reading frame of the gene coding for a destabilized version of the green fluorescence protein GFP (d2GFP) with a significant shorter protein half-life (Corish and Tyler-Smith 1999). If expressed, this gRNA in combination with WTCas9 can cause genetic alterations which often lead to loss of a functional GFP gene. By the loss of GFP signal, gRNA expression can be quantified directly. The GFP targeting gRNA was cloned into four different STAgR constructs with each four gRNA cassettes in total. In these constructs, the GFP targeting gRNA was incorporated on four different positions, followed or flanked by non-targeting control gRNAs. All STAgR plasmids as well as single gRNA plasmids were then individually transfected into HeLa cells stably expressing d2GFP and WTCas9. Eight days after transfection, cells were analyzed by flow cytometry. When only a single GFP targeting gRNA is provided to the system, 72% of cells lose GFP expression. This indicates a successful disruption of the open reading frame by induction of indel mutations. All four STAgR plasmids trigger similar GFP loss indicating that gRNAs at all four positions are expressed and functional.

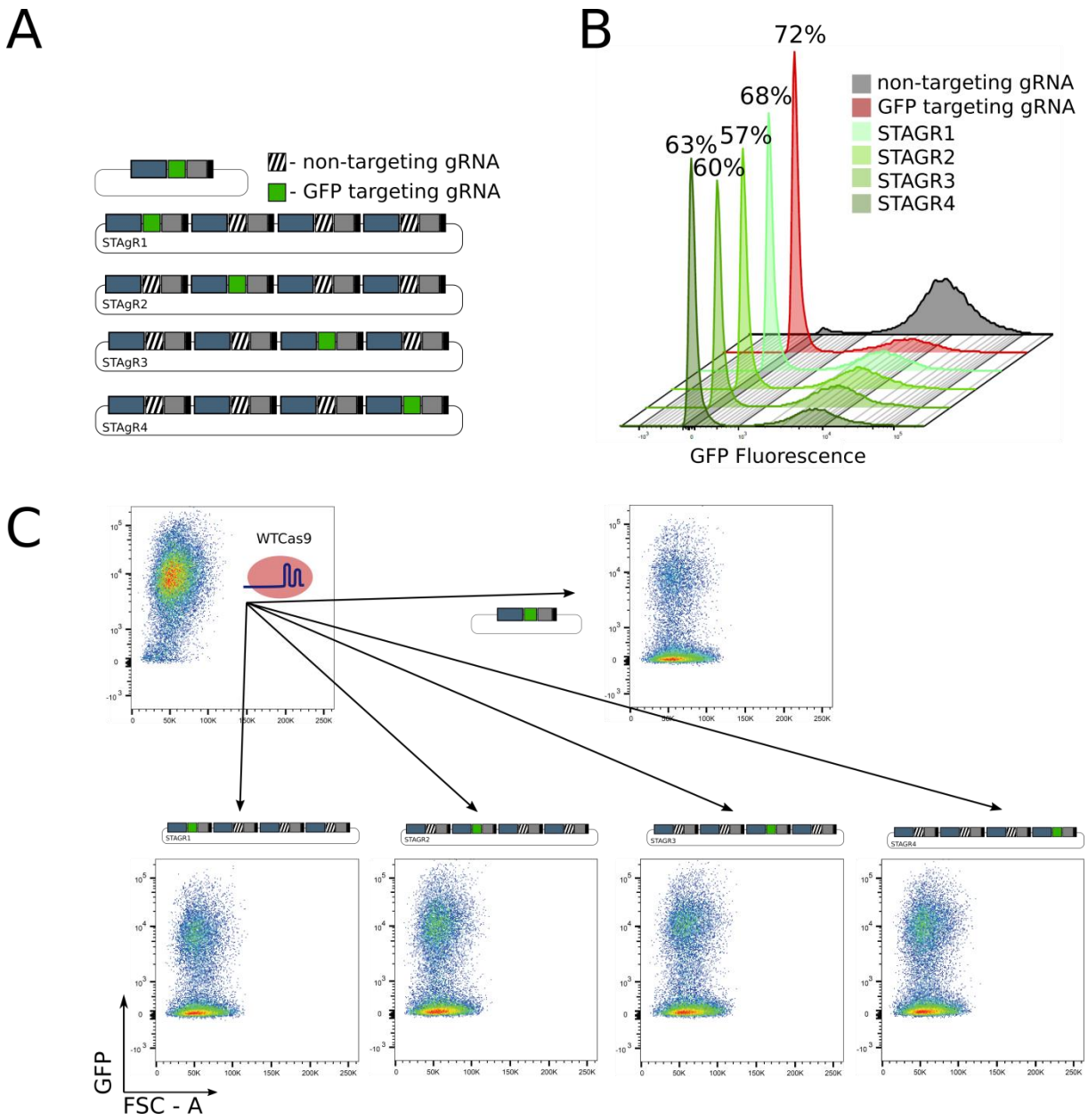

Fig. 9 | Functional validation of a 4-gRNA STAgR vector. A Five gRNA plasmids have been generated carrying a gRNA targeting the open reading frame of GFP. This gRNA is either in a single gRNA vector or four different STAgR constructs located on four different positions. These constructs were generated to make sure that all gRNAs are expressed to same levels. **B** Visualization of GFP negative cells obtained by mutation of the open reading frame of the fluorescence marker. The STAgR constructs and the single gRNA vector were transfected into a N2A cells stably expressing d2GFP, a fast degrading version of GFP. Every gRNA construct expressed the gRNA targeting GFP and therefore could guide WTCas9 to the genomic location of the fluorescence protein and induce indel mutations. This could be done to similar levels compared to the single gRNA construct, indicating that all gRNAs are expressed to similar levels. **C** Individual FACS blots of experiments shown in B. After transfection with WTCas9 and the gRNA plasmids cells clearly lost GFP expression due to the mutations induced by WTCas9. Parts of this figure were modified and taken from C. T. Breunig et al. 2018a.

1.3 STAgR is highly customizable

As the CRISPR/Cas9 based transcriptional as well as epigenomic engineering field is steadily advancing, it is important for a universal multiplexing strategy to be easily adaptable to different means. A series of strings were generated featuring different Pol III promoters. Figure 10 shows the cloning of a STAgR construct with 4 different gRNAs, each driven by different promoters (human U6, mouse U6, human 7SK and H1). In addition to promoters, the gRNA scaffold can be substituted by different sequences as well. Two MS2-binding loops (henceforth called “SAM” loop) can be integrated into the scaffold sequence in order to utilize the gRNA with an MS2 binding protein-based system (Konermann et al. 2014a). Cloning of highly customized constructs with varying promoter and scaffold sequences showed a 30% efficiency of correct assembly, comparable to that of standard STAgR constructs (Fig. 10B). The versatility and simplicity of STAgR enables the combination of different Cas9 variants, MS2 fusion proteins, and dCas9 chromatin modifiers and indicates a decisive advantage over other multiplexing systems (Fig. 11A).

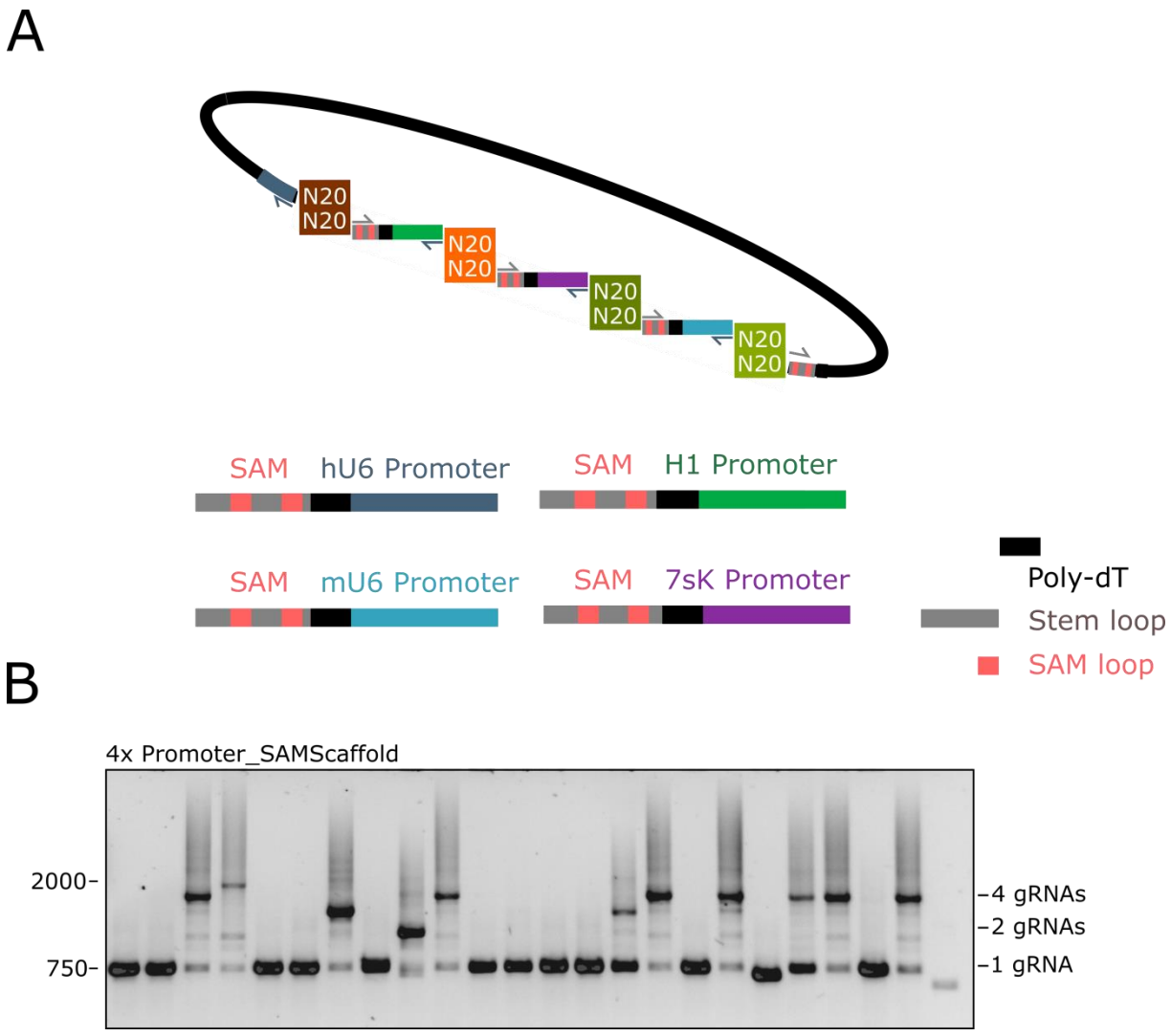

Fig. 10 | STAgR is highly customizable. A This construct was engineered to harbor four different promoters as wells as SAM gRNA stem loops to be able to combine it with additional RNA- protein interaction based targeting systems. **B** Analytical agarose gel of the indicated STAgR construct carrying four different promoters as well as different gRNA stem loops. 1.5% agarose gel, stained with SYBR Safe. Parts of this figure were modified and taken from C. T. Breunig et al. 2018a/b.

Gibson cloning is dependent on homologous sequences and STAgR cloning is based on repetitive building blocks. The limit for STAgR cloning is four gRNA cassettes when using the same promoter as well as the same gRNA scaffold. Using more than four gRNA cassettes with identical promoters and scaffold sequences never yielded the correct product, likely due to unwanted internal recombination events. However, it is possible to assemble up to 8 expression cassettes into one vector in a single step reaction by changing the gRNA driving Pol III promoter as well as the gRNA scaffold (from the conventional scaffold to SAM) after the fourth gRNA (Fig. 11B). A colony PCR ladder with all possible numbers of gRNA units is depicted in Figure 11C.

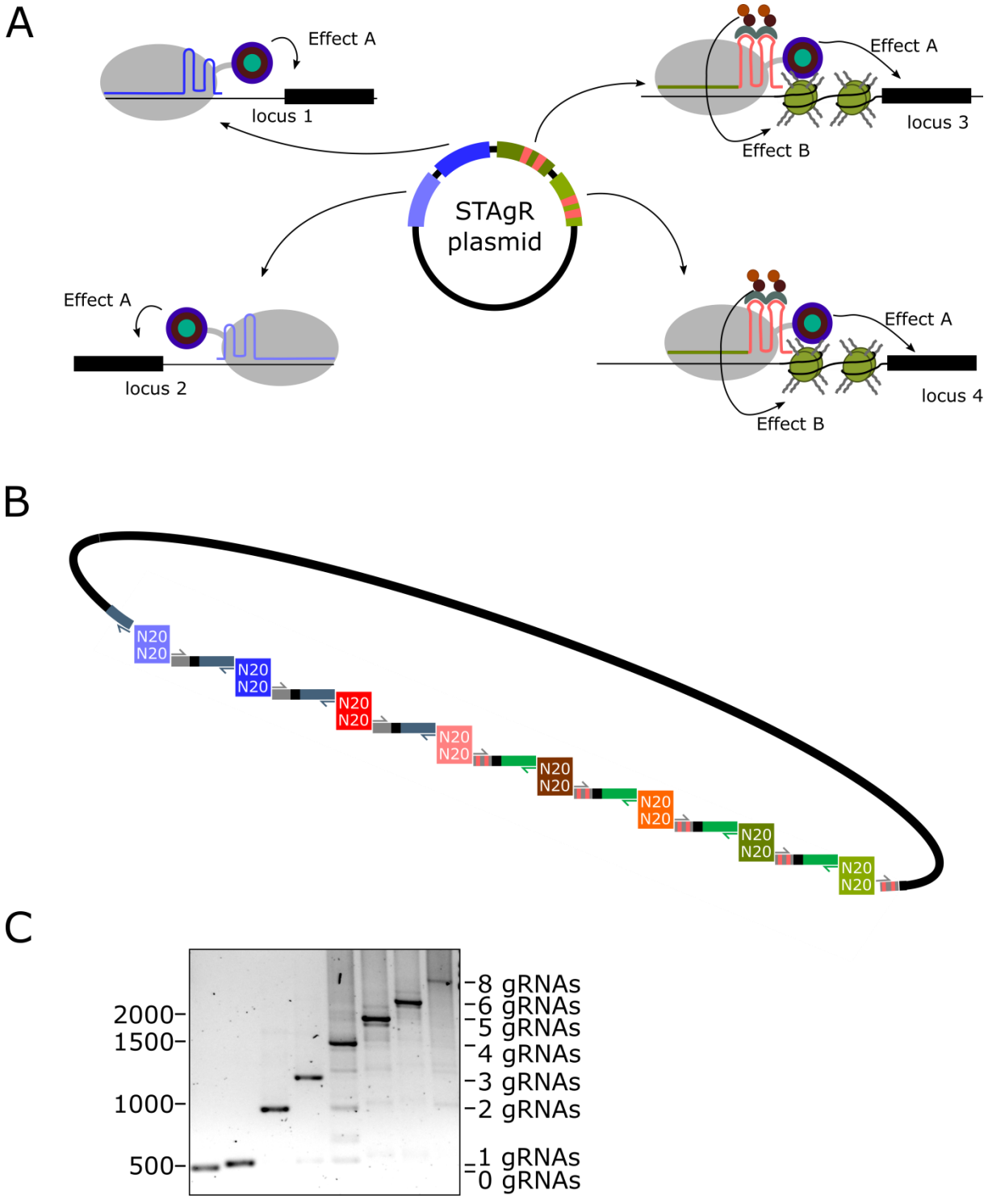

Fig. 11 | Visualization of the possibilities provided by STAgR cloning. A By combining different gRNA stem loops in one single gRNA plasmid one can target different loci with different effectors. **B** 8x STAgR could be created by changing to different promoters and different stem loops after 4 identical gRNA expression cassettes. **C** With STAgR, gRNA multiplexed vectors with 1 to 8 gRNAs can be created. This analytical gel shows a PCR of all obtained multiplexed cassettes. Parts of this figure were modified and taken from C. T. Breunig et al. 2018a.

1.4 Use of STAgR for improved and combinatorial transcriptional activation

Before potential multiplexing strategies, experiments relied on delivery of a cocktail of multiple gRNA plasmids, viruses, or molecules to cells. To test whether multiplexing gRNAs is beneficial for transcriptional engineering, a STAgR vector was produced carrying four different gRNAs. These gRNAs target the promoter regions of three different genes: the neuronal gene *Satb2*, the cardiac muscle actin gene *Actc1*, and *Ttn1* (targeted by two gRNAs) (Fig. 12A). The STAgR plasmid carrying a tdTomato fluorescence marker was transfected into P19 cells alongside a construct expressing the transcriptional activator dCas9'VPR and a GFP fluorescence marker. As a control, the cells were transfected with dCas9'VPR and a mix of single gRNA plasmids containing the exact same gRNA protospacer sequences as the STAgR plasmid. After five days, GFP^+/$tdTomato^+$ positive cells were isolated by fluorescence activated cell sorting (FACS) and RNA was extracted. Relative amount of mRNA of targeted genes was analyzed using qPCR. qPCR of the targeted genes showed that using STAgR, two out of three genes could be activated to a higher level than by using only a cocktail of single gRNA plasmids (Fig. 12B). This indicates a distinct advantage of multiplexing gRNA vectors for multiple gene activation using transcriptional engineering.

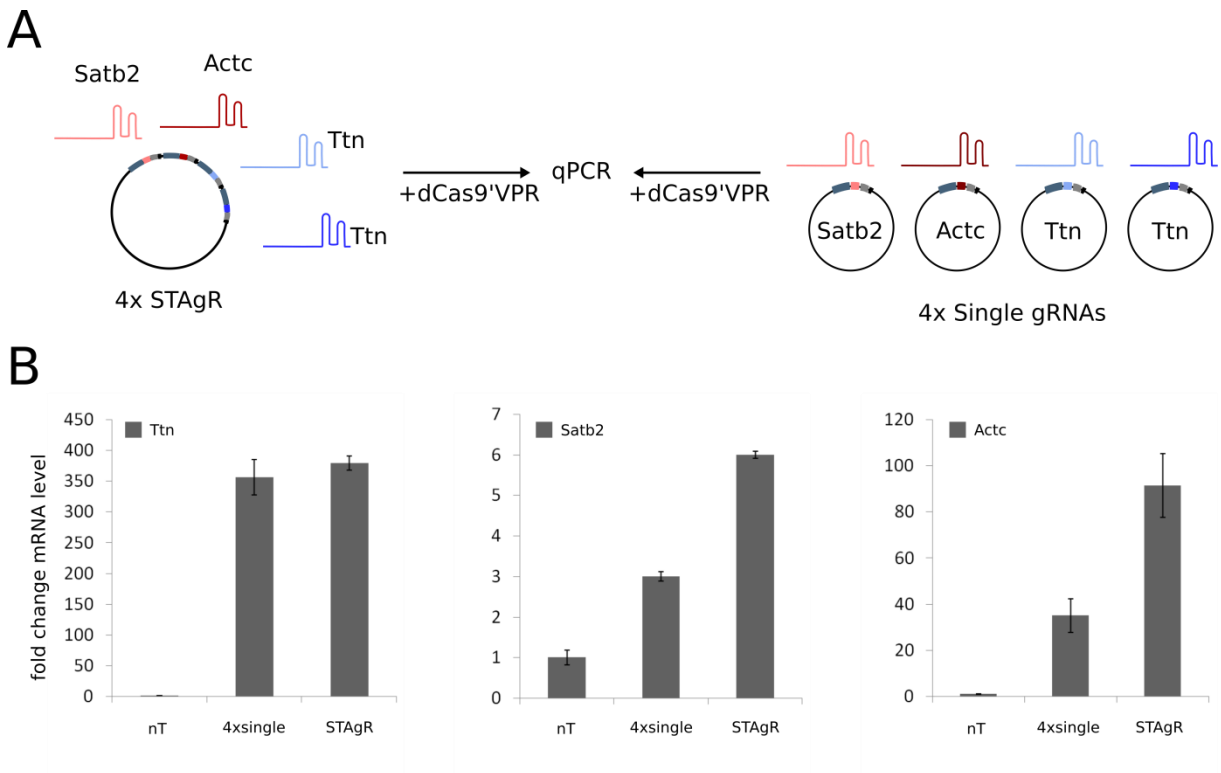

Fig. 12 | STAgR compared to single gRNA vectors. A Comparison of a 4x STAgR and a pool of single gRNA plasmids. Plasmid cocktails have been transfected into P19 cells alongside dCas9'VPR and mRNA levels were assayed by qPCR. **B** Two out of three target genes showed a higher increase of mRNA levels when the gRNAs were supplied by STAgR constructs, compared to a mix of single gRNA vectors. Error bars depict standard errors of the mean.

1.5 Simultaneous disruption of multiple genes *in vivo*

To test if Cas9 and STAgR could be used to efficiently and simultaneously disrupt multiple genes in individual cells *in vivo*, a STAgR vector was produced with gRNAs targeting the ORF of GFP and Sox2. The gRNAs were electroporated alongside a plasmid expressing WTCas9 into ependymoglia of three and a half months old GFAP-GFP transgenic zebrafish (Tg(gfap:GFP) (n=20) as previously described (Fig. 13A) (Barbosa et al. 2015, 2016) and shown in Durovic and Ninkovic, 2019. Seven days after electroporation, zebrafish brains were analyzed by immunofluorescence microscopy. In all animals analyzed, expression of GFP as well as of Sox2 is lost in a large number of ependymoglia, while control plasmids do not disrupt expression of either gene. It is striking that in most cells which lost the expression of one gene the other gene targeted is disrupted as well, certifying the efficient multiple gene targeting with multiplexed gRNA vectors using STAgR *in vivo* (Fig. 13B)

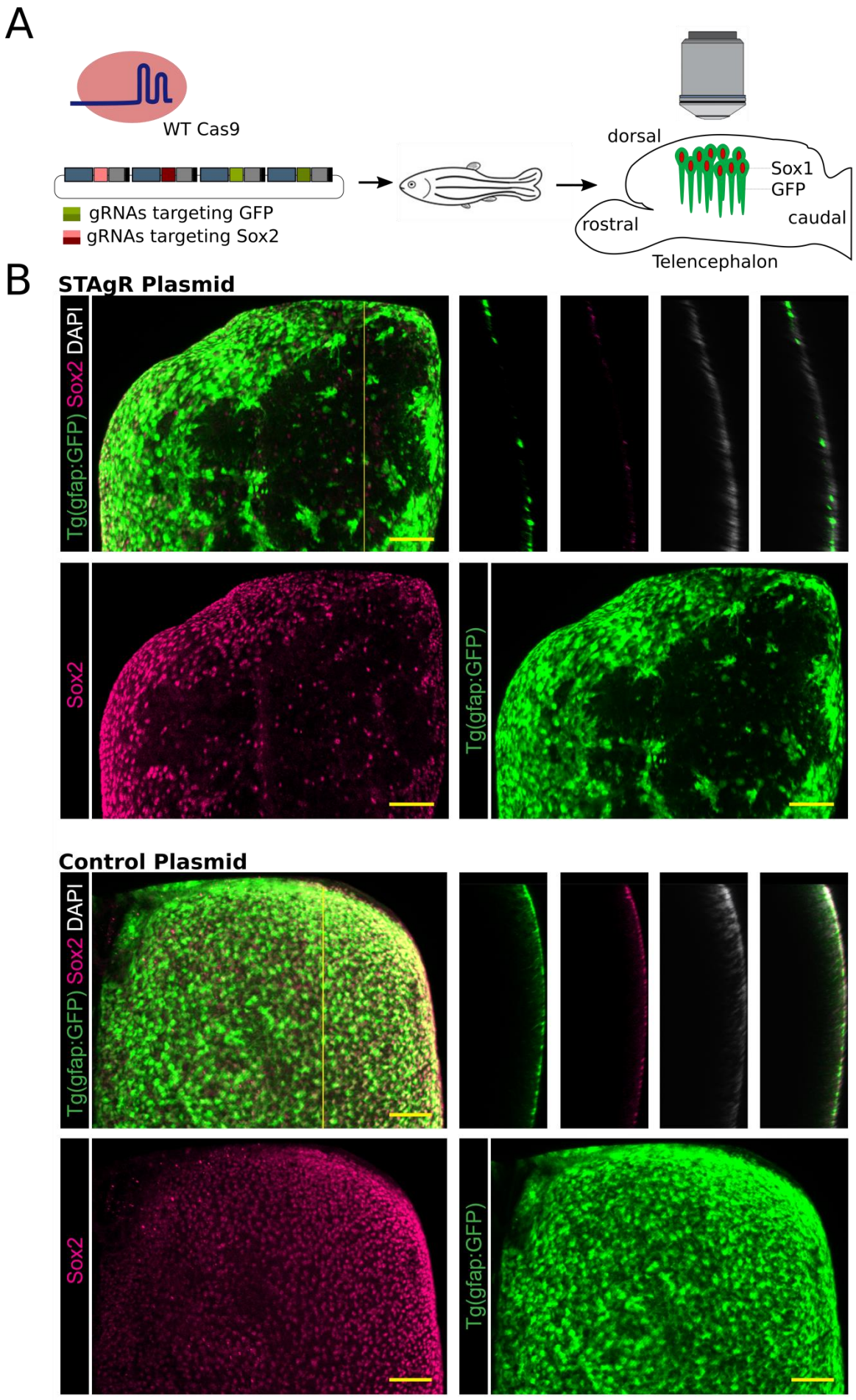
A
WT Cas9
gRNAs targeting GFP
gRNAs targeting Sox2
dorsal
Sox1
GFP
caudal
rostral
Telencephalon
B
STAgR Plasmid
Tg(gfap:GFP) Sox2 DAPI
Sox2
Tg(gfap:GFP)
Control Plasmid
Tg(gfap:GFP) Sox2 DAPI
Sox2
Tg(gfap:GFP)

Fig. 13 | *In vivo* use of STAgR. A A 4x STAgR construct with two gRNAs targeting the open reading frame of GFP as well as Sox2 were cloned and side by side with WTCas9 electroporated into GFAP:GFP transgenic zebrafish telencephali. **B** 3D reconstruction of whole mount Tg(gfap:GFP) zebrafish telencephali. WTCas9 disrupted the open reading frames of GFP and Sox2 when guided by the STAgR constructs. A control plasmid did not evoke any loss of GFP or Sox2. Scalebar: 50µm.

2. Development of novel de novo dCas9 methylation tools

As introduced in section A3.2, options for targeted *de novo* methylation is currently far from perfect. Lacking specificity and displaying significant off- target effects, CRISPR/dCas9 based *de novo* methylation requires the further development of new tools (Lin et al. 2018). During this thesis, new potential methylation tools were generated. To circumvent a possible interaction and control with and by host- factors, I designed and generated tools based on non-human or non- murine methyltransferases. I also aimed to generate tools to induce non- CpG methylation patterns. Four methyltransferases were picked for further testing. Based on functional description provided in the UniProt database (http://www.uniprot.org/) two methyltransferases, DRM2_ARATH (PaxDb number: Q9M548) and DNM1A_ORYSJ (PaxDb number: Q7Y117) were picked. DRM2_ARATH is a methyltransferase which originates from the mouse-ear cress, *Arabidopsis thaliana*. The *Arabidopsis thaliana* DNMT3 cytosine methyltransferase ortholog DOMAINS rearranged methyltransferase2 (DMR2) is in control of the non- CpG methylation pattern CpNpG and it is also responsible for asymmetric methylation patterns. DRM2 was shown to be needed in RNA-directed *de novo* methylation of cytosines in all sequence contexts (Henderson et al. 2010; Naumann et al. 2011). DNA (cytosine-5)-methyltransferase 1A (DNM1A) encoded by the gene MET1A originates from the subspecies *japonica* of *Oryza sativa* (rice). It is known to methylate CpG residues and has a significant role in *de novo* DNA methylation (Teerawanichpan et al. 2004; Yamauchi et al. 2014). It may also be involved in DNA methylation dependent gene silencing (Teerawanichpan et al. 2004) and play a minor role in DNA methylation maintenance (Yamauchi et al. 2014). The third methyltransferase, M.SSS1, is derived from the prokaryotic family of *Spiroplasma monobiae*, more specifically strain MQ1 (Renbaum et al. 1990). It is a *de novo* methyltransferase targeting exclusively CpG residues which are then completely methylated. The fourth and last methyltransferase-dCas9 fusion generated was based on a cytosine- 5- DNA methyltransferase derived from Chlorella virus NYs-1. The enzyme is called M.CVIPI and in contrast to most other mammalian methyltransferases, this enzyme recognizes the dinucleotide GpC. All constructs were generated as a fusion to dCas9 and codon optimized for mammalian expression (Fig. 14A).

To test the potential methylation capacity of the newly generated tools, a variety of transcriptional assays were performed. The first assay was based on the effect of methylation of the CAG promoter. This promoter has been reported to be sensitive to methylation. Methylation of the CAG promoter sequence results in downregulation of transcription of transgenes (Y. Zhou et al. 2014). Neuro2a cells which stably express a GFP fluorescence marker under the control of a CAG promoter were transfected with the DNA methylation fusion constructs DNMT3A and SSS1 alongside a three- times STAgR construct targeting three different sites of the CAG promoter sequence (Fig. 14B). Cells were analyzed by flow cytometry after five days. However, none of the constructs reduced the number of GFP - expressing cells, not even dCas9'SSS1 or dCas9'DNMT3A which were already reported as DNA methylation tools by others (Lei et al. 2017b; X. S. Liu et al. 2016b; Vojta et al. 2016b).

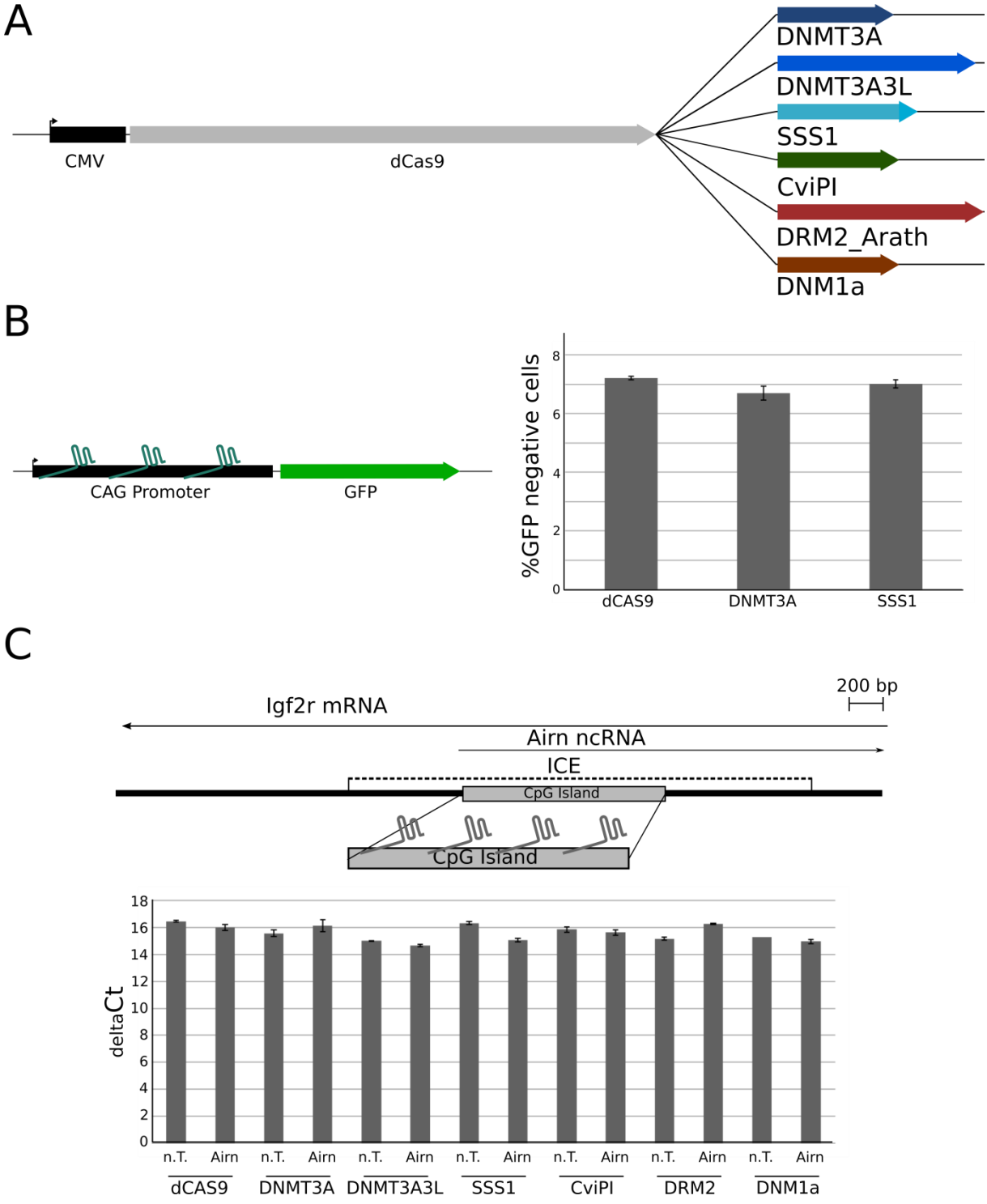

Fig. 14 | Potential new dCas9 *de novo* methylation tools A Scheme of newly produced dCas9 methyltransferase tools. **B** Three gRNAs were designed to target a CAG promoter. This STAgR was then transfected alongside DNA methyltransferases into cells expressing d2GFP under the control of the CAG promoter. Percentage of GFP negative cells was measured by flow cytometry. **C** Four gRNAs were designed to guide dCas9 fusion constructs to the ICE CpG of lncRNA Airn. Transfected cells were isolated using flow cytometry and Airn levels were determined by qPCR. Depicted are the differences between the Ct thresholds of the AIRN transcript and a housekeeper GAPDH. As a control a 4x STAgR has been transfected, carrying non targeting gRNAs ("n.T.").

To test the potential of engineered methyltransferases on a promoter known to be silenced by DNA methylation during development, I changed the experimental paradigm. Methylation of the CpG island at the 5' end of the long non-coding RNA Airn is responsible for silencing of the maternal gene copy (Koerner et al. 2012; Latos et al. 2009; Stefan H Stricker et al. 2008). Any murine cell should therefore only show expression of the paternal gene which in theory is also sensitive to methylation of its CpG island. Therefore, I reasoned that targeted methylation of this CpG island should lead to a down-regulation of the Airn transcript. To test this, I designed four gRNAs that target different parts of the Airn CpG island and combined them in a tdTomato-expressing STAgR plasmid. The gRNAs were co- transfected together with one of the dCas9-methyltransferase fusion plasmids and double-positive (GFP^+/$tdTomato^+$) cells were isolated via FACS after 4 days. Airn levels were quantified by RT PCR. However, none of the tested methyltransferases was able to change the expression level of Airn relative to non-targeting controls (Fig. 14C).

Monitoring Airn expression by qPCR did not yield any conclusive results. In order to monitor the consequences of target site methylation more easily, a methylation-sensitive fluorescence reporter was engineered. This reporter is based on a 3.7 kb region upstream of the annotated Airn transcription start site including the CpG island, which was defined to be the lncRNA's promoter. Downstream of this promoter region a tdTomato sequence was inserted (Fig. 15A). When cells were transfected with this construct, they showed mild but detectable mCherry expression. A splice acceptor sequence and an IRES sequence were inserted between promoter and fluorescence gene to ensure the transcription of functional mCherry mRNA as well as the translation to a functional red fluorescence protein if Airn transcription should be initiated sooner than after the end of its CpG island (Pelletier and Sonenberg 1988). This construct was stably integrated into a human embryonic kidney 293T (HEK293T) cell using a PiggyBAC system in order to circumvent possible host regulation of the murine Airn promoter. Over a period of 24 days, transfected cells were FACS sorted six times to isolate the cells showing the strongest expression of the mCherry reporter sequence (Fig. 15A). Once this population was stably isolated, these cells were transfected with the Airn 4x STAgR construct (now carrying a BFP Reporter) and the dCas9-methyltransferase fusion constructs. GFP^+/BFP^+ double positive cells were analyzed and the number of mCherry-negative cells scored, compared to a control population. All tested constructs did not lead to a reduction of tdTomato fluorescence. Exemplarily shown in Figure 15B are the published and therefore as positive controls chosen DNA methyltransferases DNMT3A and DNMT3A3L. However, none of the targeted methyltransferases led to a change in fluorescence reporter expression.

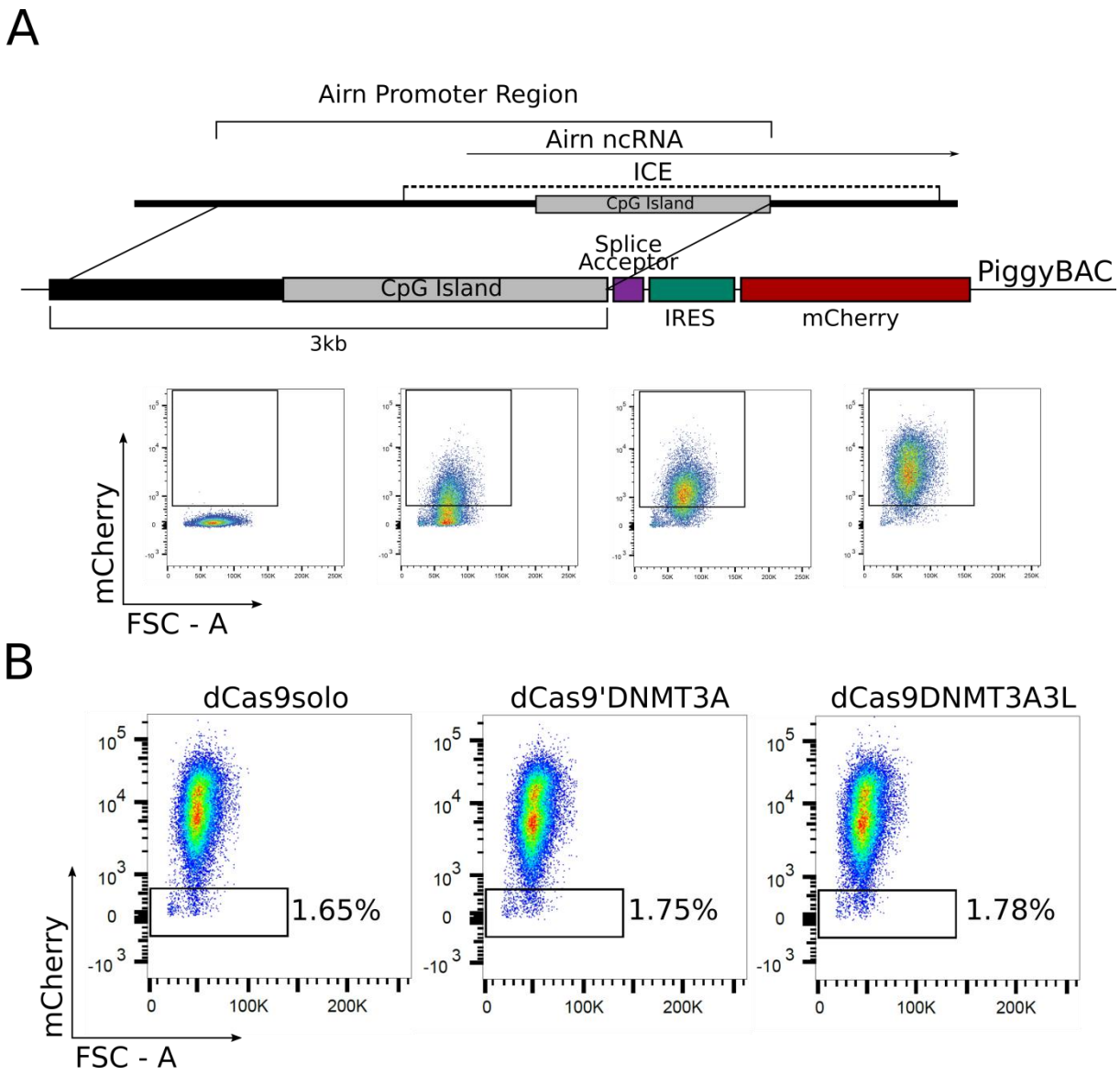

Fig. 15 | Generation of an AIRN Promoter fluorescence reporter. **A** A 3kb region including the CpG island of the Airn promoter was cloned in a PiggyBAC vector upstream of a splice acceptor and IRES and a dsRED fluorescence cassette. This vector was then transfected into HEK293T cells alongside a transposase plasmid. Cell which showed bright red fluorescence were enriched using FACS over several sorts to establish a brightly expressed fluorescence reporter driven by the Airn Promoter. **B** Airn reporter cells were transfected with gRNAs targeting the CpG island of the Airn Promoter and the dCas9-methyltransferase fusion constructs. Exemplarily shown are FACS blots of a dCas9 control, DNMT3A and DNMT3A3L.

By transcriptional read outs no changes could be observed. Next, I decided to test if targeted methylation even occurred, by analyzing the targeted sequences on a molecular level by bisulfite sequencing. For this, all methyltransferases as well as a non- methyltransferase control (dCas9'VPR) was targeted to different loci. Four gRNAs were assembled in one tdTomato- STAgR construct targeting the CpG island of Igf2r Non- Protein Coding RNA (Airn) as previously described. In addition, two gRNAs that target the promoter region of Ube2s were designed. This region is un- methylated in murine cells and was analyzed to monitor potential global methylation changes (off- target effects). P19 cells were transfected using lipofectamin with either the two- times STAgR targeting Ube2s or the four gRNA construct alongside each of the methyltransferases (DNMT3A, DNMT3A3L, DNM1A, DRM2, M.CVIPI) as well as dCas9'VPR as a control. All modifier plasmids carried a GFP expression cassette, driven by an independent CMV promoter. Two days after lipofection, positive cells for both fluorescent markers were isolated using FACS. DNA was isolated and bisulfite converted and prepared for subsequent bisulfite PCR and sequencing (Fig. 16). Surprisingly, none of the used methyltransferases resulted in higher methylation levels at targeted loci compared to base methylation levels of untreated cells or cells which obtained dCas9'VPR as a non- methyltransferase control. The strongest effects were observed from position 150 to 275 and showed approximately 1.5 fold higher methylation levels when targeted by DRM2, compared to VPR and P19. Some of the analysed cytosines (position 563 to 688) even showed lower methylation levels when targeted with DNMT3A3L or M.CVIPI (Fig. 17). The outcome of targeting the locus of Ube2s was similar; the locus remained un-methylated with all tested constructs (Fig. 18).

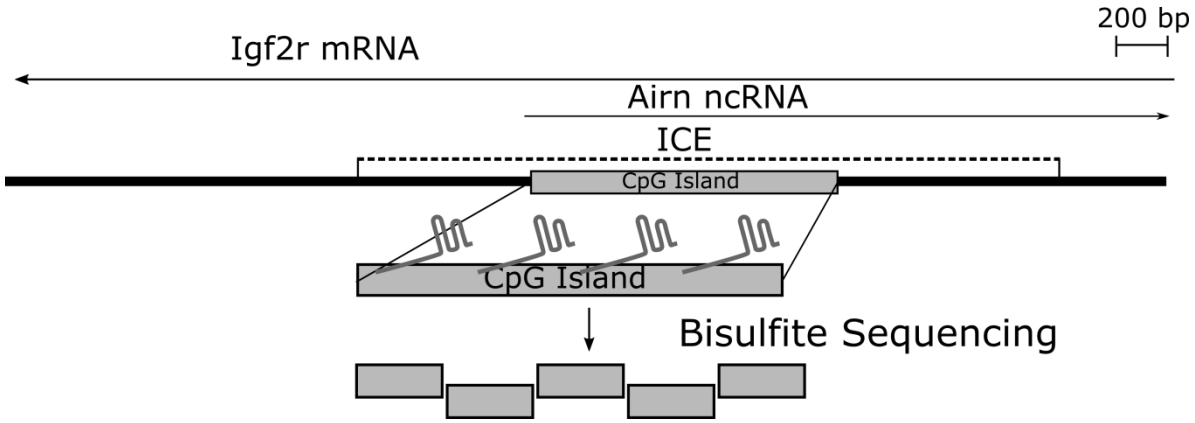

Fig. 16 | Scheme of the experimental paradigm of bisulfite sequencing of the Airn CpG island.

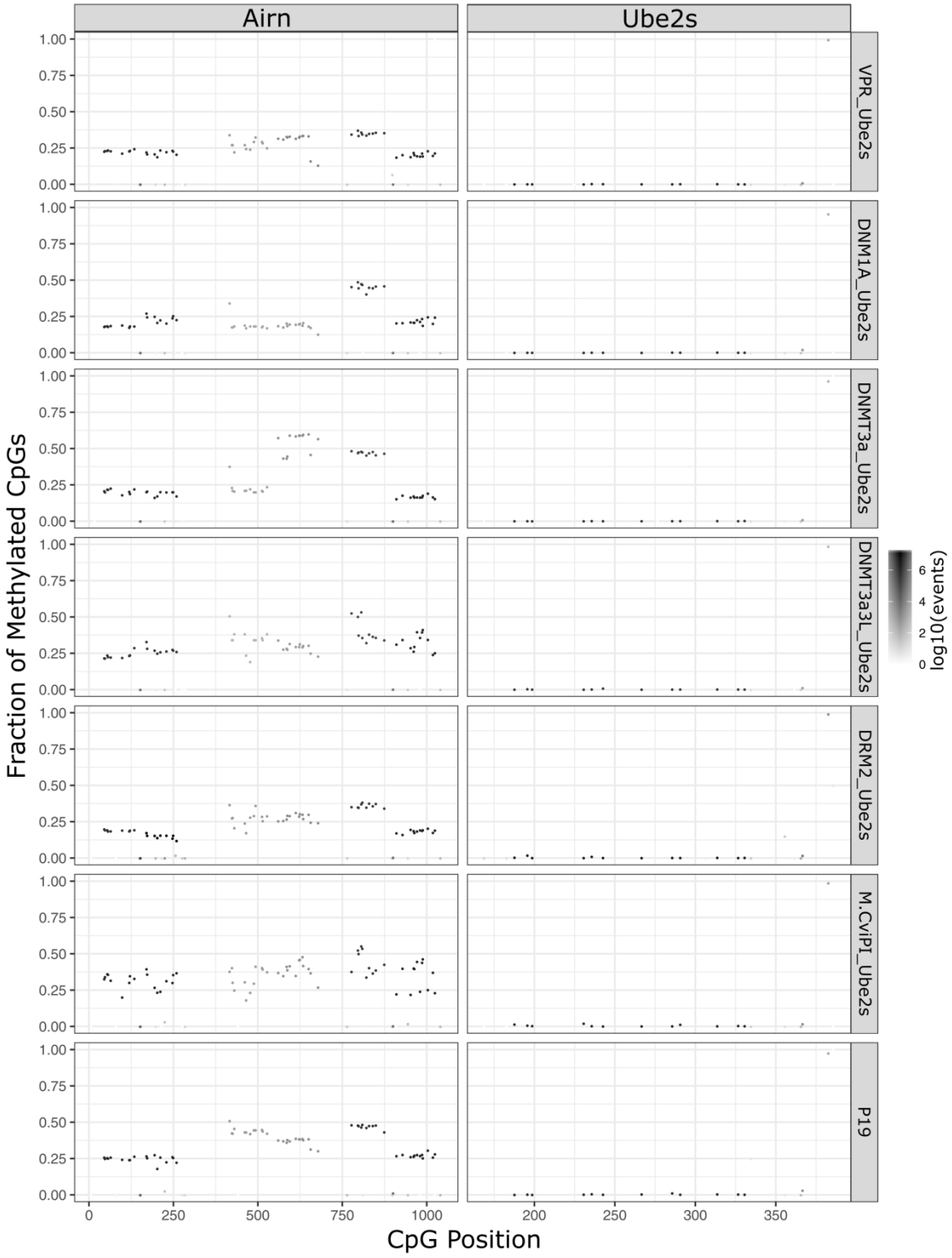

Fig. 17 | Bisulfite sequencing of the AIRN CpG island and *Ube2s* promoter after targeting the AIRN CpG P19 cells were transfected using lipofectamin. They received a mix of dCas9'Effector and a 4x STAgR construct with gRNAs targeting the AIRn promoter. Each dot represents one CpG analysed by sequencing. The darker the dot the more methylation signal. The methyltransferases DNM1A, DNMT3A, DNMT3A3L, DRM2 and M.CVIPI were targeted to the CpG island of the Airn locus. dCas9'VPR was used as a negative control. The promoter region of *Ube2s* was analysed to control for potential unspecific treatment effects. "P19" resembles the baseline. Here non- transfected cells were analyzed.

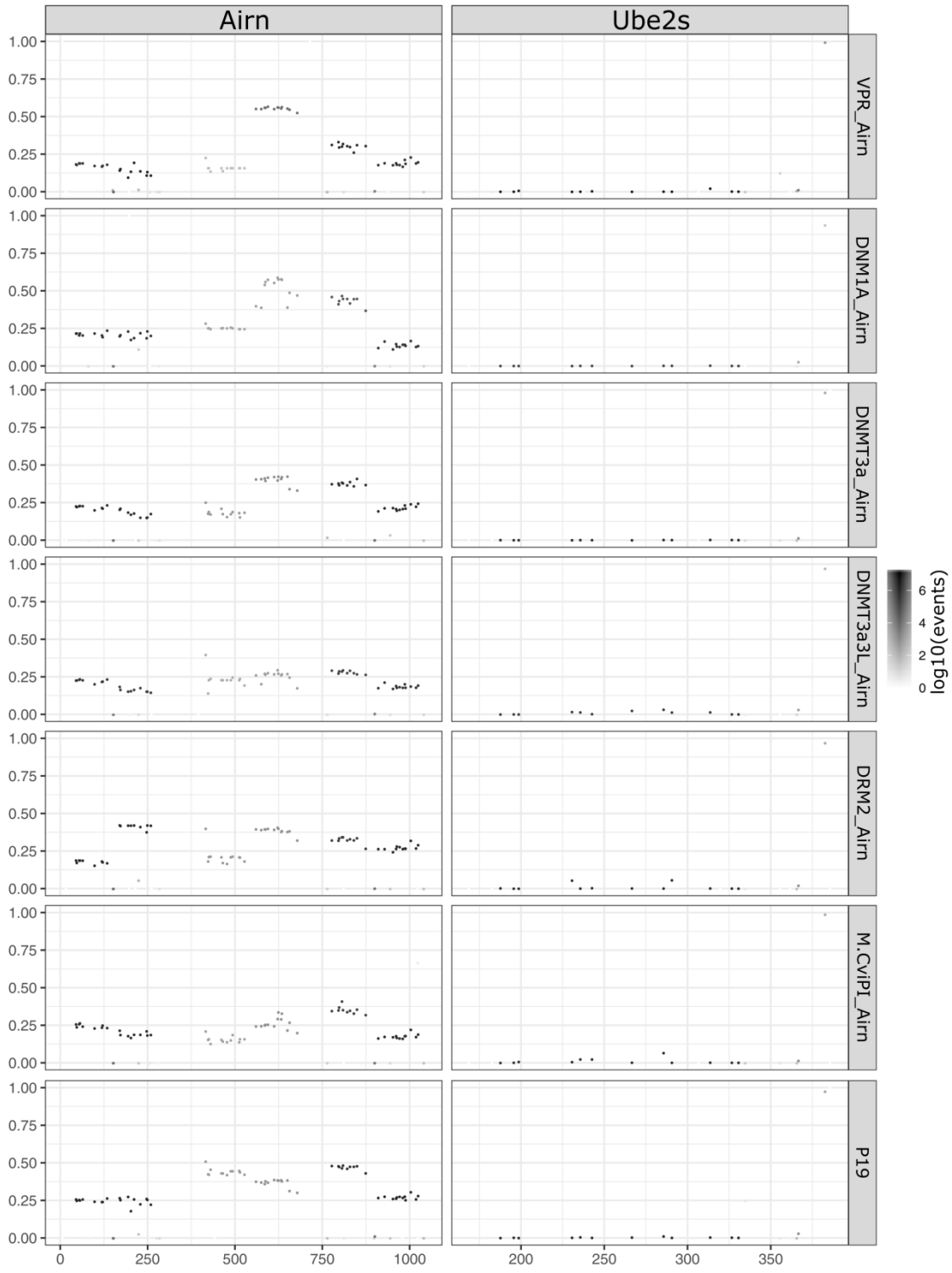

Fig. 18 | Bisulfite sequencing of the AIRN CpG island and *Ube2s* promoter after targeting the *Ube2s* promoter P19 cells were transfected using lipofectamin. They received a mix of dCas9'Effector and a 2x STAgR construct with gRNAs targeting the *Ube2s* promoter. Each dot represents one CpG analysed by sequencing. The darker the dot the more methylation signal. The methyltransferases DNM1A, DNMT3A, DNMT3A3L, DRM2 and M.CVIPI were targeted to the promoter region of the gene *Ube2s*. As a non- active control dCas9'VPR was used.

3. Manipulation of DNA methylation marks associated with Alzheimer ’s disease

Developing tools to be able to manipulate disease associated methylation marks was an overall goal of this PhD project. This should be done to be able to directly link methylation to disease development or progression. The chromatin marks which were planned to be manipulated were reported to be hypermethylated in Alzheimer’s disease. These differentially methylated positions (DMPs) were, amongst others, in close proximity to the Alzheimer’s Disease associated genes *ANK1* and *RHBDF2* (cg05066959, cg11823178, cg05810363, cg23968456, cg03169557) (Fig. 5/19) (De Jager et al. 2014; Lunnon et al. 2014).

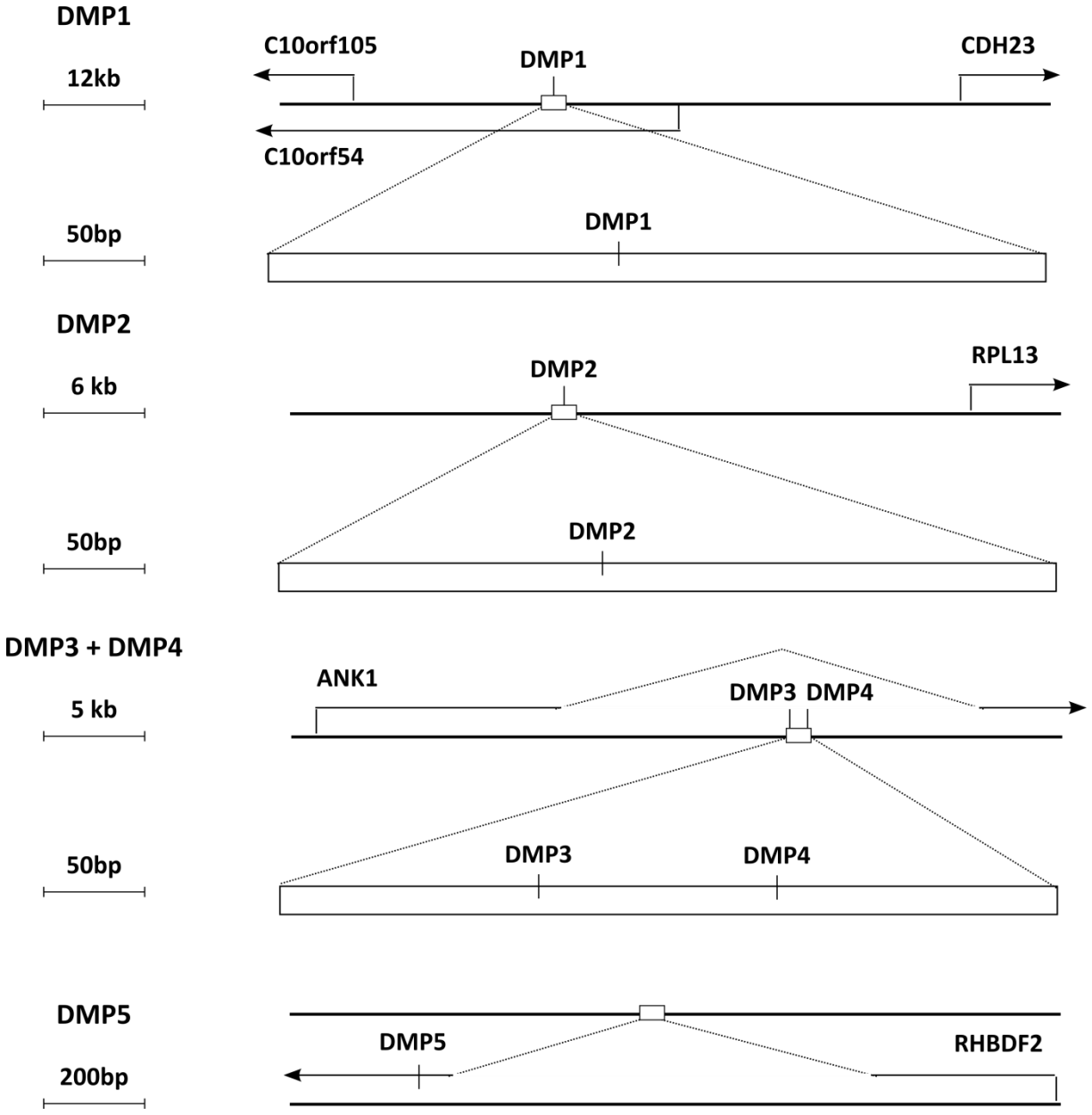

Fig. 19 | Scheme of the different methylated positions found in two independent EWA studies.

The absolute methylation levels of analyzed samples during the conducted EWAS are not apparent from the published data and an access to raw data was not given. Hence, I first set out to determine the baseline methylation status at the loci of interest in the model systems, in which I planned to manipulate them. These were human embryonic neural stem cell lines CB130, CB152 and CB660 and human induced pluripotent stem cells (iPSCs) as well as neurons derived from these cells (Fig. 20A). To gain insight into the methylation status of the loci in an AD-dependent manner, two engineered iPSC lines were analyzed as well. These lines carry heterozygous and homozygous mutations in the amyloid precursor protein (*APP*) and presenilin 1 (*PSEN1*) associated with early-onset Alzheimer's disease (Paquet et al. 2016). Hereafter, cells harboring these mutations are referred to as "P4C4" and "P2B5". They were compared to a non- engineered line (7889SA, hereafter "WT"). DNA was isolated and bisulfite converted. The loci were amplified, libraries prepared and analyzed by next generation sequencing (NGS) (Fig. 20B/C).

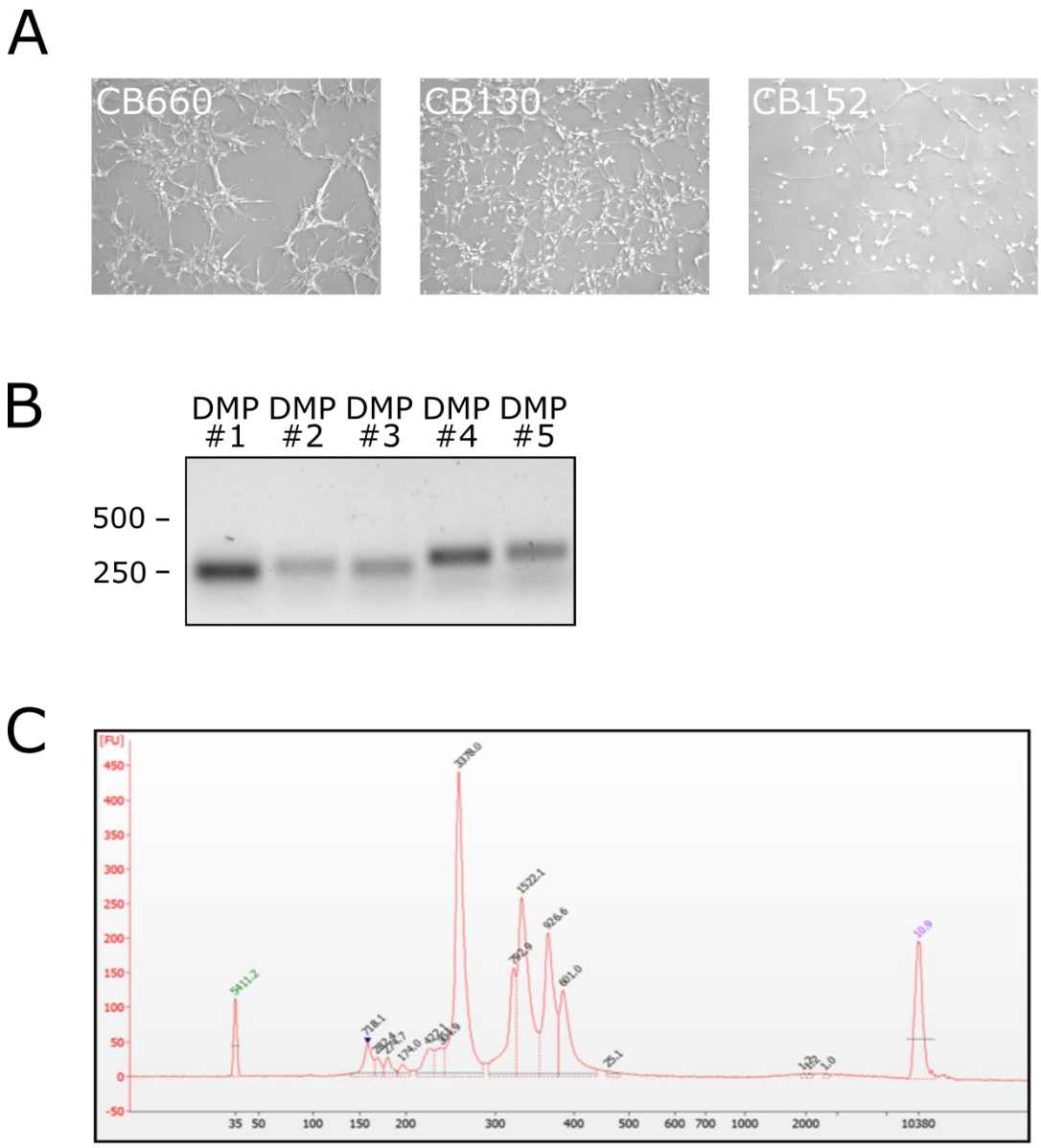

Fig. 20 | Bisulfite sequencing of the 5 DMPs. A Brightfield images of the three human neural stem cell lines on which this study should have been based, CB660, CB130, and CB152. **B** Analytical agarose gel depicting the different loci after bisulfite treatment and site specific PCR. **C** Representative image of a bisulfite sequencing library, analyzed via BioAnalyzer.

Surprisingly iPSCs of all three genetic backgrounds already carry high methylation levels at all the positions analyzed. Nearly all of the sites whose hypermethylation has been associated to Alzheimer's disease progression show methylation rates higher than 90%. Only DMP1 showed methylation rates lower than 90% (83% in WT iPSCs, 79% in P2B5 iPSCs). The different disease associated mutations did not yield any significant differences in methylation levels (Fig. 21A). Next, I tested three different human foetal neural stem cell lines. These stem cell lines conveniently ensure a renewable and scaleable supply of tripotent (astrocytes, oligodendrocytes and neurons) cells which provide a valuable resource for applied

neurobiology (Sun et al. 2008). In total, three different neural progenitor cell lines (CB130, CB152, CB660) were planned to be used and were therefore analyzed on their current methylation status of DMP1 to DMP5. Three out of five DMPs in all neural progenitor lines displayed high methylation states. The methylation levels ranked from 95% (DMP3 CB152) to 99% (DMP2 CP152, DMP4 CB660). Merely DMP1 and DMP5 showed a different picture. At CpG cg05066959 (DMP1) bisulfite sequencing revealed that only around 50 to 60% of analyzed cells of cell lines CB130 and CB660 are fully methylated. Furthermore in the cell line CB152, DMP1 is methylated to 83%. With DMP5 the inconsistency continues; methylation levels varied here from around 50% (CB130 and CB152) to 92% (CB660) (Fig. 21C). This clearly indicates the high variability of methylation rates of the analyzed loci dependent on the genetic background.

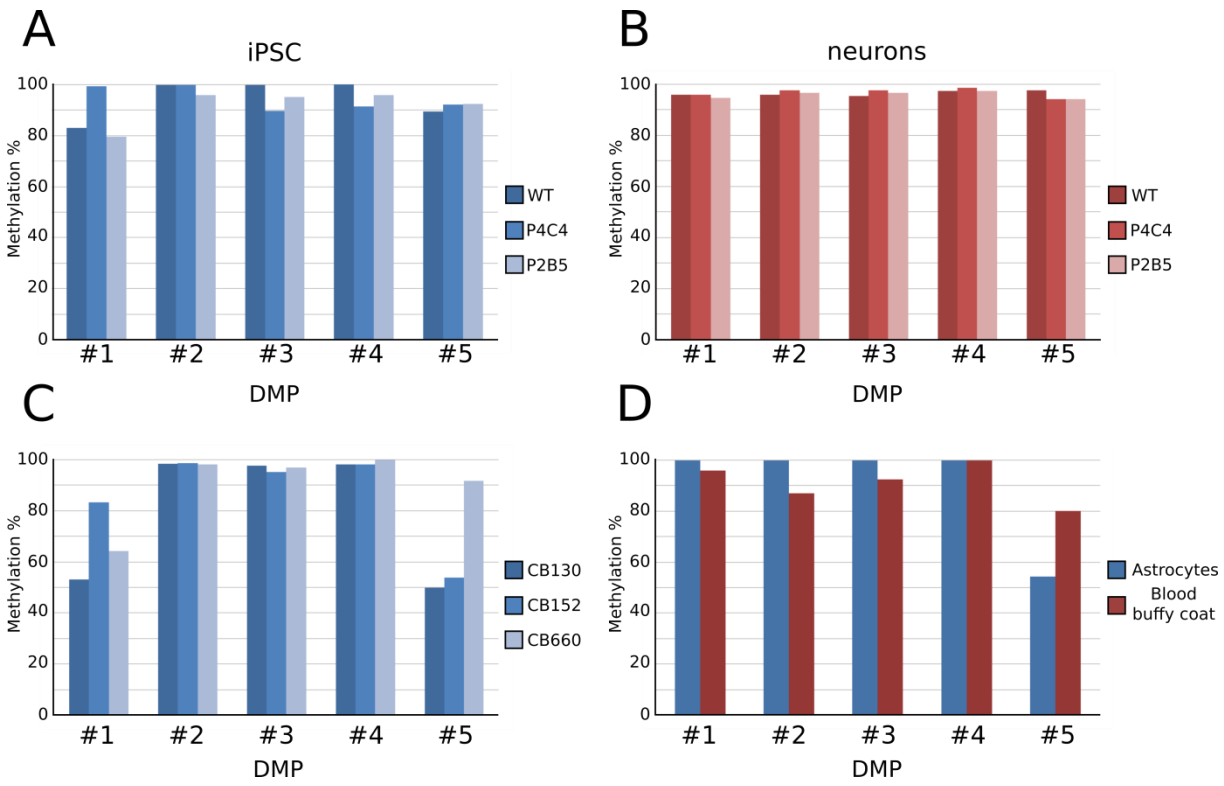

Fig. 21 | Bisulfite sequencing data of different cellular cultures. The analyzed loci DMP1 - 5 refer to cg05066959,cg11823178, cg05810363, cg23968456, cg03169557. **A** Methylation status of different iPSC lines. Strains which were analysed were WT iPSC and two iPSC lines carrying familiar Alzheimer's disease mutations. **B** Methylation status of different neuronal lines. The following strains were analysed: WT neurons and two neuron lines carrying familiar Alzheimer's disease mutations. **C** Methylation status of the three neural stem cell lines shown in Fig20A. **D** Methylation status of astrocytes generated *in vitro* as well as a non-cultured, control cells isolated from the buffy coat of human blood.

To test the disease-affected cellular type, neurons derived from previously described iPSCs were analyzed next. Here, all DMPs analysed showed methylation levels higher than 90% and the different disease mutations did not cause any differences in methylation levels (Fig. 21B). Even though neurons are the affected cell type, other cellular subclasses could be responsible for disease development as well. The EWA studies analyzed methylation rates not as cell type specific as conducted during this thesis. This is why the spectrum of evaluated cell types was extended. From human iPSC derived astrocytes were analyzed for their current methylation status at the different methylated positions. Overall, DMP1 to DMP4 showed elevated methylation levels. Here a striking 99.9% of all analyzed cells harbored fully methylated CpGs at all positions. In astrocytes DMP5 shows reduced methylation levels. This CpG dinucleotide is fully methylated in only 54.5% of the analyzed cellular population (Fig. 21D). Again, individual DMPs were not as highly methylated as in other samples, further indicating large variation between different cellular types. Nonetheless, this shows clearly that not only iPSCs, neurons or the different neural stem cells show high methylation rates at the analyzed loci, but astrocytes as well.

Reportedly, *in vitro* culturing can have severe influence on the global methylation level and can induce aberrant hypermethylation in specific regions over extended proliferation (Meissner et al. 2008). It is additionally debatable if methylation patterns *in vitro* resemble methylation levels in corresponding *in vivo* celltypes (de Boni et al. 2018). To exclude that this holds true for the analyzed positions and the encountered hypermethylation is an artefact of *in vitro* culturing and differentiation, cells from the buffy coat of human blood was analyzed. In these *in vivo* control cells, methylation levels ranged from 80% (DMP5) to 99.8% (DMP4) and overall showed a comparable picture to all other analyzed *in vitro* samples (Fig. 21D). As it still remains unclear whether epigenetic patterns found in *in vitro* differentiated neurons resemble those detectable in native brains neurons, human brain cortex tissue was analysed in the same way as previously described (de Boni et al. 2018). Here white matter tissue was separated from grey matter tissue and analysed individually. Grey matter samples showed methylation levels of 96.6% (DMP1), 77.9% (DMP2), 91.9% (DMP3), 88.9% (DMP4) and 79.8% at DMP5 (Fig. 22A). The white matter sample displayed slightly reduced methylation levels with 97% at DMP1, only 65.7% at DMP2, 83.5% at DMP3, 84.6% at DMP4 and 79.6% at DMP5. Overall the methylation did not differ dramatically from previously analysed tissue (Fig. 22B).

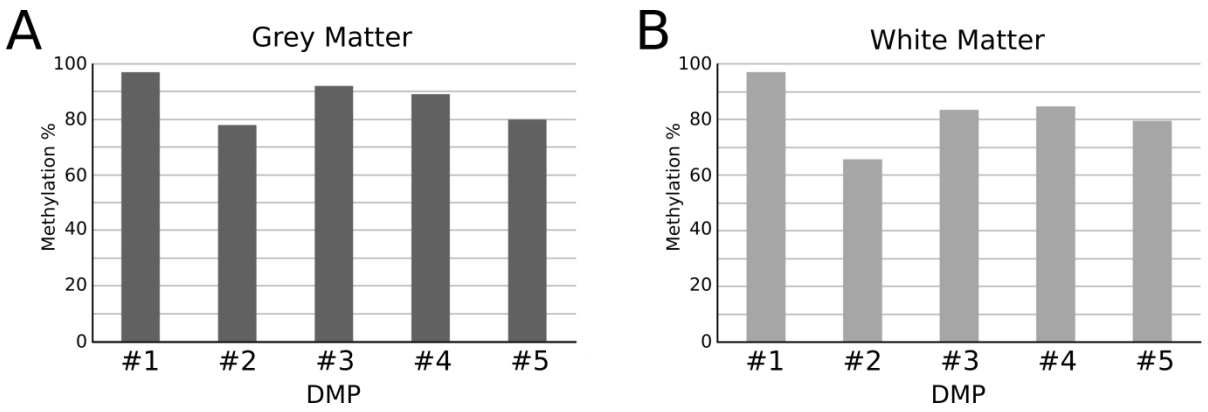

Fig. 22 | Bisulfite Sequencing data of human brain samples. A Methylation status of the 5 DMPs in post mortem human grey matter from cortex samples. **B** Methylation status of the 5 DMPs in post mortem human white matter from cortex samples.

During Bisulfite sequencing and after conversion, the different loci are amplified with strand specific primers. This means that during the classical version of this procedure one actively selects for one strand or the other (Darst et al. 2010). DNA methylation is generally a symmetric chromatin modification which means that the cytosines of a CpG dinucleotide are modified on both strands (L. Zhao et al. 2014). Nonetheless, this pattern is temporarily disrupted during DNA replication, when the newly synthesized and unmethylated daughter-strand forms a asymmetrically methylated CpG dyad called hemimethylated DNA (Sharif and Koseki 2018). This state was thought to not exist permanently, as either the still methylated strand was thought to be demethylated or vice versa, the non- methylated strand to be modified. But apparently this did not hold true, as about 10% of all CpGs in embryonic stem cells seem to be hemi-methylated permanently (L. Zhao et al. 2014). To confirm previously obtained data and to rule out possible hemi-methylation, the bottom strand of the five DMPs was analysed as well.

Figure 23 shows the differences of methylation levels in percent of top and bottom strand. Here, four different examples are shown as representatives for the different analyzed cell- and tissue types. In P4C4 iPSCs, P2B5 neurons, human blood buffy coat and human white matter, none of the differences between the two strands are higher than 15%. Both analyzed strands show some variation, but nonetheless both sides of each CpG are equally hypermethylated, confirming the previously obtained datasets (Fig. 24).

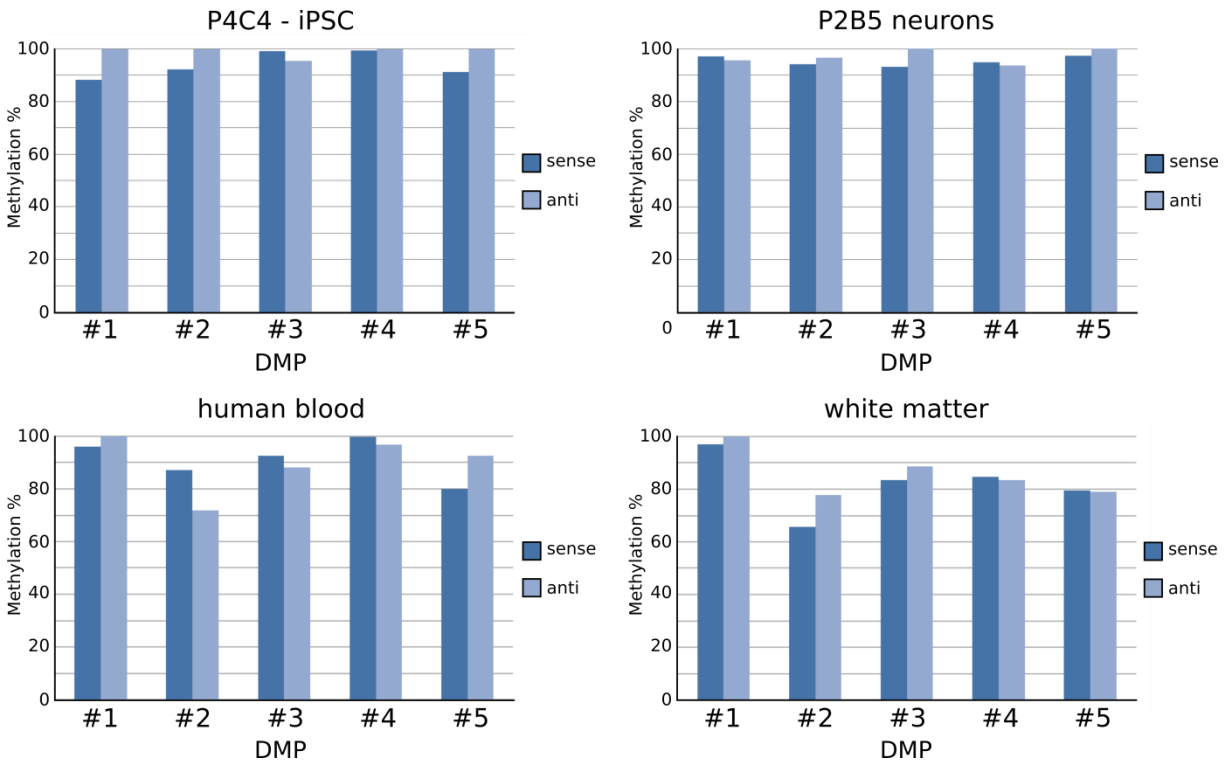

Fig. 23 | Bisulfite sequencing data of the antisense sequences of the five DMPs from previously analysed samples. Exemplarily for all samples P4C4 iPSCs, P2B5 neurons, blood and white matter are shown.

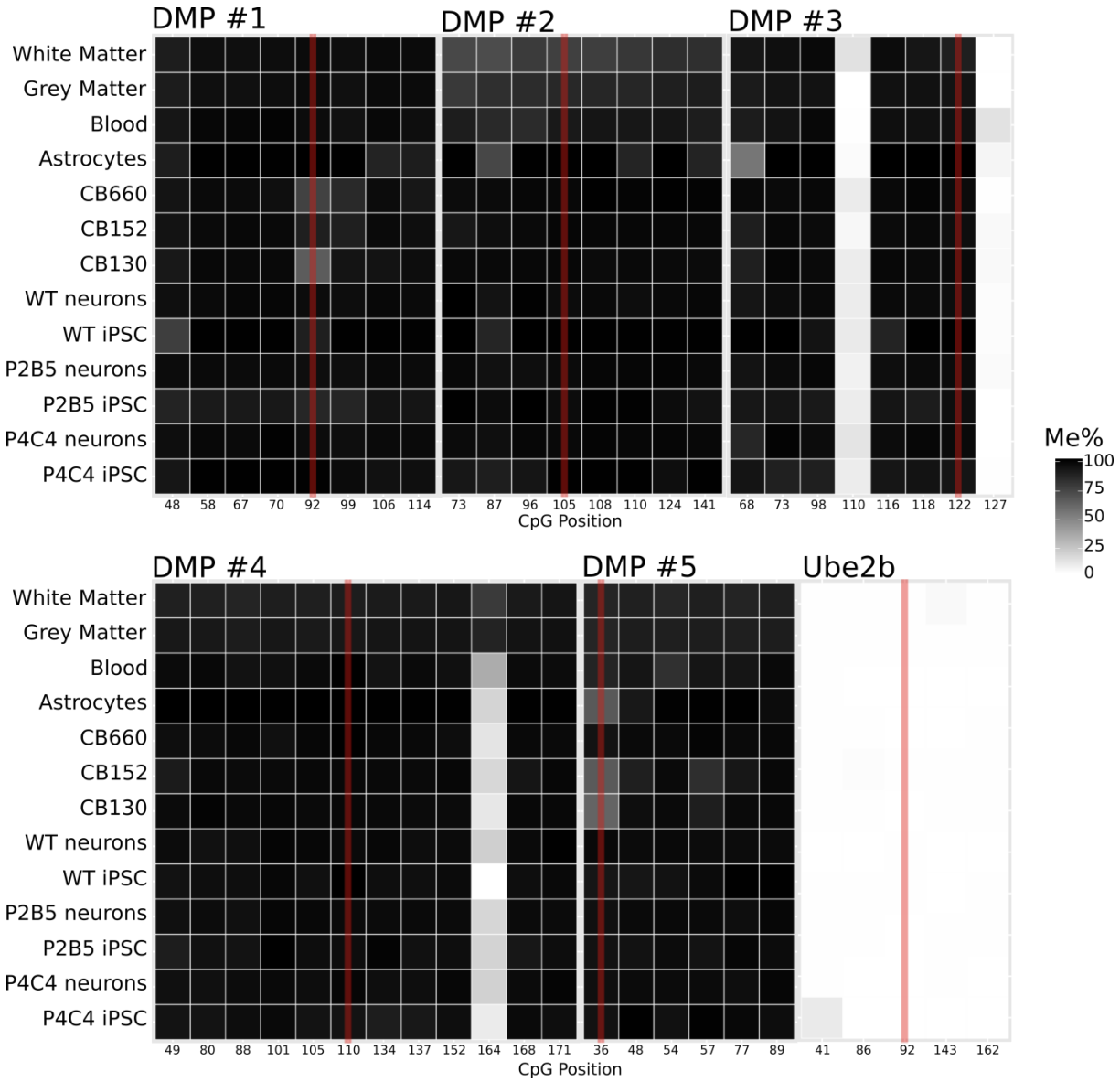

Fig. 24 | Visual summary of bisulfite sequencing data of sense loci. The darker the squares the higher methylated are the different positions. Numbers indicate the CpG dinucleotides in the analysed sequences. The red line marks the CpG islands which were previously found to be methylated in Alzheimer's disease. The locus of Ube2b was analysed to exclude errors during bisulfite conversion.

4. Transcriptional engineering of layer specific subtype defining transcription factors to achieve neuronal reprogramming

Transcriptional engineering, the manipulation of endogenous gene copies with dCas9 activators holds a tremendous potential for certain questions in biology. Reprogrammed neurons often display a lack of maturity. This means that cells can be transformed into this desired cell type, the newly generated neurons though show for example expression of deep layer markers, even if located in the upper layers of the brain (Gascón et al. 2016). I reasoned that targeting and activation of multiple factors at once, even if individual factors only play a minor role, could help to orchestrate cells during the transformation process to a subtype specific state. With the establishment of the STAgR technique, I developed a solid basis for extending the transcriptional engineering tools towards these applications.

4.1 Candidates for callosal projection neurons

All gRNAs were chosen making use of the UCSC genome browser track "CRISPR10K". This track combines various algorithms to assign a quality score for every single gRNA. The score predicts potential off target effects and binding efficiency (Bae et al. 2014; Doench et al. 2014; Doench et al. 2016; Haeussler et al. 2016; Moreno-Mateos et al. 2015). Since published data indicates that two gRNAs targeting a promoter region are improving for solid gene activation (Chavez et al. 2015; Cheng et al. 2013; Maeder et al. 2013), I designed two gRNAs for each gene. Since it has been reported that gRNAs should bind in close proximity to the gene's transcriptional start site, one in the first 100bp upstream and the second within 300bp (but at least 100bp apart from each other) (Wang, La Russa, and Qi 2016), I followed these principles of gRNA design (Fig. 25).

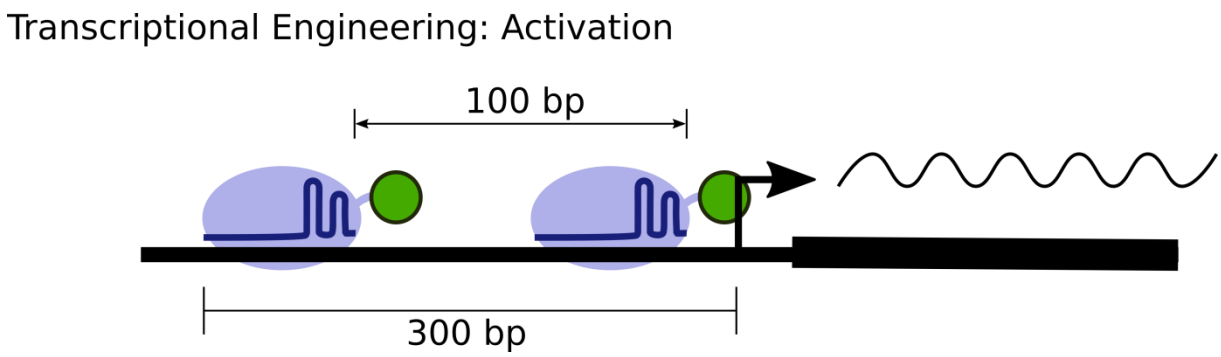

Fig. 25 | Scheme of transcriptional engineering setup. To successfully induce the transcription of a target gene with dCas9 based tools one needs to target a locus with two different gRNAs. These gRNAs should target within 300bp and should be located at least 100bp apart from each other.

The candidates, which have been chosen as potential callosal projection neuron reprogramming factors were *Satb2, Cux2, Cux1, Mef2c, Tle2, Lhx2, Bhlhb5, Brn2* and *Nurr1*. It has been tested if dCas9 based transactivators can upregulate mRNA levels when targeted in different cell lines (Fig. 26- 30). Firstly, two different genes have been in the focus, *Satb2* and *Cux2*. *Satb2* is located on murine chromosome 1 and has three annotated isoforms with different transcriptional starting sites which are all around 500 bp apart (Fig. 26A). For *Satb2,* two sets of two gRNAs each were designed, targeting different isoforms. The gRNAs S1 and S2 targeted the isoform starting at Chr1:56,793,986 (Gencode Transcript: ENSMUST00000114415.9), whereas gRNAs S3 and S4 targeted the variant with gencode transcript: ENSMUST00000042857.13. For both sets, single gRNA plasmids carrying a tdTomato fluorescence reporter were generated and transfected alongside a plasmid carrying a dCas9'VP64 fusion protein and a fluorescence reporter into P19 cells. After five days, double positive cells were isolated via FACS, whole RNA was isolated and *Satb2* levels analyzed by qPCR. Compared to a non-targeting control, in combination with dCas9`VP64, gRNA S1 and gRNA S2 could raise the mRNA level of *Satb2* 6-fold. When guided by gRNA S3 and S4, mRNA levels were increased around 9.2 times, indicating that the latter gRNAs are more potent. A combination of all four gRNAs did not raise the mRNA levels of *Satb2* any further. The second gene targeted was *Cux2* (Cut- like homebox 2). I tested sets for two different transcriptional start sites of *Cux2* containing three gRNAs each. The gRNAs C2.1, C2.2 and C2.3 targeted the annotated starting site of transcript variant 2 (Gencode Transcript: ENSMUST00000111752.9) whereas gRNAs C2.4, C2.5 and C2.6 targeted transcript variant 1 (Gencode Transcript: ENSMUST00000086317.11) (Fig. 26B). When applied alongside dCas9'VP64, neither gRNA set 1 nor gRNA set 2 were able to increase mRNA levels of *Cux2* to more than 2.5 fold.

As the CRISPR field is rapidly evolving, novel tools are generated constantly. Building on dCas9'VP64, Chavez et al. created a hybrid fusion protein existing of classical VP64, p65, a subunit of transcription factor NF- κB and Rta, a transcription factor of Epstein- Barr virus (Chavez et al. 2015). This novel transcriptional activator termed VPR was shown to be significantly more potent when fused to dCas9 and targeted to an engineered fluorescence reporter (Chavez et al. 2015). To test this advanced tool, P19 cells were transfected with a construct providing an overexpression of dCas9'VPR alongside the gRNAs which were found to be most potent with dCas9'VP64 in activating transcription of *Satb2* and *Cux2*. This time gRNAs were also applied individually to test for the minimum requirements to induce mRNA levels of both factors significantly. As seen in Figure 27, the application of VPR enhanced the

induction of *Satb2* mRNA levels in comparison to VP64 roughly 5- fold, to an overall fold increase of 50- times over a non- targeting control. This confirmed VPR to be a more potent transcriptional activator. Furthermore, it was apparent that the combination of gRNAs S3 and S4 showed a synergistic effect, as single applications did not add up to the same mRNA levels of Satb2. For *Cux2* however, single gRNAs as well as the set of gRNA C2.1 to C2.3 did not increase the mRNA levels to more than 2- fold, showing no further improvement by the use of dCas9'VPR. As there is one additional transcriptional starting site annotated for *Cux2*, another set of three gRNAs was designed and tested (Gencode Transcript: ENSMUST00000168288.8). However, these gRNAs did not activate *Cux2* transcription either (data not shown) suggesting that other limitations or barriers to transcriptional engineering could interfere with a successful induction, as we have experienced before (Baumann et al. 2019).

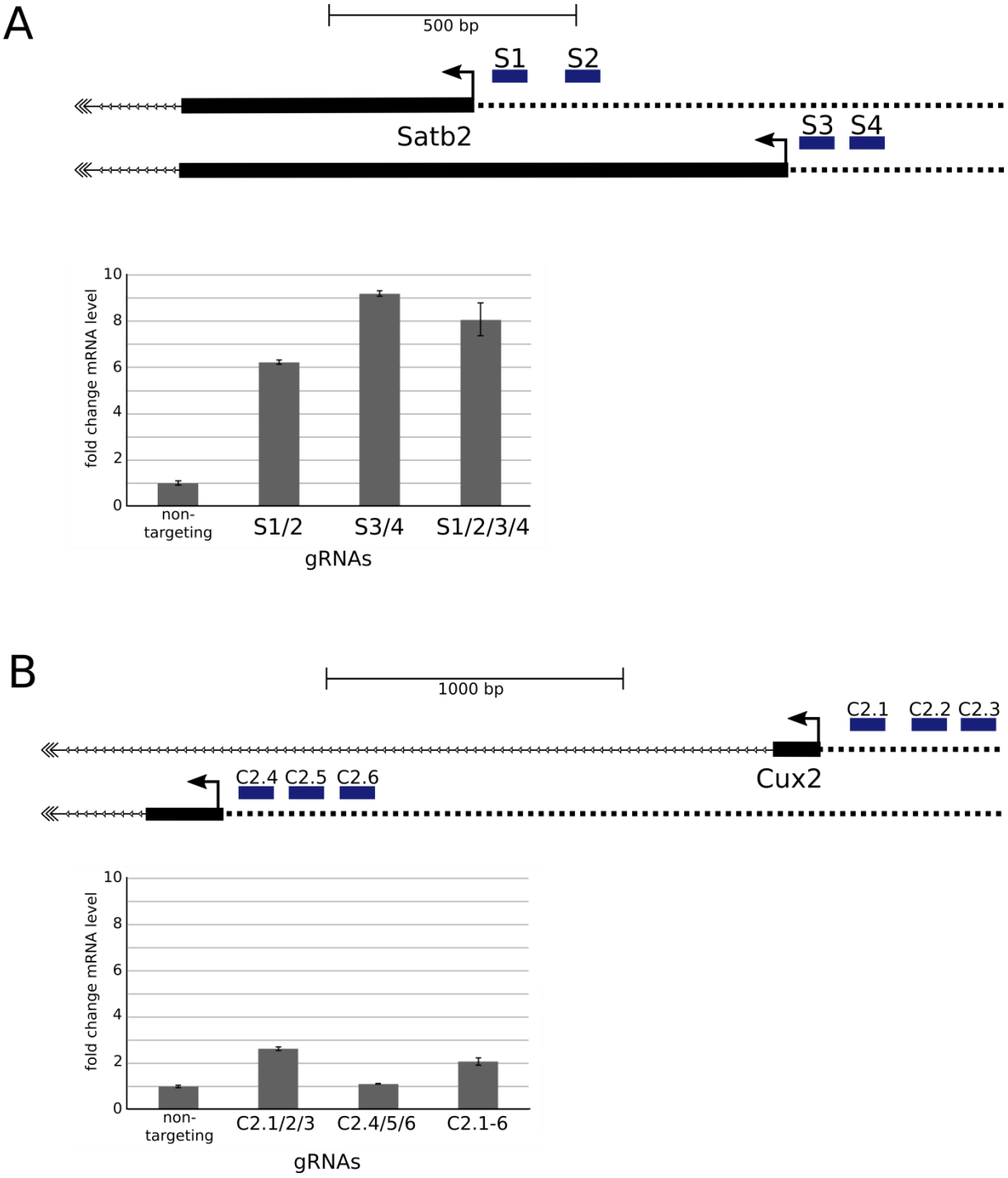

Fig. 26 | Schemes of gRNA binding at Satb2 and Cux2 loci as well as induction by dCas9'VP64. **A** Four gRNAs have been designed for two different annotated transcriptional starting sites for *Satb2*. P19 cells were transfected with transcriptional activator dCas9'VP64 and the different sets of gRNAs. The graph depicts the mRNA levels of *Satb2* analysed via qPCR. **B** Six gRNAs have been designed for two different annotated transcriptional starting sites for *Cux2*. P19 cells were transfected with transcriptional activator dCas9'VP64 and the different sets of gRNAs. The graph depicts the mRNA levels of *Cux2* analysed via qPCR.

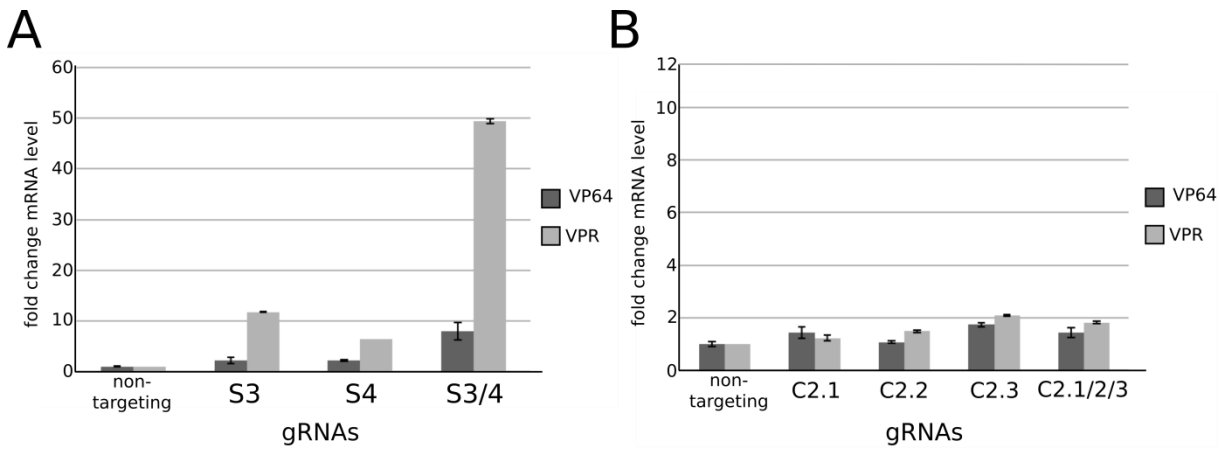

Fig. 27 | Comparison of dCas9'VP64 and dCas9'VPR. The different gRNAs were supplied to two different transcriptional activators. **A** P19 cells were transfected with dCas9'VP64 or dCas9'VPR and the different gRNA combinations. mRNA levels were analysed by qPCR. **B** Comparison between VP64 and VPR by targeting the *Cux2* locus with three different gRNAs.

To test targeted gene activation for a larger set of subtype specific transcription factors I designed a pair of gRNAs for *Mef2c*, *Cux1*, *Tle2*, *Lhx2*, *Bhlhb5*, *Brn2*, and *Nurr1* targeting an annotated transcriptional start site (Fig. 28A). Similar to *Satb2*, *Bhlhb5* (Gencode Transcript: ENSMUST00000026120.7), *Lhx2* (Gencode Transcript: ENSMUST00000143783.8), *Brn2* (Gencode Transcript: ENSMUST00000178174.2) and *Nurr1* (Gencode Transcript: ENSMUST00000028166.8) mRNA levels could be elevated when targeted with dCas9'VPR in P19 cells (Fig. 29/30A). However, as seen for *Cux2*, transcription of *Cux1* (Gencode Transcript: ENSMUST00000004097.15), *Tle2* (Gencode Transcript: ENSMUST00000146358.7) and *Mef2c* (Gencode Transcript: ENSMUST00000005722.13) were only minorly or not induced by CRISPR transactivators (Fig. 29A).

To test whether the transcriptional activation is dependent on the cellular system, I targeted these factors in two additional cellular models, postnatally isolated *ex vivo* astrocyte cultures and isolated mouse embryonic fibroblasts (MEF) (Fig. 28B). Similar as in P19 cells, transcriptional levels of *Bhlhb5*, *Tle2* and *Satb2* were increased in astrocytes and fibroblasts, although to slightly varying degree (Fig. 29B/C). Transcriptional induction of *Lhx2*, *Brn2*, *Nurr1* and *Cux1* varied in the different cellular models used (Fig. 29A/B/C). However, mRNA levels of *Mef2c* as well as *Cux2* were not increased by dCas9'VPR in astrocytes nor in fibroblasts (Fig. 29B/C).

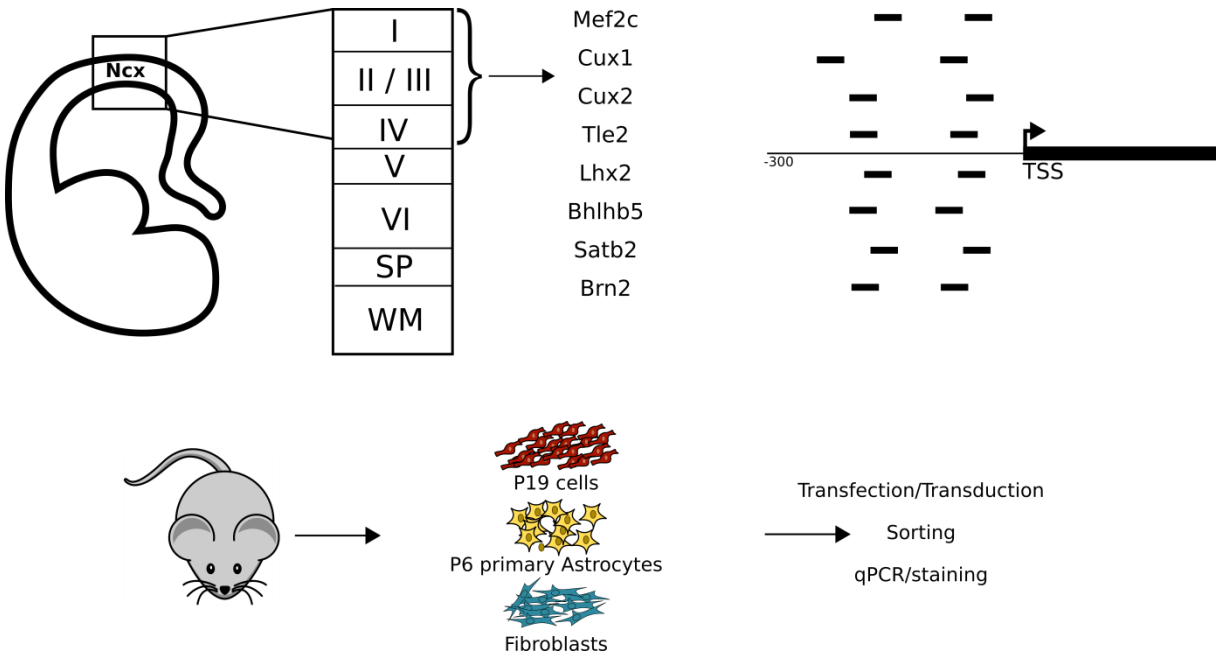

Fig. 28 | Overview of factors chosen as candidates for callosal projection neuron reprogramming. **A** All derived factors were shown to influence the development of the upper cortex layers. Black bars indicate the positions relative to the transcription start sites of the genes. **B** Scheme of the different in vitro models which were used and experimental paradigm of transcriptional activation.

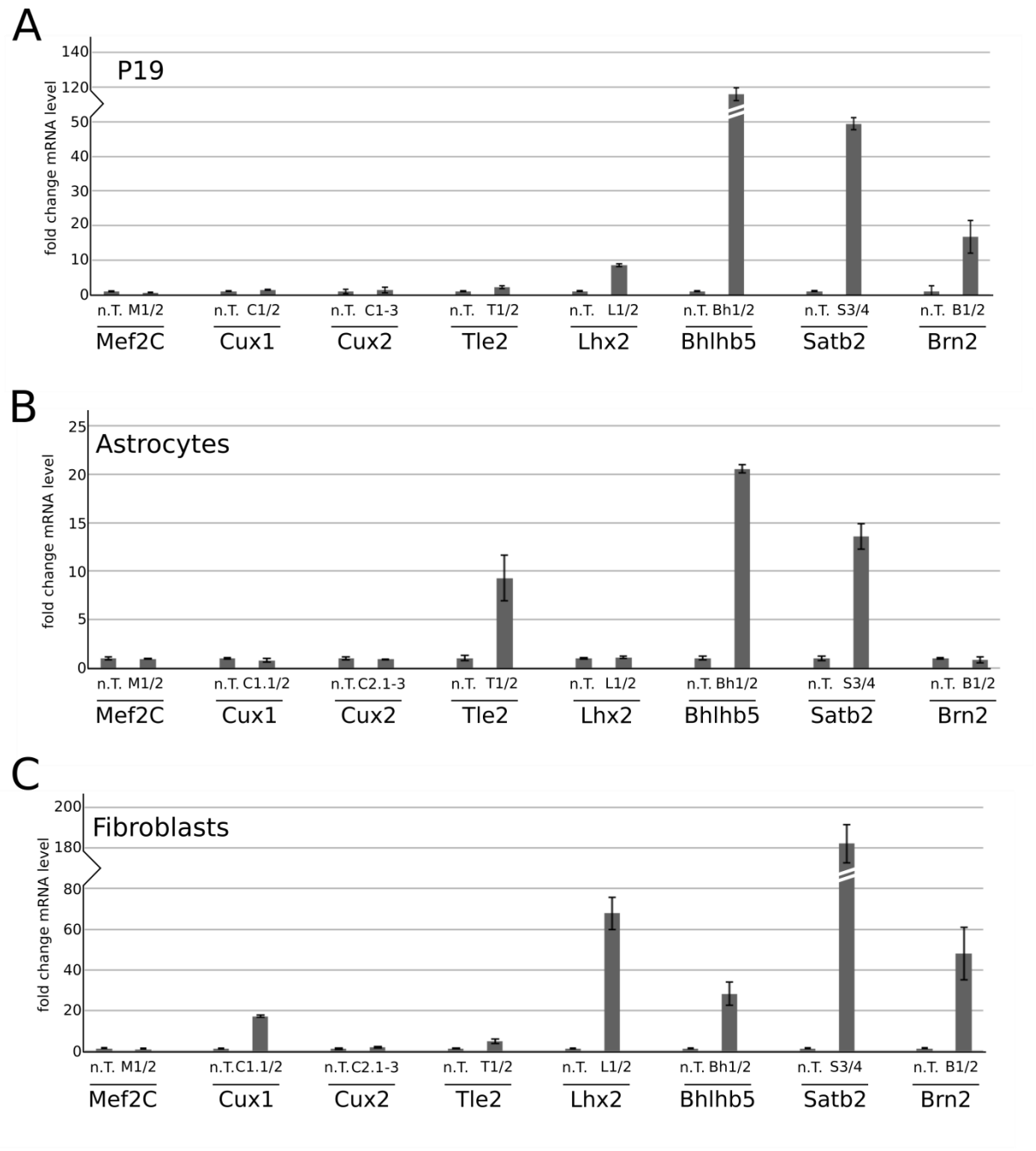

Fig. 29 | Transcriptional manipulation of potential callosal projection neuronal reprogramming factors. A Activation of *Mef2C, Cux1, Cux2, Tle2, Lhx2, Bhlhb5, Satb2* and *Brn2* in P19 cells using sets of two different gRNAs each. **B** Activation of *Mef2C, Cux1, Cux2, Tle2, Lhx2, Bhlhb5, Satb2* and *Brn2* in primary astrocyte cultures using sets of two different gRNAs each. **C** Activation of *Mef2C, Cux1, Cux2, Tle2, Lhx2, Bhlhb5, Satb2,* and *Brn2* in fibroblasts using sets of two different gRNAs each.

Since, *Mef2c* and *Cux2* could not be activated significantly and *Lhx2*, *Cux1,* and *Brn2* did not respond to transactivation in astrocytes, I tested whether this unresponsiveness is caused by targeting the wrong annotated transcription start site or wrong gRNA position. For this, alternative gRNA sets were designed, generated, and applied. Targeting with alternative gRNAs or targeting different transcription start sites improved mRNA induction for some of the factors, other levels could not be raised this way (Fig. 30A/B/C). For *Brn2*, three more gRNAs were tested in different combinations. With gRNA set B3/B5, *Brn2* transcription could be raised higher than with previous sets in astrocytes (Fig. 30B). For *Lhx2* ("ENSMUST00000000253.5") and *Mef2c* ("ENSMUST00000197146.4" and "ENSMUST00000185052.5"), two alternative gRNA sets were applied. Out of two gRNA pairs each, one increased mRNA levels, compared to previously targeted transcripts (Fig. 30B). For *Cux1* ("ENSMUST00000176216.8") no gRNA set was found which raised levels over basal expression in astrocytes (Fig. 30A). To test whether transcriptional activation with these alternative gRNAs is variable in different cellular systems, they were applied in P19s and in fibroblasts. Consistent with previous data, mRNA induction in both cellular systems was overall higher, but transcription of similar factors was induced (Fig. 30A/C).

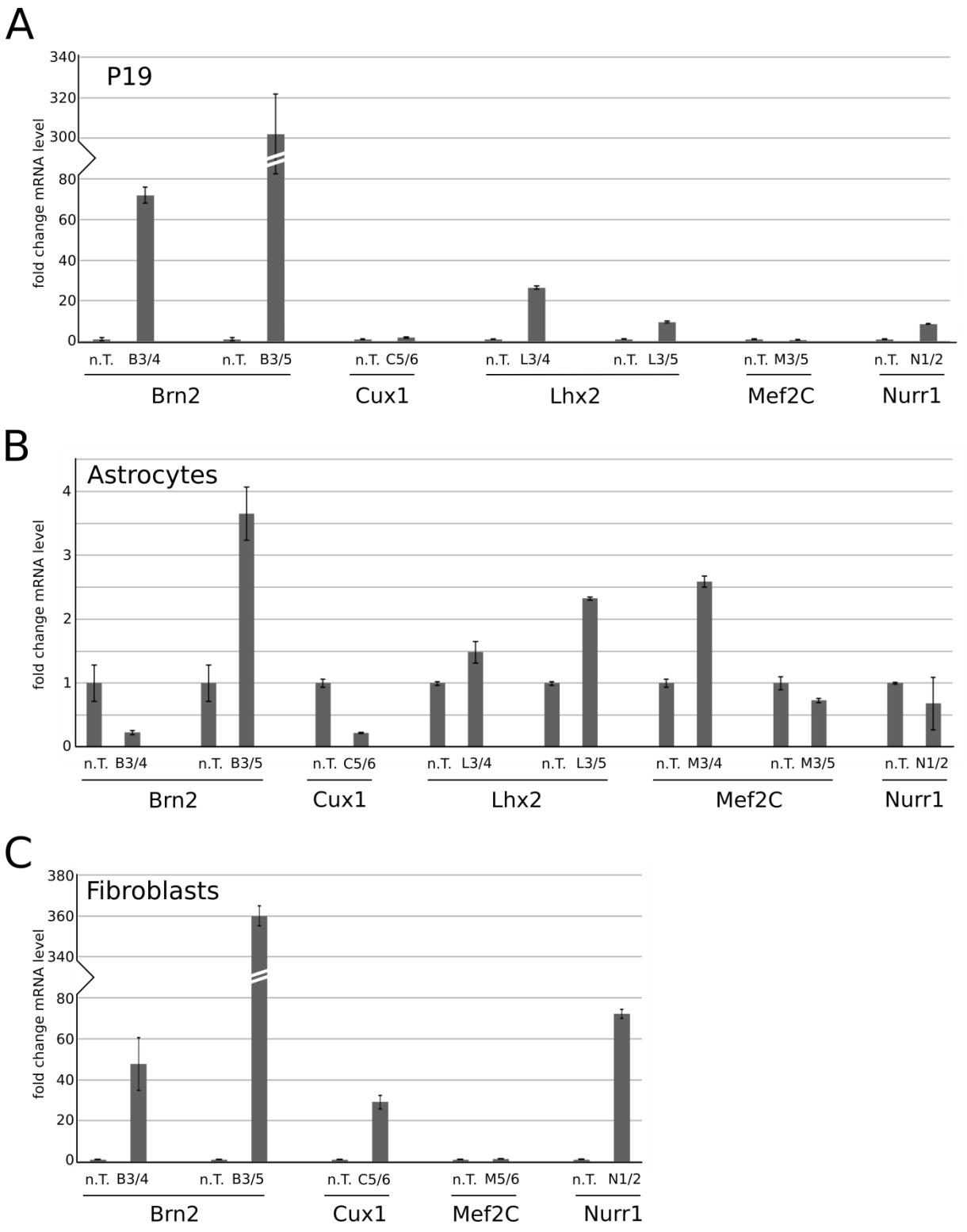

Fig. 30 | Transcriptional manipulation with alternative gRNA sets of potential callosal projection neuronal reprogramming factors. Targeting with alternative gRNA sets of the factors which did not show a distinct activation in the first round. **A** in P19 cells **B** in astrocytes and **C** in fibroblasts.

4.2 Generation of an 8x STAgR and simultaneous activation

Since in the previous experiments, *Satb2*, *Bhlhb5*, *Lhx2*, and *Tle2* have been successfully induced by Cas9- based transactivation in astrocytes, I combined the most potent gRNA pairs onto two 4x STAgR plasmids. The gRNAs targeting the *Satb2* promoter region (gRNAs S3 and S4) were combined with the set for *Bhlhb5*, as well as *Lhx2* targeting gRNAs L3 and L5 with the pair for Tle2 (T2 and T3). All of these gRNAs were generated featuring the SAM gRNA scaffold to be compatible with all available dCas9 as well as MS2 based transcriptional activators. These 4xSTAgR expression cassettes were combined to an 8x gRNA expression vector (Fig. 31). To test whether simultaneous delivery and expression of eight gRNAs expression cassettes affect transcription activation, these constructs were tested alongside a plasmid coding for dCas9'VPR featuring a tdTomato reporter in primary astrocytes and fibroblasts. However, the qPCR analysis shown in Figure 31 indicates that the simultaneous activation had little adverse effect on the transcriptional level of the individual factors in astrocytes. All factors can be induced to comparable levels as when the gRNAs are supplied individually. In fibroblasts, transcription of all factors was induced but for two out of four factors, namely *Satb2* and *Bhlhb5*, this induction was overall lower compared to the individual gene targeting. This overall indicated that multiplexed gRNA plasmids can be used to induce expression of multiple transcription factors simultaneously.

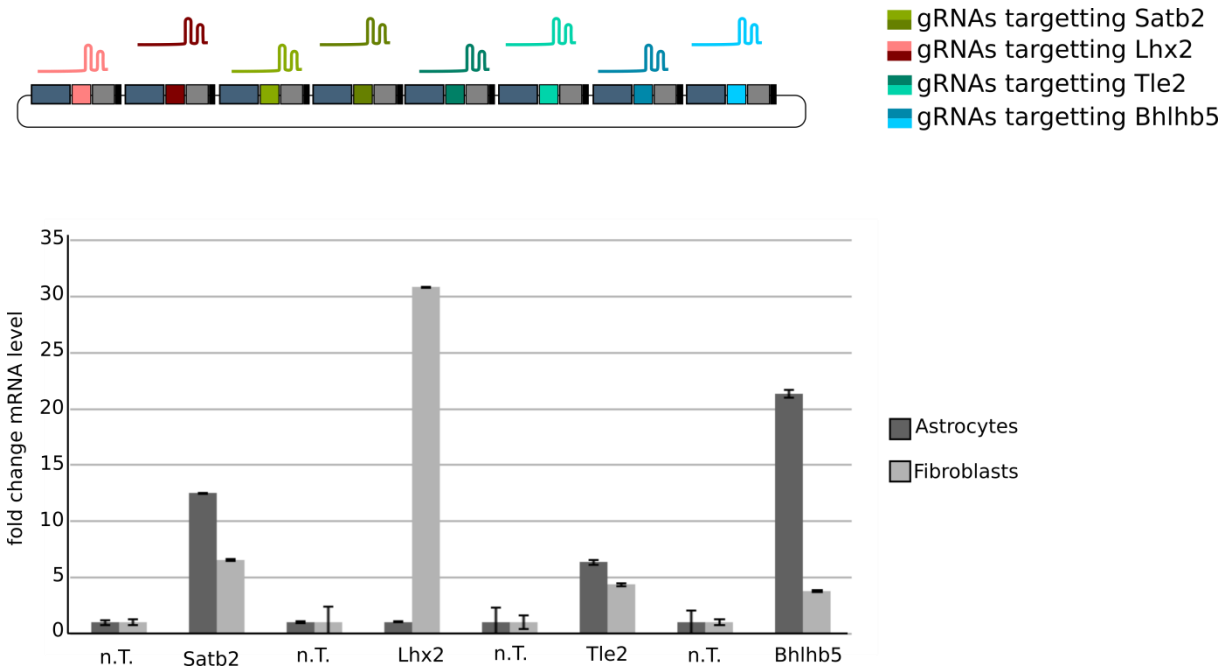

Fig. 31 | Generation of 8xSTAgR with potential callosal projection neuron reprogramming factor targeting gRNAs. dCas9'VPR was supplied with 8xSTAgR in Astrocytes and Fibroblasts and mRNA levels have been depicted via qPCR.

4.3 Development of a gRNA dependent reporter system

To create a system, which provides the possibility to identify cells, which received both, gRNAs as well as dCas9 transactivators, I generated a reporter construct, regulated by the CRISPR transactivator itself. It is based on a minimal CMV promoter, which on its own is not strong enough to drive the fluorescence reporter, but does so, if it is targeted with the transactivator. To implement this strategy I included upstream of this promoter the targeting sequence of a used gRNA (e.g. *Satb2* targeting gRNA S3). When this gRNA is expressed, it binds not only to the endogenous *Satb2* promoter but will also bind the promoter region of the fluorophore reporter, subsequently inducing its transcription (Fig. 32A). I tested this *functional activator reporter* (FAR) system in P19 cells as well as in astrocytes. A plasmid coding for dCas9'VPR and a tdTomato fluorescence protein was transfected alongside the GFP functional activation reporter plasmid to monitor for activator expression. If no gRNA is supplied, GFP expression is not detectable by flow cytometry or microscopy (Fig. 32B/C). This changes if gRNA S3 is provided to guide dCas9'VPR to the promoter region of the reporter plasmids. When analyzed by flow cytometry, 35% of all cells show bright fluorescence (Fig. 32B). This induction was also detectable by fluorescence microscopy (Fig. 32C). Utilization of this system does not only directly show which cell obtained the full system (even if subdivided into different vectors or viral particles), it also frees fluorescence channels for potential marker analysis by immunohistochemistry.

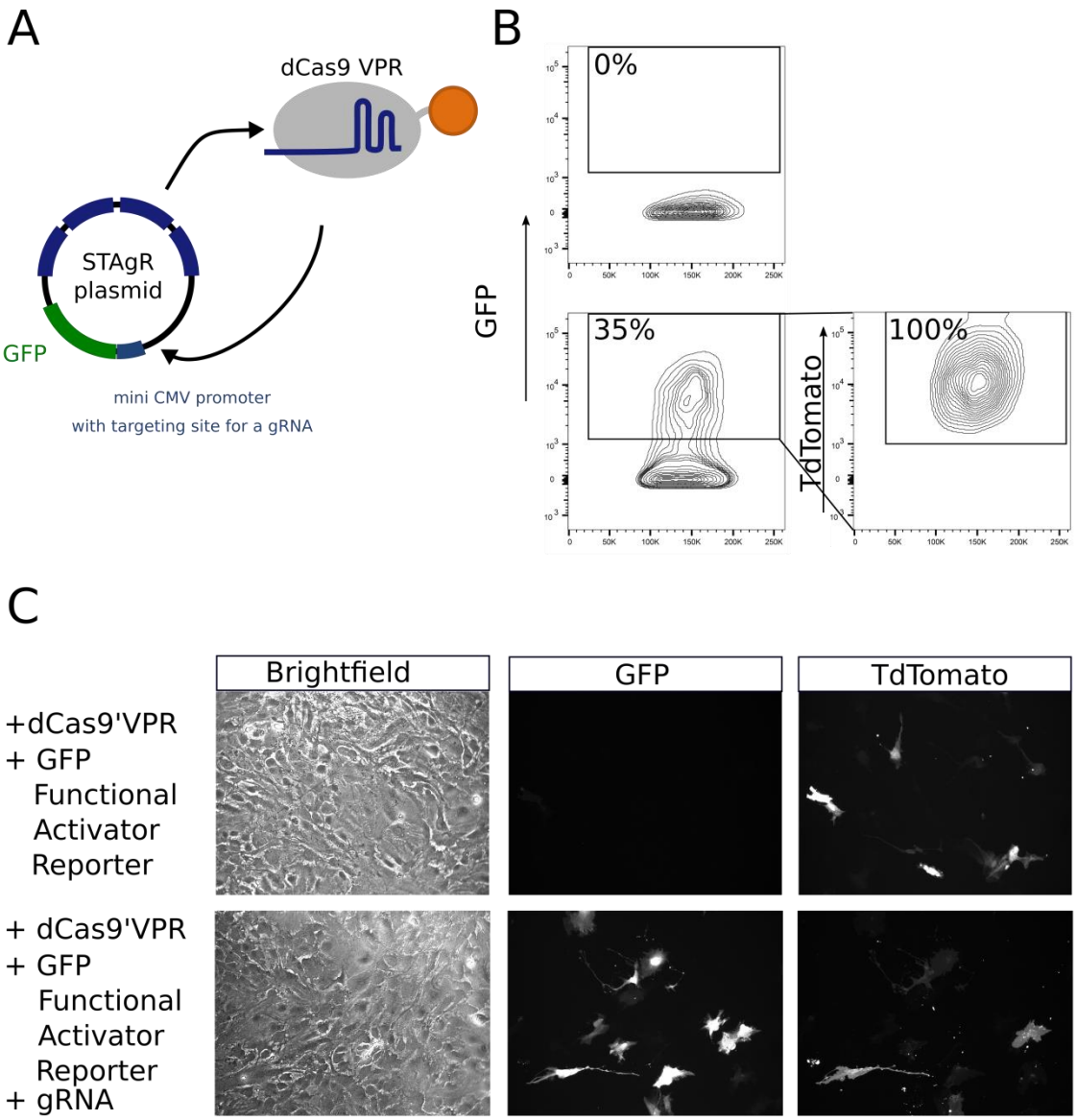

Fig. 32 | Establishment of a Functional Activator Reporter. **A** Concept of the established Functional Activator Reporter. A gRNA will not only bind the endogenous promoter of a gene of interest but also the minimal CMV promoter region upstream of a fluorescence gene. Transcriptional activators will then induce its expression, highlighting the cells which got all parts of the system simultaneously. **B** Cells that only obtained the transcriptional activator and the reporter did not show any green fluorescence when analysed by flow cytometry (upper square). When dCas9'VPR was supplied with a gRNA targeting the reporter, 35% of all cells showed green fluorescence out of which 100% were dCas9 positive. **C** Imaging of a living astrocyte culture which obtained either no gRNA but dCas9'VPR (TdTomato) and the reporter plasmid (GFP) or the whole system and a targeting gRNA.

4.4 Adaption of the functional activator reporter to lentiviral delivery

To test whether the designed and established experimental strategy based on the *FAR* reporter is suitable for viral delivery, I chose an alternative dCas9 activator toolset. As conventional dCas9'VPR fusion constructs exceed the packaging limit of a lentiviral particle, I chose a toolset which is based on the interaction of a repeating peptide array with an antibody- fusion protein, termed dCas9'SunTag (Fig. 33A) (Tanenbaum et al. 2014). This made it possible to separate the artificial transcription factor fusion GCN'p65'HSF1 with its shuttle and anchor dCas9'SunTag to be able to stay well under the maximum packaging limit of a lentivirus particle. The GCN antibody coupled artificial transcription factors were combined with the 8xSTAgR construct like depicted in Figure 33B. Surprisingly when the 8x STAgR construct was packed with the additional GCN cassette, the *FAR* was expressed even without the trans-activator itself, losing its actual purpose (Fig. 33C). Without the GCN cassette however, the 8xSTAgR construct carrying the functional activity reporter only showed GFP expression when combined with a dCas9'VPR over expression. To test whether this leakiness can be prevented, the position of the GFP functional activator reporter's expression cassette was changed to generate different cassette orders (Fig. 33B). However changing the GFP functional activator reporter's position or orientation on the plasmid did not improve its leakiness. This indicates that combining the FAR with dCas9'SunTag based transactivators introduces unreliability.

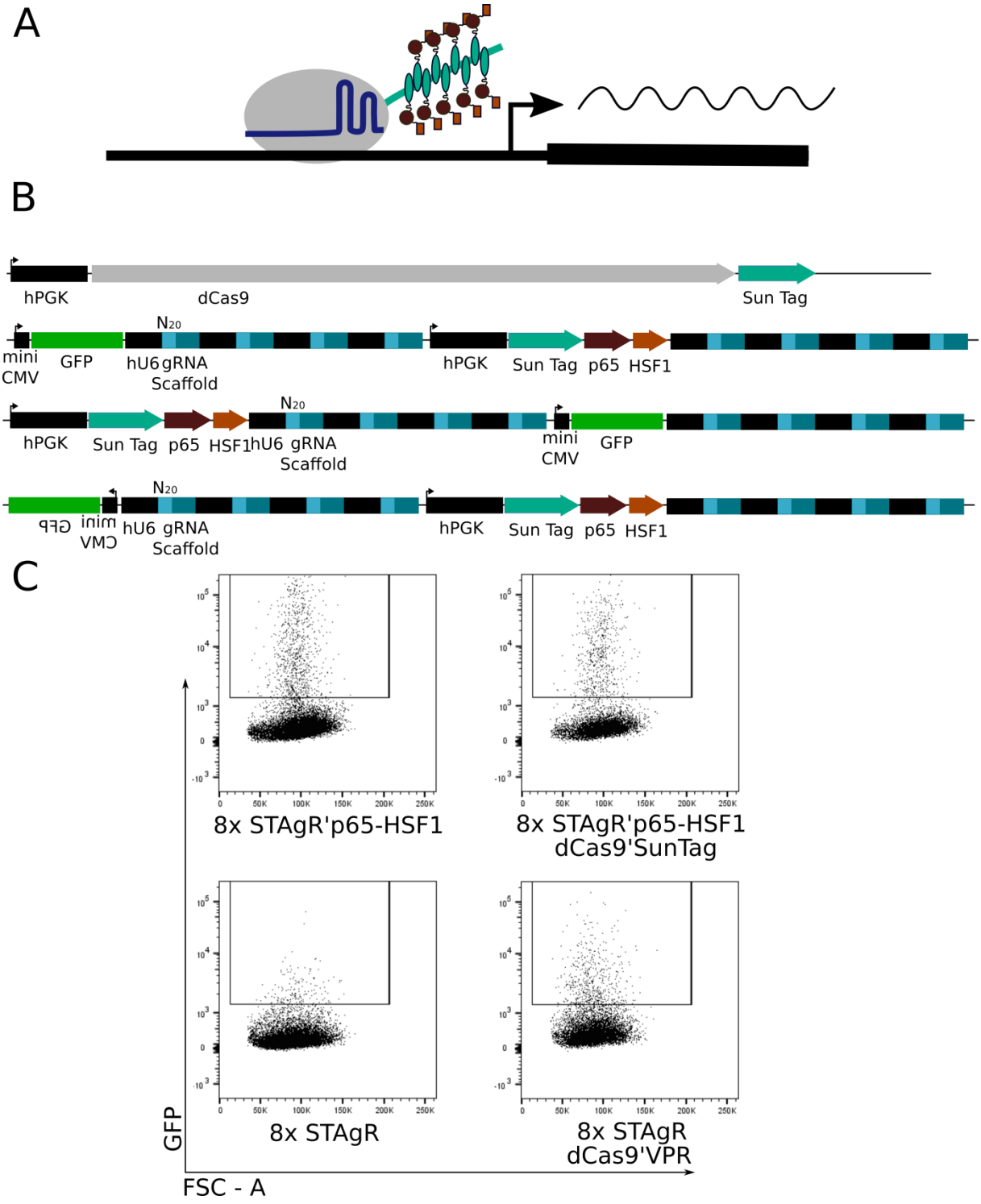

Fig. 33 | Transfer of the functional activator reporter into a lentiviral system for potential in vivo usage. A Overview of the dCas9SunTag system. **B** Schematic overview of the different constructs generated. **C** Flow cytometry blots showing GFP expression in dependence on which viral particles were provided.

In order to test if the FAR system is compatible with a different transactivator system, it was tested in primary mouse embryonic fibroblasts derived from the dCas9Activator mouse line (dCAM) (Fig. 34A) (Giehrl- Schwab et al. unpublished). The activator system in this transgenic mouse is based on dCas9'VPR which is supported by MS2 based artificial transcription factors which help to accumulate a high amount of activators at a target site (Konermann et al. 2014a). The transgene is under the control of a CAG promoter which is suppressed by a transcription Stop cassette, flanked by loxP sites and therefore removable using Cre recombinase (Hermann et al. 2014). Mouse Embryonic Fibroblasts (MEFs) were extracted from the dCAM mouse line and the loxP-STOP-loxP site was subsequently removed in vitro by transfecting a plasmid coding for Cre recombinase and a tdTomato fluorescence protein. The transfected cells ($tdTomato^{+}$) were isolated by FACS and expanded. Viral particles were generated which featured a functional activator GFP reporter with a binding site for *Satb2* targeting gRNA S3 and the corresponding single gRNA expression cassette. Cells were then transduced with this virus and analyzed by immunohistochemistry. When transduced with the single gRNA control particle, cells show widespread GFP expression. However when infected with the particle, containing an 8x STAgR construct also carrying a GFP reporter with an S3 gRNA binding site, only few cells showed GFP expression (Fig. 34B), indicating that the FAR is sensitive to the number of gRNAs used, especially in viral settings.

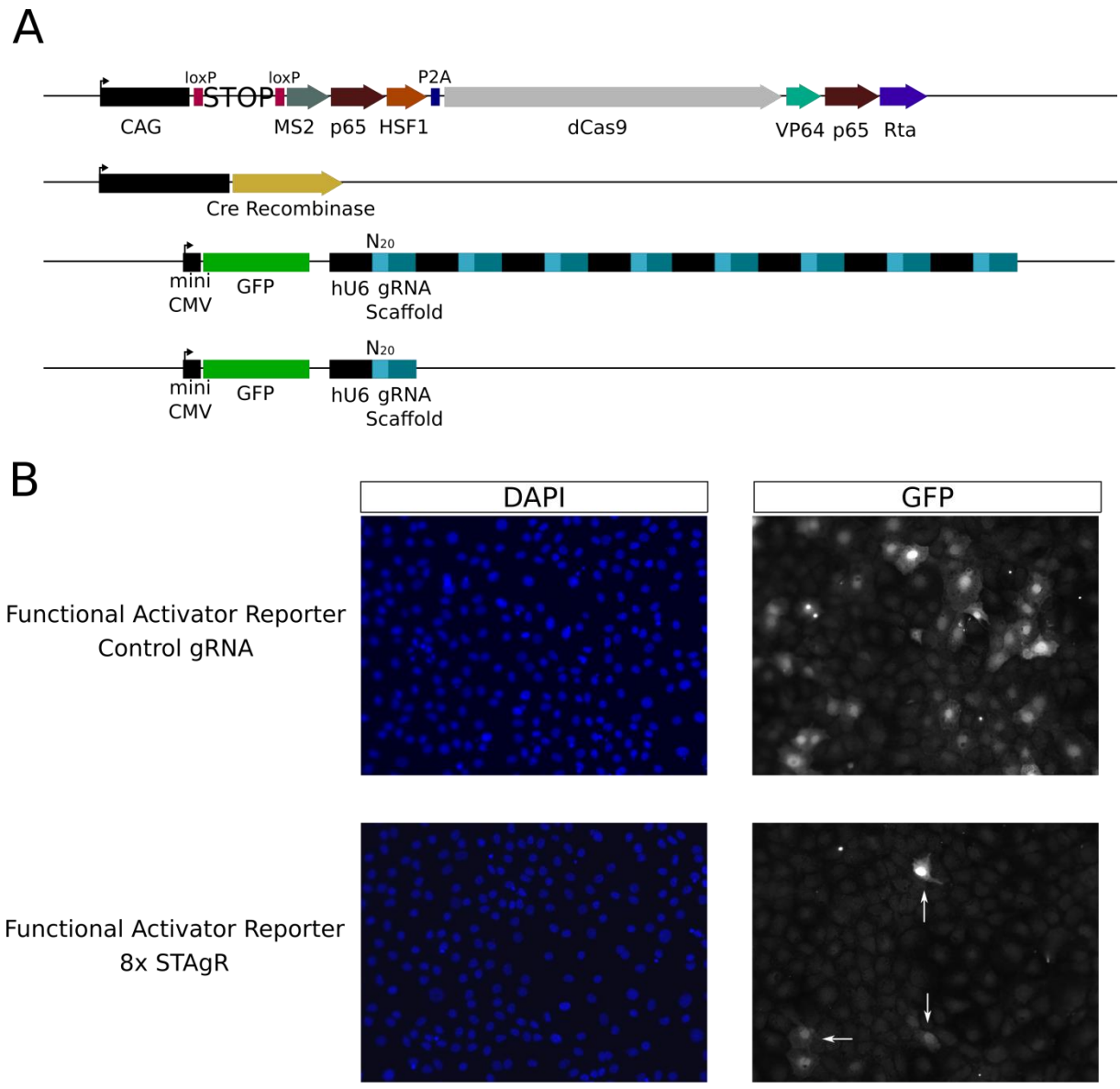

Fig. 34 | Viral particles used in dCas9'Activator mouse-derived fibroblasts. A Schematic overview of the dCas9'Activator transgene engineered in the mouse line and the different lentiviruses used. **B** Immunohistochemistry of cultures infected with the functional activator reporter and either a control gRNA virus or the 8xSTAgR virus.

To test whether the low count of GFP positive cells is due to the repetitive character of the 8xSTAgR construct leading to low titer, I generated a construct, which carried the 8x STAgR gRNA expression cassettes but also coded for a constitutively expressed GFP under a CMV promoter. In two other constructs, the gRNA targeting the functional activator reporter was decoupled with its target to form two smaller lentiviral constructs (Fig. 35A). The lentiviral construct featuring the constitutively expressed GFP as well as the combination of both smaller viruses was applied *in vitro*. Whereas the culture transduced with the virus featuring the constitutively expressed GFP showed bright green fluorescence, the decoupled functional

activator reporter did not result in GFP expression (Fig. 35B). This suggests that the functional activator reporter is incompatible with lentiviral delivery and I therefore abandoned it for *in vivo* experiments focusing on constitutively expressed reporters.

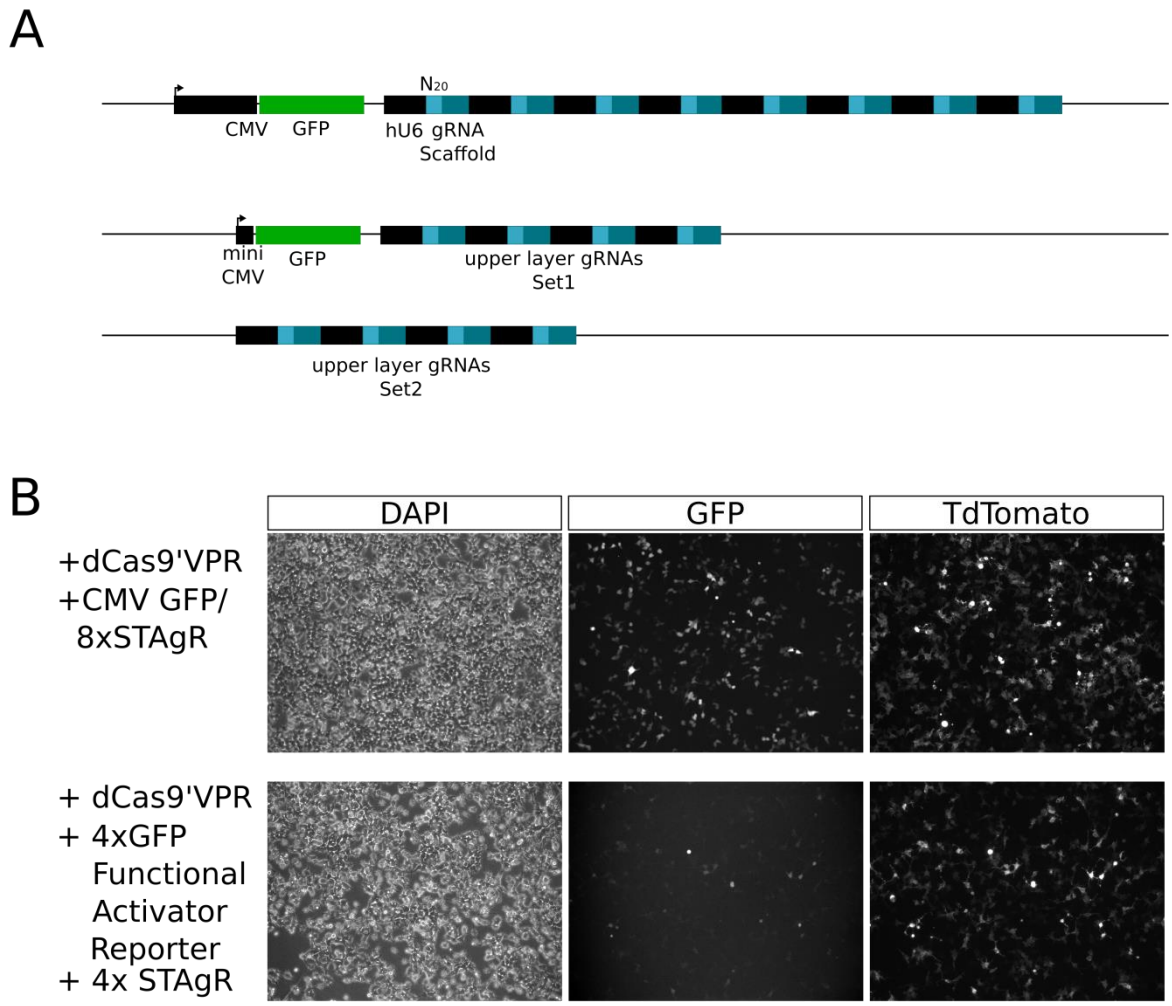

Fig. 35 | Viral particle optimization for *in vivo* usage. A Schematic overview of the viral particles used. **B** Immunohistochemistry of P19 cultures infected with the constitutively expressed GFP 8xSTAgR and the decoupled functional activator reporter. After transduction, cells were transfected with dCas9'VPR'TdTomato

4.5 In vivo injection after traumatic brain injury

To be able to apply this system *in vivo*, I made use of the dCAM, crossed with a line that carries the Cre recombinase under the control of the Aldh1L1 promoter (Tien et al. 2012) (Fig. 36C). Offspring was genotyped using primers and protocols depicted in Tables 10/11. $dCAM^{+}/Cre^{+}$ double positive individuals were grown until three months of age. Mice were treated as described in chapter D5.3 to mimic a traumatic brain injury and injected with viral particles after three days (Fig. 36A/B). The mice were perfused and the brains were isolated and post-fixed for 24 hours. Brain slices of 50µm were prepared and analyzed by

immunohistochemistry (Fig. 36B). Figure 36B shows the cortex of a three months old mouse. GFAP staining (white) indicates the area of the stabwound as astroglia start to proliferate in the grey matter after acute injury (Simon, Götz, and Dimou 2011). After viral injection, cells with astrocyte morphology were identified which showed strong GFP expression and therefore obtained the 8xSTAgR gRNA construct. However whether the gRNAs in combination with the proneural factors NEUROD1 and NEUROD4 lead to layer specific reprogramming still needs to be elucidated and could not be accomplished until the end of this thesis.

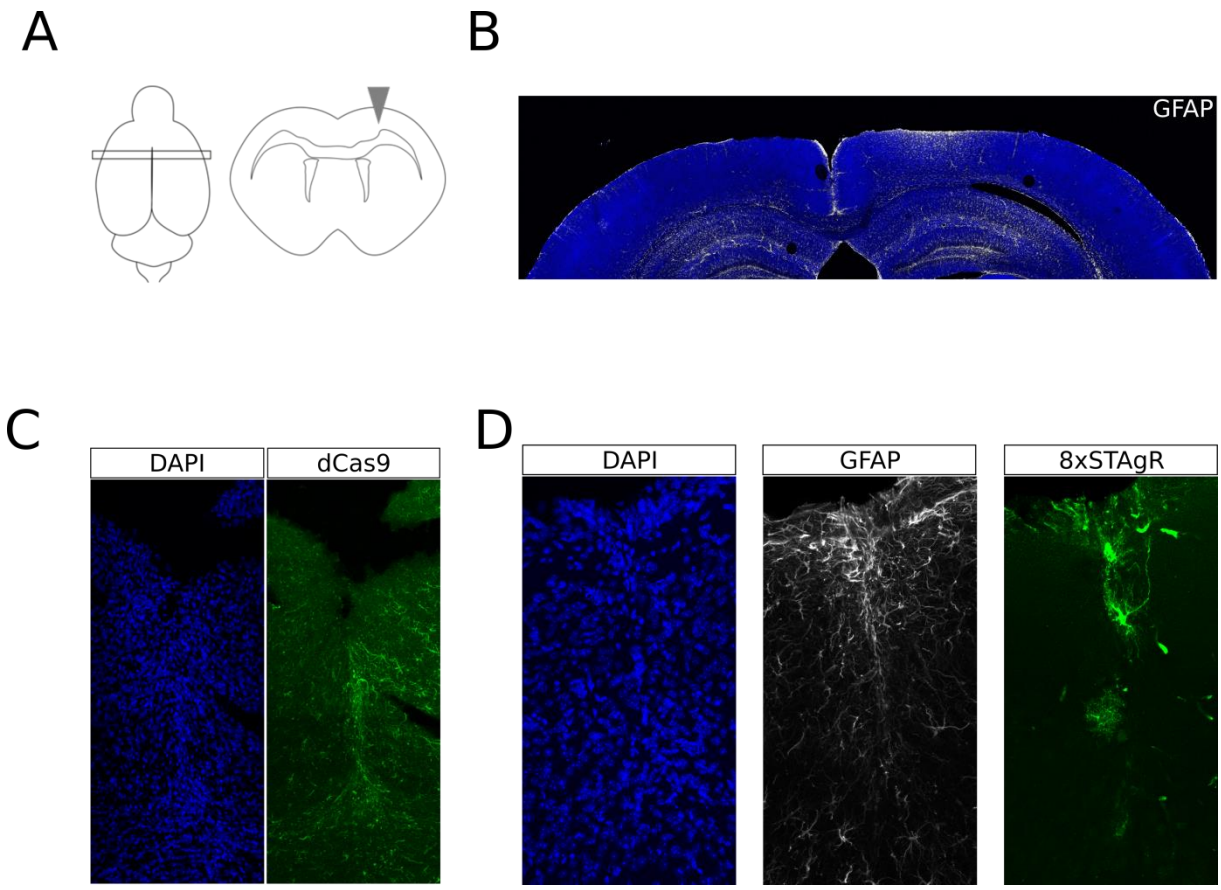

Fig. 36 | Selective targeting of astrocytes with dCas9'VPR and STAgR at a site of brain injury *in vivo*. A Schematic overview of injury paradigm. **B** Immunohistochemistry of a 70µm brain slice at the injury site. GFAP staining indicates the location of injury. **C** dCas9 staining at an injury site of a dCas9 activator mouse crossed with an Ald1h1-Cre mouse line. Selective dCas9 expression can be seen in reactive astrocytes accumulating around the injury site. **D** Staining of GFAP (white) and GFP (green) after stabwound and injection of a 8xSTAgR lentiviral particle, carrying a constitutive expressed GFP.

C. Discussion

1. STAgR cloning based gRNA Multiplexing

Experimental paradigms using Cas9/dCas9 to target multiple genes or loci need to avoid critical bottlenecks. In any approach that aims to target multiple genes or loci, the implementation of a reliable multiplexing strategy is essential to ensure each cell receives all the desired gRNA sequences. Co-transfection of large numbers of gRNA expression vectors will result in only a small fraction of cells receiving all essential targeting information in form of gRNAs in stoichiometric levels. It is possible to clone each gRNA into a different vector with a unique selection marker. However, the number of selectable constructs (antibiotic as well as fluorescent markers) is limited. An alternative approach is to clone multiple gRNA expression cassettes into a single-vector. Sequential insertion of these cassettes is cumbersome and time-consuming. Furthermore, CRISPR/Cas9-based approaches often necessitate a comprehensive validation of gRNA sequences. This implies that a flexible and customizable multiplexing strategy is advantageous. By using the N20 protospacer sequence as homology region for Gibson assembly, STAgR cloning provides said requirements in a fast, cheap, and highly efficient way. At the time of publication of the manuscript, STAgR enabled the cloning of an unprecedented number of gRNA cassettes in a single reaction. It is a simple method that does not rely on expensive or restricted materials and is easy to learn. The method enables comprehensive highly customizable gRNA multiplexing and makes it available to a large scientific community. STAgR cloning allows the utilization of most common gRNA vectors, thereby enabling a large set of experimental paradigms. Furthermore, its flexibility makes it compatible with various CRISPR-based approaches. A recent study has shown that combining different Cas9 tools can help to unravel the effect of epigenetic barriers on transcriptional reprogramming (Baumann et al. 2019). This only hints the potential of combining a conventional dCas9 targeted modifier or transcriptional activator with other protein- RNA interaction based targeting systems like the MS2 system (Konermann et al. 2014a). With STAgR, a combination of different modified gRNA stem loops is fairly easy. Loci can be targeted with transcriptional activators with dCas9 based tools and others additionally with chromatin modifiers to remove epigenetic barriers by MS2 based targeting, while gRNAs are provided from one vector. With this, STAgR provides a possibility to further push and combine epigenetic and transcriptional engineering tools. More conventional WTCas9 based genetic engineering approaches could also heavily profit from this multiplexing strategy.

I showed that multiplexed gRNA vectors with the STAgR strategy can be reliably generated with high efficiency. However, the efficiency of the enzymatic assembly is dependent on the molar ratio the individual building blocks are represented and the reaction duration. I also encountered that efficiencies are dependent on the sequences of the generated N20 overhangs. Given that the enzymatic reaction, on which STAgR is based, is highly dependent on homologous sequences, certain motifs have to be avoided as N20 sequences. I found that polyT stretches and especially sequences which resemble the first 15bp of the used promoter can lead to premature termination of the STAgR reaction. Furthermore, the order of the individual N20 sequences seems to influence STAgR efficiencies. If a certain construct could not be obtained, a simple interchange of the gRNA's sequential order could often solve this problem.

One concern while designing this technique was that the repetitive character of the STAgR constructs could oppose a problem for the transcriptional machinery. A multitude of similar promoters in close proximity could lead to promoter skipping and therefore lead to imbalanced expression of the individual transcripts. RNA Polymerase III transcription termination is dependent on a oligo(dT) stretch on the non-template strand (Arimbasseri, Rijal, and Maraia 2013). To prevent potential read-through of RNA Pol III and creation of non- separated multiple gRNA transcripts each expression cassette was equipped with a pair of oligo(dT) termination cassettes. These precautions have proven to be effective, as I could show that each gRNA is transcribed to a functional molecule using a genetic assay using WTCas9 and a gRNA targeting the open reading frame of the fluorescence protein GFP. By providing WTCas9 with a variety of STAgR constructs in which this gRNA was located on different positions of four different constructs, I showed that each single gRNA of a 4x STAgR constructs is expressed at similar levels. This is crucial as the functionality and the effect of CRISPR, as a bipartite system is highly dependent on its two components. If the amount of Cas9 or dCas9 effector fusion is stable in a system, the number of different gRNAs could limit the quantity of Cas9 for each single target site. Further, if gRNAs are differentially represented in a system, the amount of Cas9 effector would be highly variable for the different targeting sites. This may not be very crucial for WTCas9 approaches as the induction of doublestrand breaks and indel mutations can be a unique event in a cell. For transcriptional or epigenomic engineering approaches however, this may be rather significant as the binding of the two Cas9 versions seems to be different. WTCas9 has to undergo a conformational change before DNA cleavage (Nishimasu et al. 2014). This only occurs after PAM recognition, pairing of the seeding sequence and extensive binding of the gRNA to its

genomic complement (X. Wu et al. 2014). dCas9 however does not require extensive binding of the full sequence and is already bound after PAM recognition, DNA melting and the alignment of the seeding sequence, making it more likely to bind off- target sites and thereby reducing the amount of dCas9 available at the on- target site (X. Wu et al. 2014). I could further show that gRNA multiplexing is beneficial for transcriptional activation compared to a pool of single gRNA plasmids. If a cell obtains a multiplexed gRNA vector, the overall amount of dCas9 effector has to be subdivided over more targeting sites. The technical limitations of an e.g. transfection makes it more efficient to deliver one single plasmid with all targeting information than multiple plasmids with one gRNA sequence each.

The advantages and the potential of convenient gRNA multiplexing strategies are obvious. Therefore, other labs have also developed and published gRNA multiplexing strategies. Some of them are based on the sequential activity of Type IIS restriction enzymes called Golden Gate Cloning. These enzymes cut outside of their recognition sequences to create 4bp overhangs which can be used to assemble multiple fragments (Engler, Kandzia, and Marillonnet 2008). Golden Gate Cloning-based strategies may share some advantages with STAgR cloning but need multiple rounds of cloning to generate desired vectors. This can take up to two weeks of time (Lowder et al. 2015; Sakuma et al. 2015b; Vad-Nielsen et al. 2019). Using PCR to generate building blocks does save a tremendous amount of time, however it is only fair to mention that the end-product requires sequencing of the assembled gRNA cassettes as PCR can introduce errors. Modern polymerases have been engineered to be highly efficient and therefore PCR- induced errors occur extremely rarely. This strategy has also been adapted to Golden Gate cloning to great success, assembling 9 different gRNA cassettes in one reaction and published shortly after STAgR cloning (Zuckermann et al. 2018).

2. dCas9 based methylation tools

The establishment of STAgR provided a fundamental basis for various scientific approaches using transcriptional as well as epigenomic engineering. To find evidence of a causal connection between DNA methylation and disease development, I found that there is a necessity to generate novel epigenomic engineering DNA methylation tools. Previous studies already showed that dCas9-based DNA methylation is possible (Amabile et al. 2016; X. S. Liu et al. 2016a; Stepper et al. 2017a; Vojta et al. 2016a). Even if methylation could be induced in targeted attempts, it spread over a wider area. This and the fact that not only site specifically, methylation was raised but overall high off- target effects could be monitored,

limits the utility of these systems. Site specific methylation would be necessary to assess the effect of DNA methylation at a specific locus. Furthermore, as the methyltransferases are all derived from and used in mammalian systems, there could be potential host factor interference or interaction with the engineering tools. Therefore, I tested viral (M.CviPI), bacterial (M.SSS1) and plantal (DNM1a and DRM2) methyltransferases for the use in human and murine cell systems. One of the generated methyltransferases (M.SSS1) was published during the execution of this thesis. Lei *et al.* showed that their version of dCas9'M.SSS1 could be engineered to be more centralized and more efficient in its *de novo* methylation than any other tool published before (Lei et al. 2017a). This suggests that methyltransferases derived from different species could hold a potential advantage over mammalian derived ones.

To test their methylation capacity, those unusual methyltransferases were applied in a variety of transcriptional and molecular assays. The first assays which were conducted were based on the fact that methylation can be a hallmark of promoter silencing, especially artificial promoters like CMV and CAG (Y. Zhou et al. 2014). Furthermore, methylation of the CpG island of the promoter of the long non coding RNA Airn was shown to be responsible for gene silencing of the maternal copy (Koerner et al. 2012; Latos et al. 2009; Stefan H Stricker et al. 2008). Targeted methylation of this locus therefore was thought to be able to manipulate Airn expression directly. I chose this locus as a further potential target for the methyltransferase tools and as readout for their potential methylation capacity. I did not only monitor Airn RNA levels but also generated a reporter construct which when methylated was hypothesized to reduce transcription of subsequent gene and therefore show a loss of fluorescence intensity. Both assays however did not give clear indications of *de novo* methylation. To have a better view at the molecular level, two different loci have been analyzed by bisulfite sequencing after targeting with the constructed methylation tools. In my experiments, not even the published positive controls DNMT3a and DNMT3a3l induced *de novo* methylation of the analyzed loci.

There are several possible explanations for the failure of these approaches. Expression of the constructs was confirmed by immunohistochemistry stainings of dCas9 (data not shown). Furthermore, time plays a crucial factor in *de novo* methylation, as reportedly targeted methylation by dCas9'DNMT3a can take up to five days to be detectable (Vojta et al. 2016b). Others showed that with different methyltransferases, like dCas9'MQ1 or dCas9'DNMT3a3l, this effect can be rather immediate (Lei et al. 2017; Stepper et al. 2017). The conducted

experiments were all in a timeframe of two to seven days. Targeted methylation could also be dependent on the targeted loci. Preferred targets of previously conducted studies were promoter regions with CpG islands (Vojta et al. 2016). As the chosen target, the Airn promoter harbors a CpG which can be methylated during development, it was rather surprising that not even positive controls resulted in *de novo* methylation. It could be that the Airn CpG or the promoter of Ube2s are too tightly regulated by the host cell and that any *de novo* methylation could be countered by either de-methylation or cells whose loci were successfully methylated simply died. To rule out any cell type specificity the experiments have been repeated with another murine cell line (N2a) (data not shown). None of the conducted experiments showed any neither positive nor conclusive result.

3. Alzheimer's diseases associated differentially methylated positions

Alzheimer's disease is undoubtedly one of the biggest burdens of modern society. As public attention rises, more and more studies have looked into genomic alterations with genome wide association studies to find hints for causes of Alzheimer's disease (Lambert et al. 2013). These studies could even identify high risk genes, however only a small proportion of Alzheimer's disease patients develop those familial forms. As these studies failed to explain the underlying risk for AD genetically, it was postulated that epigenetic variation could play a significant role in disease development (Ertekin-Taner 2010). Notably, two epigenome wide association studies independently identified a set of differently methylated positions which were found to be hypermethylated in two different Alzheimer's disease cohorts (De Jager et al. 2014; Lunnon et al. 2014). De Jager *et al*. and Lunnon *et al.* provide data which shows a correlation between the differentially methylated positions and Alzheimer's disease progression, suggesting that there potentially is a causative relationship. The five significant hits reported by both studies were differentially methylated positions in close proximity to the genes of RHBDF2, RPL13, C10orf54- CDH23 and ANK1 (Fig. 5). Network analyses even revealed a connection of some of these genes to known Alzheimer's risk genes, supporting the idea that the hypermethylation of these DMPs in not only a result of early disease development but may be a cause.

I was planning to test this putative causal relationship by manipulating the differentially methylated positions with epigenomic engineering and link these methylation marks to potential Alzheimer's disease indicators. I reasoned it would be best to manipulate these marks in cells which allow a subsequent differentiation in disease-relevant cell types. Hence, initial experiments were conducted in a variety of human embryonic neural stem cell lines

(Sun et al. 2008). The absolute changes in methylation levels were not reported in the EWAS studies and an access to raw data was not given. Therefore, I first analyzed the methylation level at the loci of interest. Surprisingly, all five loci were already methylated to a high degree in all three neural stem cell lines analyzed. Similarly, iPSCs and *in vitro* differentiated neurons and astrocytes from three different genetic backgrounds all showed high methylation levels at the analyzed loci. To rule out a potential *in vitro* artifact, I analyzed the buffy coat (mixture of leukocytes and thrombocytes) of human blood and post mortem collected human cortical tissue by bisulfite sequencing. All of these samples displayed high methylation levels (above ~80%) comparable to analyzed *in vitro* derived samples. This was further confirmed by analysis of the antisense strand of all samples, displaying minor variations but overall high methylation levels.

As the initial paradigm was to raise the methylation levels at those loci and see if they have influence on measurable Alzheimer's disease characteristics, I reasoned that the already high methylation levels at the DMPs do not leave any room for further increase and significant differences between patients and healthy individuals are likely too small to indicate causality. Even if both studies delivered convincing evidence for an association of differential methylation and Alzheimer's pathology, limitations remain (Lord and Cruchaga 2014). Both studies utilized Illumina's HumanMethylation450 platform for quantifying methylation levels. While these studies were conducted, this platform was the gold standard to determine genome-wide methylation levels. Technical restrictions of this array do not allow the investigation of areas which are not part of the pre-designed probe set. This means that overall DeJager and Lunnon only looked at 2% of all CpGs in the human genome. This could mean that disease-relevant loci might have been missed. Furthermore, this technique does not allow distinguishing between methylated and hydroxymethylated CpGs (Fig. 2). As those two DNA modifications have been reported to possess contradictory effects on gene regulation, the statement about the methylation levels of the DMPs and the potential outcome for gene regulation of genes nearby, could be the exactly the opposite (Coppieters et al. 2014). EWAS are also highly dependent on the composition of the analyzed tissue. The brain is composed of various cell types, and slight variation in cell composition could be mistaken for epigenomic changes. This heterogeneity can be compensated by utilizing cell sorting techniques to be able to isolate and analyze specific cell types. In these specific epigenomic changes can be linked to distinct populations. Technical advances like single- cell epigenomic profiling will presumably ameliorate this problem (Kelsey, Stegle, and Reik 2017).

Even if EWAS hold a tremendous potential for unraveling epigenomic miss-regulation in diseases, reported hits have to be critically examined. EWAS hits should be subsequently validated by epigenomic engineering to prove causality and not only hypothesize about it. Moreover, EWAS should be seen as a supplementary method to fully elucidate molecular miss-regulation in disease. Recent advances in single cell transcriptomics have proven to effectively being able to identify transcriptionally distinct subpopulations in Alzheimer's disease samples (Mathys et al. 2019). This allows to reveal transcriptional alterations in specific cell populations and to link these to AD pathology. Like this, alternate transcriptional profiles can be identified which emerge early during pathogenesis and reveal new risk genes whose miss- regulation could contribute to disease development. These miss-regulated genes could then subsequently be epigenetically analyzed to further elucidate possible reasons for miss-regulation and how to revert them.

4. Utilizing CRISPR for subtype specific transcriptional manipulation

Utilizing CRISPR based transcriptional activators for neuronal reprogramming holds great potential. The bipartite nature of these tools and its dependence on providing the target information by small RNA molecules simplify simultaneous targeting and activation of a large number of endogenous genes. Entire gene regulatory networks can be manipulated to control cellular fate. With STAgR, I created a multiplexing strategy which made these approaches simpler. Because of the vast variety of different neuronal types common in the brain, direct reprogramming to specific subtypes is still one of the biggest challenges. Lost neurons after traumatic brain injuries or as a cause of neurodegenerative diseases should be replaced with the subtype lost. Only if this milestone can be reached, direct reprogramming will be applicable as a replacement therapy. Huge efforts in single-cell transcriptomics have been made to identify factors which drive these specific fates in various brain structures (Chen et al. 2017; Delile et al. 2019; Loo et al. 2019; Telley et al. 2016; Zeisel et al. 2015). These datasets help to shortlist transcription factors potentially relevant to drive a specific cellular fate. I have chosen a range of factors which was thought to orchestrate a cell to the subtype of upper layer callosal projection neurons. These factors were Satb2, Cux1, Cux2, Brn2, Nurr1, Bhlhb5, Lhx2, Tle2, and Mef2c. I generated gRNAs which targeted the promoter regions of each of these genes. Different transcriptional activators have been tested over the time, to find the best system. I confirmed dCas9'VPR to be the more potent transcriptional activator over dCas9'VP64 (Chavez et al. 2016). Furthermore, targeting with two gRNAs can result in a synergistic effect on transcriptional activation. This is in line with

other publications, showing that induction of transcription seems to be dependent on the amount of programmable transcription factors targeted to a transcription start site. Consequently, systems which accumulate artificial transcription factor molecules at a promoter region can be more efficient than simple single transcription factor fusion constructs (Chavez et al. 2016).

Throughout the conducted experiments, I noticed that not all genes are equally activated transcriptionally in one cell type. I generally observed three classes of genes. The first group does not respond significantly to transcriptional activation. Multiple gRNA sets, which targeted different annotated transcription start sites, were not able to increase mRNA levels indicating that other barriers cause this unresponsiveness. Another group of genes showed minor (3 to 10-fold) transcriptional induction after targeting with dCas9'VPR. The last group of genes is highly responsive as mRNA levels could be raised by up to thousand fold compared to endogenous levels. Interestingly, these groups of genes were not always consistent in the different host cells I utilized. This suggests that individual genes can react differently in one cell type or the other. Each individual cell type may tightly control expression of certain genes, which overrules dCas9'VPR. Which specific mechanisms underlie this tight control, still needs to be elucidated. Studies suggest that chromatin modifications could play such a role (Luz-Madrigal et al. 2019). Indeed, we have experienced that a targeted de- methylation can lead to an increase in transactivation by dCas9'VP64 (Baumann et al. 2019). This further emphasizes the potential of combining transactivators and chromatin modifier orchestrated by gRNA expression of a highly customized gRNA construct.

5. Utilizing CRISPR for *in vivo* reprogramming

With the establishment of the functional activator reporter (Section B3.4), I thought to have found a solid way to target multiple endogenous promoters *in vivo* and follow the activation of subsequent genes and a potential transdifferentiation. However, this system did not translate well into viral vectors which set me back to the use of conventional fluorescence reporters. Even if a lot of effort has been expended to optimize and simplify the use of dCas9 transcriptional activators, I encountered various difficulties to translate and utilize this system in *in vivo* experiments. Undoubtedly, the advantages of dCas9 activator systems have been thoroughly discussed. However, if there is a dependency on viral vectors to deliver all components, one also faces size limitations as the most competent dCas9 transactivators can exceed the packaging limit of one single lentivirus (Kumar et al. 2001). Even after various

attempts to utilize ways to split dCas9 activators on two different lentiviral particles, the titers have not been high enough for *in vivo* usage (Tanenbaum et al. 2014; Zetche, Volz, and Zhang 2015). The chance to work with a dCas9 activator transgenic mouse line vastly simplified these experimental paradigms.

If this system is able to help orchestrating the process of subtype specific reprogramming still remains an open question and could not be answered during the conduct of this thesis. Next experiments will be *in vivo* injections of gRNA and NeuroD1/ NeuroD4 packed viral particles into the somatosensory cortex after brain injury. Crossing the dCas9 activator mouse line, whose transgene expression is silenced with a loxP-STOP- loxP cassette with mice expressing Cre recombinase under the murine promoter of aldolase, limits expression of the activators to astrocytes. After a given amount of time, cells which obtained gRNAs and pro- neural factors should be analyzed in regard to their morphology, cell type specific and especially subtype specific markers like NeuN, CUX1 or CTIP2 (Mattugini et al. 2019).

Should this approach prove successful, one should use the tremendous amount of transcriptomic data to identify potential factors defining other neuronal subtypes to push the specificity of direct reprogramming.

D. Materials and Methods

1. Materials

1.1 Hard- and software

This work was written on an Acer Aspire V Nitro running Windows 10 Professional and using the text processing software Microsoft "Word" 2010. Images were processed with GIMP (GNU Image Manipulation Program) Version 2.6, ImageJ Version 1.48p (Wayne Rasband, USA), "Inkscape" Version 0.91 (Free Software Foundation, Inc., Boston, USA) and Zeiss Zen blue Version 2.6 (Carl Zeiss Microscopy GmbH, Jena, Germany). Nucleic acid as well as protein sequences were analyzed using "Snapgene" Version 3.3 (GSL Biotech, Chicago, USA) or "Serial Cloner" Version 2.6.1 (Serial Basics). Literature and database searches were performed with the online tool provided by the National Center for Biotechnology Information (NCBI, http://www.ncbi.nlm.nih.gov/).

1.2 Chemicals, reagents, media and supplements

All experiments done during this work were performed using chemicals of analytical grade and unless otherwise noted, are listed in Table 1.

Table 1 | List of used reagents and chemicals plasmids for different expression systems.

Name	Catalogue	Manufacturer
6x DNA loading dye	R0611	Thermo Fisher Scientific
Agarose	870055	Biozym, Oldendorf
Aqua poly mount	18606	Polysciences
Bovine Serum Albumine	A2153-1KG	Sigma-Aldrich
DAPI Nuclear Staining Dye	1351303	Bio-Rad Laboratories
ECL Luminol Reagent	sc-2048	Santa Cruz Biotechnology
Ethanol, 99.9%	9065.2	Carl Roth
GeneRuler 1kb DNA ladder	SM0313	Thermo Fisher Scientific
Gibson Assembly Master Mix	E2611	NEB
HotStar Taq	203203	Qiagen
Methanol	34860-1L-R	Sigma-Aldrich
Nuclease-free water	AM9932	Life Technologies

Paraformaldehyde	158127-5G	Sigma-Aldrich
Poly-D-Lysine	P6407-5MG	Sigma-Aldrich
Phusion DNA Polymerase Master Mix	M0531S	NEB
PowerUp™ Sybr Green Master Mix	A25742	ThermoFisher Scientific
SYBR Safe DNA Gel Stain	5001208	Life Technologies
Triton-X 100	T8655.1	Biomol
Bovine serum albumin	A9418	Sigma-Aldrich
Accutase	A6964-100ML	Life Technologies
BDNF	PHC7074	Gibco
Blasticidin S	R21001	ThermoFisher Scientific
Cryotubes	10577391	Thermo Fisher Scientific
DMSO	D5879-100ML	Sigma-Aldrich
EGF	78006	Stemcell Technologies
Fetal calf serum	C8056-500ML	Sigma-Aldrich
Hygromycin B	10687010	ThermoFisher Scientific
Lipofectamin® 2000	11668027	ThermoFisher Scientific
Puromycin	A1113803	ThermoFisher Scientific

1.3 Antibodies

Table 2 | List of used primary and secondary antibodies.

Antibody	**Antigen**
Non-commercial primary antibodies	
rat IgG2a Cas9 Clone 8641-1	spCas9
Commercial primary antibodies	**Source / Product# / Lot#**
mouse IgGI anti- GFAP	Sigma- Aldrich / G3893 / 083M4785
chicken anti- GFP	Aves Labs Inc. / GFP- 1020 / GFP697986
rabbit anti- RFP	Rockland / 600-401-379 / 33235

commercial secondary antibodies	
Alexa Fluor 546 goat- anti- rat IgG	Invitrogen / A11081
Alexa Fluor 488 goat- anti- mouse IgG	Invitrogen / A11039
Alexa Fluor 546 goat- anti- rabbit IgG	Molecular Probes / A21207
Alexa Fluor 647 goat- anti- mouse IgG1	Invitrogen / A21240

1.4 Plasmids

Plasmids used in conducted experiments were part of the Stricker laboratory plasmid library.

Table 3 | Used plasmids for different expression systems.

Insert	Reporter	Backbone /Name
hU6_gRNAScaffold	Neomycin	MLM3636/ gRNA Neo
hU6_ SAM loop	Neomycin	MLM3636/ SAM Helper
hU6_gRNAScaffold	GFP	MLM3636/ green STAgR
hU6_gRNAScaffold	TdTomato	MLM3636/ red STAgR
hU6_gRNAScaffold	BFP	MLM3636/ blue STAgR
hU6_gRNAScaffold/miniCMVGFP	GFP	MLM3636/ Functional Activator Reporter
Lenti_gRNA vector	GFP	plKO1
dCas9'VP64	Hygromycin/GFP	pcDNA3

dCas9'VPR	Hygromycin/GFP/ RFP	pcDNA3
dCas9'DNMT3a	Hygromycin/GFP	pcDNA3
dCas9'DNMT3a3L	Hygromycin/GFP	pcDNA3
dCas9'SSS1	Hygromycin/GFP	pcDNA3
dCas9'CviPI	Hygromycin/GFP	pcDNA3
dCas9'DMN1a	Hygromycin/GFP	pcDNA3
dCas9'DMR/ARATH	Hygromycin/GFP	pcDNA3
Lenti_dCas9_SunTag	-	plKO1

1.5 Oligonucleotides

Oligonucleotides have been used to amplify sequences of interest for Gibson cloning, Sanger sequencing or quantitative RT PCR. Oligonucleotides for Gibson cloning have been designed using the NEBBuilder (https://nebuilder.neb.com/). Primer3Plus was used for qPCR primer design (http://primer3plus.com/cgi-bin/dev/primer3plus.cgi) wheras Bisulfite Sequencing primer were designed with MethPrimer 2.0 (Urogene, http://www.urogene.org/cgi-bin/methprimer2/MethPrimer.cgi). All primers were purchased either from ThermoFisher Scientific or Metabion.

Table 4 | Used oligonucleotides.

Oligonucleotide	Sequence	Usage
8xgRNASeq_fwd1	GAGACGCAGGGAGGGAT	Sequencing
8xgRNASeq_fwd2	AGCGGGCGAAGCCAGTGA	Sequencing
8xgRNASeq_rev1	CGTTTGGGGAAGGCCAC	Sequencing
DNMT3A3L_SeqPrimer	TCTGGAGCACGGCAGAATAG	Sequencing
GFP Seq fwd	GGCAAGCTGACCCTGAAGT	Sequencing
GFP Seq rev	TCTAGATCCGGTGGATCCC	Sequencing

GFPbeginningSeq_rev	TCCAGCTCGACCAGGATG	Sequencing
hPGK_seqF	GGTCTCGCACATTCTTCAC	Sequencing
p65_seqR	GCTGCTGAAACTCAGAGTTGTC	Sequencing
STAgR_minimalCMVseq_fwd	CAAGGTCGGGCAGGAAGA	Sequencing
StAgR_seq_fwd1	GAGTTAGGGGCGGGACTATG	Sequencing
StAgR_seq_fwd2	ACTGGATCCGGTACCAAGG	Sequencing
AIRNmid_fwd	CTTCCTCAACCTGCCTGAAG	qPCR
AIRNmid_rev	GTTGTCGGTGTCGAGGTTTT	qPCR
Bhlhe22 _qPCR_fwd	CCGAGTCCAGACGTTCACTT	qPCR
Bhlhe22 _qPCR_rev	GCCCGTGTAGATCGTGTCAT	qPCR
Brn-2 _qPCR_rev	GCCTCTGAGTCCAATCCCGC	qPCR
Brn-2_qPCR_fwd	GCTGGTTGATGGGTCCGGAA	qPCR
Cux1_qPCR_fwd	GCTGAGATACGCTTAGCACTTGAGT	qPCR
Cux1_qPCR_rev	CGGGTCTGTCCAAACCTCTATACA	qPCR
CyclophilinA_fwd	CAAAGCCACGGATCAATCTT	qPCR
CyclophilinA_fwd	GACGTGTTGCGCACTTAACG	qPCR
CyclophilinA_rev	CCCGGGAATAGTGAAACTGA	qPCR
CyclophilinA_rev	ACGACATAGATTGGGCTTAATGCT	qPCR
Lhx2_qPCR_fwd	CACATCCTCAAGCCTCCAAGAA	qPCR
Lhx2_qPCR_rev	AAAGGAGACAGTCTTGGCCAGTGT	qPCR
mCux2_qPCRfwd	CCCACCGTGTTCTTCGACATT	qPCR
mCux2_qPCRrev	GGACCCGTATGCTTTAGGATGA	qPCR
Mef2c_qPCR_fwd	TTTCCTCAAATGCCCCAAG	qPCR

Mef2c_qPCR_rev	TTTCTGTCTCCTGTTACAAAACCA	qPCR
mSatb2_qPCRfwd	CCTCAAGACGAACACCGTCAT	qPCR
mSatb2_qPCRrev	GCGCATCCTGGACCTGTAGT	qPCR
Tbr1_qPCR_fwd	CCTACTACAACGGCGTGGGCACTGT	qPCR
Tbr1_qPCR_rev	GTCACGATCCAGGTGTTCAGCATCG	qPCR
Tle2_qPCR_fwd	GACCAGTTCCGCCCGTTT	qPCR
Tle2_qPCR_fwd	CACATCCTCAAGCCTCCAAGAA	qPCR
Tle2_qPCR_rev	GCAAGACCACAAAATATTGAAAAGAC	qPCR
Tle2_qPCR_rev	AAAGGAGACAGTCTTGGCCAGTGT	qPCR
AldoCreGeno_fwd	CCTGTCCCCTTGCACAGTAG	Genotyping
AldoCreGeno_rev	CGGTTATTCAACTTGCACCA	Genotyping
Cas9 F	TCTTCGGCAACATCGTGGACG	Genotyping
Cas9 R	CGGTTCTTGTCGCTTCTGGTCAGCA	Genotyping

1.6 gRNA Sequences

gRNAs used during the conducted experiments are listed in Table 5.

Table 5 | gRNA sequences

Target	Sequence
Cux2 gRNA1	GGGGAGCACGGAGAGCGCGC
Cux2 gRNA2	GACGGCGCCTGGACTGGCGG
Cux2 gRNA3	GGGTCCAGCCCGGGTGTTGG
Cux2 gRNA4	TTTACGGTCCCCGTCGCCCG

Cux2 gRNA5	TCTGAATCGATATAAAGAGG
Cux2 gRNA6	ACAGGCCTGTCCAGGTGACA
Satb2 gRNA1	GCGGTGGACCAGTCTGGCTT
Satb2 gRNA2	CCTGTGCCTCCTCCGCAGCC
Satb2 gRNA3	CACCGAGAAAAGTTGCTCCG
Satb2 gRNA4	GAAGTGGCCTTCCCCAAACG
Cux2 gRNA7	TCTCTCTCTCTCGTTGCAGA
Cux2 gRNA8	ACAAGTTTCTGTAACTTACA
Cux2 gRNA9	CATTTTTGCCCTTAGGCACT
Tle2 gRNA1	GCGCGCGCCTCTGGAGCCGT
Tle2 gRNA2	TTGCCTAATTTCTCTCCCCC
Tle2 gRNA3	TGGAACCGAAGAAGCAGAGC
Lhx2 gRNA1	GAGACGCAGGGAGGGATCCG
Lhx2 gRNA2	GGAGCGGGCGAAGCCAGTGA
Lhx2 gRNA3	TCCTCAACCCCAGGTTCCAG
Lhx2 gRNA4	GCCCCAGACCGAAGCCCAGA
Lhx2 gRNA5	CTTCAATTCTCCCAGTGGCT
Lhx2 gRNA6	CGCTTGGGTAGCGTTGCGCG
Mef2c gRNA1	TCTTGTTCCAAGATTATTCT
Mef2c gRNA2	ATTTTGGATAGACTTCCGAT
Tbr1 gRNA1	GCAGTGGTCACAAAGCTTAA
Tbr1 gRNA2	GACGATCATGGCAAATTGAA

Bhlhb5 gRNA3	GCAGTTGTTGGGTTACTAAC
Bhlhb5 gRNA4	TGCTGCCTGTCTTCAGACCT
Cux1 gRNA1	GCGCGCGGGAAAAAGGGTGA
Cux1 gRNA2	GCGCCCTTTAGGTGAGCTGC
Cux1 gRNA3	CGTGAAAGTGACTGCGGAGC
Cux1 gRNA4	ATTGTCAACCGGTGTCGCCC
Cux1 gRNA5	GCCCGCCTGCTGCCTCCTGG
Cux1 gRNA6	TTCGGACTCCATGGCTGAGG
Brn2 gRNA1	GGAGAGAGCTTGAGAGCGCG
Brn2 gRNA2	GCGGTATCCACGTAAATCAA
Brn2 gRNA3	CCAATCACTGGCTCCGGTC
Brn2 gRNA4	GGCGCCCGAGGGAAGAAGA
Brn2 gRNA5	GGGTGGGGGTACCAGAGGA
Cited2 gRNA1	AGCTTACTCGCAATAACAAG
Cited2 gRNA2	TTTGATTAAACCACACCAAG
NeuroD1 gRNA1	CCGTGAGCTGAGCAACGAGC
NeuroD1 gRNA2	TGGACGCGTGCGCGATTGCG
NeuroD1 gRNA3	AGACCATATGGCGCATGCCG
CAG Promoter gRNA1	TTTCCATTGACGTCAATGGG
CAG Promoter gRNA2	ATTATTTTGTGCAGCGATGG
CAG Promoter gRNA3	CGGGAGGGCCCTTTGTGCGG
CAG Promoter gRNA4	TTTTATGGTAATCGTGCGAG

CAG Promoter gRNA5	GCCTCGGGGCTGTCCGCGGG
AIRN Promoter gRNA1	GGGTAGGATTCCGTTGCAAG
AIRN Promoter gRNA2	GAACTACACGAGGGCCGATA
AIRN Promoter gRNA3	GACCTGATCCGCGGTTTGCG
AIRN Promoter gRNA4	GCACAAGGGCAGGGTTCCGA
TTN gRNA 1	GAGCCGGGCTGTAAGGATGT
TTN gRNA 2	GCTAAATTTAGCCTTTCAGAAG
ActcI gRNA 1	GGCTCCAAGAATGGCCTCAG
ActcI gRNA 2	GGGAGGGGCAGGCCAGCAAG
Ube2s gRNA1	AGGTGGGCCTGAGGCCTAGC
Ube2s gRNA2	GTCCGAGGAGTGCAGGAAGG
miniCMV Reporter Plasmids	ACCAATTCAGTCGACTGCCC
miniCMV/teton/CMV	GTAGGCGTGTACGGTGGG
„uni CMV“	

2. Microbiological methods

2.1 Strains

For molecular cloning and plasmid production the *E. coli* XL-1 Blue strain (Stratagene/Agilent Technologies) was used.

Genotypes:

E. coli

Top10 - F- mcrA Δ(mrr-hsdRMS-mcrBC) φ80lacZΔM15 ΔlacX74 nupG recA1 araD139 Δ(ara-leu)7697 galE15 galK16 rpsL(Str^R) endA1 λ^-

STBL3 - F- glnV44 recA13 mcrB mrr hsdS20(rB-, mB-) ara-14 galK2 lacY1 proA2 rpsL20 xyl-5 leu mtl-1

2.2 Media

LB medium:

1% (w/v) tryptone

0.5% (w/v) yeast extract

1% (w/v) NaCl

LB agar

LB medium + 1.5% (w/v) agar

SOC Medium

2% (w/v) tryptone

0.5% (w/v) yeast extract

10 mM NaCl

2.5 mM KCl

10 mM $MgCl_2$

10 mM $MgSO_4$

20 mM glucose

2.3 Cultivation of *E. coli*

The different *E. coli* strains were cultivated in LB medium at 37°C and at approximately 200 rpm. LB agar dishes were incubated at 37°C. Selection of successfully transformed clones was done by adding antibiotics to either LB medium or LB agar. Used antibiotics were Ampicillin (100 µg/ml) and Kanamyin (50 µg/ml).

2.4 Transformation of *E. coli* Top10 and Stb3

The frozen and chemically competent bacteria were thawed on ice. 50- 200 ng of plasmid DNA were added to 20- 50 µl bacterial suspension and incubated on ice for at least 20 min. After heatshocking the cells at 42°C for 45 s, the cells were chilled on ice for additional 2 min. Then 10x the volume of used bacterial suspension LB (for XL1 Blue/ Rosetta 2 DE3+) or SOC (for DH10Bac) medium was added and the suspension was incubated at 37°C for at least 20 min on 200 rpm. The cells were then plated onto LB agar plates containing antibiotics and incubated at 37°C overnight or LB medium containing antibiotics was inoculated, directly.

3. Molecularbiological methods

3.1 Isolation of plasmid DNA from *E. coli* Top10 / STBL3

Depending on the desired amount of isolated DNA, 2- 300 ml LB (+ corresponding antibiotic) were inoculated with the previous transformed *E. coli* strain and incubated at 37°C for at least 12h. The cells were harvested and centrifuged at 4000g, 4°C and for 15 min. Alkaline lysis and DNA purification was done by using anion exchange columns, which were as well as the different used buffers, provided by ThermoScientific (Mini/Maxi-Kit) and according to the manufacturer's protocol.

3.2 Determination of DNA concentrations in solutions

DNA concentrations in solution were determined by measuring the optical density at a wavelength of 260 nm. This was done using a ND-1000 spectrophotometer (PeqLab). OD_{260nm}= 1 correspond to a concentration of 50 µg/ml double-stranded DNA. The purity of DNA was determined by the quotient of absorptions at 260 and 280 nm.

3.3 Restriction digestion of DNA

Sequence specific enzymatic restriction digestion of DNA was done using site-specific endonucleases from NEB (Frankfurt a. M., Germany). 200 ng to 1 µg of DNA was diluted in enzyme specific buffers and incubated with 1 to 4 units of endonuclease for 1h at 37°C. The enzymes were either inactivated at 65°C for 20 min or removed by gel electrophoresis (4.3.4) as well as appropriate purification kits.

3.4 Separation and analysis of DNA fragments by agarose gel electrophoresis

10x TBE buffer

0.5 M Tris

1.3% (v/v) H_3BO_3

20 mM EDTA

6x DNA loading buffer

50% (v/v) glycerol

0.02% (w/v) Orange G

Solutions with different sized DNA molecules have been supplemented with 6x DNA loading buffer (to 1x) and separated by loading onto 1% (w/v) agarose gels containing 0.5 µg/ml SYBR Safe (Invitrogen) in TBE. The gels were run at 120 V for 25 to 40 min. Separated DNA fragments were visualized with a UV transilluminator at 324 nm and size analyzed by using 1kb ladder (ThermoFisher Scientific).

3.5 Gelextraction of DNA fragments

For gel extraction of DNA fragments, buffers and anion exchange columns, provided by ThermoScientific (Gel Extraction Kit) were used according to manufacturer's protocols. Elution of DNA was done in 15 µl ddH_2O.

3.6 DNA Purification with AMPure Magnetic Beads

After PCR or enzymatic digestion, DNA samples were purified with magnetic AMPure XP Beads. Per 1 µl sample, 1.8 µl AMPure XP beads were added and the solution was incubated for 2 min on RT. The beads and the DNA fragments were separated from the residual liquid using a magnet and then washed twice with 70% Ethanol. The pellet was air dried and dissolved in 15-20 µl H_2O to release the bound DNA fragments. Purified DNA was separated from the beads using a magnet and transferred to a new 1.5 µl reaction tube for subsequent usage.

3.7 Dephosphorylation of DNA-fragments

To avoid religation of digested linearized vectors, the 5'- phosphate was removed by addition of 1 U phosphatase (NEB, "Antarctic Alkaline Phosphatase", AAP) together with the appropriate reaction buffer. The solution was incubated for 30- 45 min at 37°C and the enzymes were removed by either AMPure XP beads or by gel electrophoresis.

3.8 Ligation of DNA fragments

The linearized and dephosphorylated vector was enzymatically ligated with a DNA fragment of interest by adding 1 U T4 DNA-ligase. The reaction was performed in a volume of 20 µl 1x T4 ligation buffer, over-night at 16°C or at RT for 10min to 2h.

3.9 Gibson Cloning

If not otherwise indicated all constructs used in this work were generated with Gibson cloning (Gibson et al. 2009b).

5x Gibson isothermal reaction buffer

25% (w/v) PEG-8000

500 mM Tris-HCl pH 7.5

50 mM MgCl2,

50mM DTT

5mM NAD

1mM each of the four dNTPs

1.33x Gibson Master Mix:

Taq ligase (40u/µl): 50 µl

5x isothermal buffer: 100 µl

T5 exonuclease (1u/ul): 2 µl

Phusion polymerase (2u/ul): 6.25 µl

Nuclease-free water: 216.75 µl

Overhang primers for Gibson assembly were designed using the online tool NEBBuilder (https://nebuilder.neb.com/#!/) and are listed in 4.1.5. Fragments were generated using Phusion High Fidelity DNA Polymerase (NEB) according to manufacturer's protocol. PCR fragments were analyzed by gel electrophoresis and isolated using AMPure XP beads. After determining the DNA concentration as described in 4.3.2., DNA fragments were combined in a molar vector to insert ratio of 1:3 to a total volume of 2.5µl and 0.5 pmol. 7.5 µl of Gibson Master Mix were added and the reaction was incubated at 50 °C for 45 to 60 min. The reaction was then transformed into chemically competent bacteria as described in 2.4.

3.10 STAgR Cloning

All multiplexed gRNA vectors were generated according to the protocol developed during this thesis (Breunig et al. 2018a; Breunig et al. 2018b).

3.11 single gRNA Cloning

Expression vectors for single gRNA expression, are all based on the plasmid pMLM3636 (Addgene plasmid 43860). The vectors were either Neomycin selectable (gRNA_Neo), carried a fluorescence marker gene (STAgR_TdTomato or STAgR_GFP) or a minimal CMV Promoter Reporter construct. All vectors contained the hU6 Promoter as well as the gRNA stem loop (scaffold) or the SAM loop (Mali et al. 2013) separated by an AgeI restriction site, which was used for vector linearization. gRNA sequences were ordered as 80bp single

stranded DNA oligos, whereas a 5' overhang (TCTTGTGGAAAGGACGAAACACCG) and a 3' overhang (GTTTTAGAGCTAGAAATAGCAAGTTAAAATAAGGCT) were added to the 20bp protospacer sequence for subsequent cloning. Single gRNA double stranded DNA cloning fragments for Gibson cloning were generated by Phusion PCR using "LibGen_U6_fwd" and "LibGen_Scaffold_rev" as primers and the corresponding 80bp single stranded DNA oligos as template. After PCR gRNA fragments were isolated as describe in 4.3.6 and used in a Gibson Assembly reaction as described in 4.3.9. The reaction was transformed into chemically competent bacteria and incubated for 16h at 38 °C. DNA was isolated as described in 4.3.1 and clones were analyzed by Sanger Sequencing using "STAgR_seq_fwd2" as a sequencing primer.

4. Cell biological methods

4.1 Mammalian cell lines

The following mammalian cell lines were used.

Hek 293T	Human embryonic kidney cell transformed with SV 40 large T antigen
MEF	Mouse Embryonic Fibroblasts derived from embryonic tissue
N2a	Murine neuroblastoma cell line
P19	Murine embryonic carcinoma cell line derived from embryo- derived teratocarcinoma.

4.2 Cultivation of mammalian cell lines

Cells were cultivated in DMEM medium (Dulbecco's modified eagle medium) supplemented with 10% (v/v) FCS (fetal bovine serum, Biowest/Sigma) and 1% penicillin/streptomycin (10000 U/ml penicillin, 10000 µg/ml streptomycin). Additional supplements for specific cell lines are listed in table 6. Cells were grown in a monolayer in cell culture dishes at 37°C and an atmosphere containing 5% CO_2. Cells were, depending on the cell density, split up to twice a week in ratios from 1:4 up to 1:10. To do so, the media was removed and the cells were washed with 1x PBS followed by 5 min incubation with 16 µl/cm^2 Trypsin/EDTA solution at 37°C. Cells were suspended in fresh DMEM medium, pelleted for 2 min at 300g (Megafuge 8R, Thermofisher Scientific) and then diluted in an appropriate amount of medium for a following distribution on new cell culture dishes.

Table 6 | Volume of transfection reagents and medium.

Cellline	Supplements
Hek293T	-
MEF	10 mM HEPES Buffer Solution
	1 mM Sodium pyruvate solution
N2a	1x MEM NEAA
P19	1x MEM NEAA

4.3 Storage of mammalian cells

For long time storage, cells were trypsinized or resuspended by pipetting, pelleted by centrifugation (5 min, 300g) and then resuspended in FCS with 10% (v/v) DMSO. The cells were then aliquoted into cryo vials. The vials were slowly frozen in isopropyl at -80°C.

When reutilized, cells were thawed in a 37°C water bath and pelleted by centrifugation for 1 min at 300g. The supernatant was removed and the pellet resuspended in fresh medium before it was transferred into a cell culture dish.

4.4 Transfection of mammalian cells

If not otherwise indicated, cells were transfected using Lipofectamin 2000 (L2K, Thermofisher Scientific). All cells were either seeded or cultivated until a cell confluence of 80% and the media was changed prior to the transfection to the corresponding media but without any antibiotics. For each transfection sample, the DNA (appropriate amount can be seen in table 7) was diluted in Opti-MEM (Gibco) and mixed gently. Lipofectamine was vortexed prior to usage and diluted in another 1.5 ml reaction tube in Opti- MEM. After incubation of both tubes for 5 min on RT the diluted DNA was added to the diluted transfection reagent and the mix was incubated for 20 min on RT. The full reaction was added drop- wise to wells containing cells and medium.

Table 7 | Volume of transfection reagents and medium.

Plate Size	Volume of plating medium	Volume of dilution medium	DNA	L2K

24- well	500 µl	2x 50 µl	0.8 µg	2 µl
12- well	1 ml	2x 100 µl	1.6 µg	4 µl
6- well	2 ml	2x 250 µl	4 µg	10 µl

4.5 Preparation of primary Astrocyte cultures

Astrocyte medium

DMEM – F12 50:50 (+Glutamax)

1% (v/v) penicillin/streptomycin

10% (v/v) FCS

B27

EGF/FGF

For primary astrocyte cultures animals were taken at postnatal day 5-7. The pups were decapitated and the brains were isolated and transferred to a dish with Hank's Buffered Salt Solution (HBSS). After removing the meninges, the two hemispheres were separated and the cortical matter was dissected from the underlying striatum as well as the hippocampi. This tissue was then transferred to a 15 ml tube with astrocyte medium and dissociated with a P1000 by repeatedly pipetting up and down. The cell suspension was then transferred to a poly-Lysine coated T25 tissue culture flask and incubated in a cell culture incubator for one week before further processing.

4.6 Transfection of primary Astrocyte cultures

Cells were seeded one day prior to transfection. Seeding densities can be taken from table 9. Before transfection the astrocyte medium was removed and collected in a 50 ml falcon ("conditioned astrocyte medium"). The appropriate amount of Opti- MEM was added to each well and the cells were put back into the incubator. DNA as well as lipofectamin was diluted in Opti- MEM in two separate 1.5 ml reaction tubes, according to table 9, incubated for 5 min and then the DNA dilution was added to the transfection reagent dilution. This mix was incubated for 20 min at RT and then added drop- wise to the cells. After 4 h the transfection mix was removed and the prior collected conditioned astrocyte medium was added to the cells.

Table 9 | Seeding density and volume of reagents for Astrocytes transfection

Plate size	Cell number	Volume of plating medium	Volume of dilution medium	DNA	L2K
24 well	60000	300 µl	2x 50 µl	600 ng	0,75 µl
12 well	100000	600 µl	2x 100 µl	1200 ng	1,5 µl
6 well	350000	1 ml	2x 125 µl	2000 ng	3 µl

4.6 Indirect immunofluorescence microscopy

4.6.1 Staining of Tissue Culture on coverslips

Cells were seeded on poly-l-lysine treated coverslips. Cells were then fixed in 4% (v/v) paraformaldehyde (in 1x PBS) for 20 minutes at 37°C followed by permeabilization with 0.1% (v/v) Triton X-100 (in 1x PBS). Next, cells were blocked in 10% FBS for 30 minutes at RT. Cells were then incubated overnight (at 4°C) with the appropriate primary antibodies, diluted in 3% BSA (in 1x PBS). Coverslips were then washed with 1x PBS supplemented with 0.1% Triton X-100 for 1x 5 min and additionally with 1x PBS for 3x 5 min at RT. Primary antibodies were detected using secondary antibodies with fluorophores, diluted in 0.1% Triton X-100 (in PBS) at 1:1000 and incubated for 2h at RT. Following this, coverslips were washed one time with PBS supplemented with 0.1% TX100 (Sigma) and twice with 1x PBS only. Finally, DNA was stained with DAPI (1 µg/ml) for five minutes at RT. Coverslips were mounted on top of slides using Aqua- Poly mounting medium and stored until further analysis.

4.6.2 Staining of free floating brain slices

After taking out them out of the storing solution, the brain slices were washed on a shaker with PBS for 10 min at RT. The tissue was blocked and permeabilized by incubation in PBS, supplemented with 0.5% (v/v) TritonX100 and 10% (v/v) normal goat serum (NGS) for 30 min to 2 h at RT on a shaker. Primary antibodies were diluted appropriately, in the previous described blocking solution. Slices were then incubated overnight at 4°C on a shaker. Brain slices are washed 3- times with PBS prior to incubation with secondary antibodies, which are diluted 1:500 in blocking solution. Secondary antibodies are left on the slices for 2 h at RT on

a shaker. Chromatin is stained with DAPI diluted 1:1000 in PBS for 10 min at RT. The slices were then washed another 3 times with PBS and were then mounted on glass objective slides.

5. Animal methods

5.1 Mouse strains

B57BL6/J Aldh1l1-Cre

B57BL6/J ROSA26_dCas9-VPR_CRKI, carrying a transgene consisting of a CAG Promoter followed by a loxP STOP loxP cassette. This loxP STOP loxP site prevents expression of the transcriptional activation machinery consisting of the MS2 RNA binding protein fused to the transcription factor p65 and heatshock protein HSF1 (Konermann et al. 2014b). This transcriptional frame is continued by a P2A sequence and dCas9 fused to VP64, p65 and Rta (Chavez et al. 2015).

B57BL6/J ROSA26_dCas9-VPR_CRKIxAldh1l1-Cre. To provide Cre expression in Aldh1l1 positive cells.

5.2 Genotyping of transgenic mice

Lysis buffer

1 M NaCl

1 M Tris/HCl pH 8.5

10% SDS

0.5 M EDTA

10mg/ ml Proteinase K

Genotyping was performed by PCR on genomic DNA extracted from ear clip biopsies. Ear clips were incubated with 0.5 ml lysis buffer at 55°C in a shaker (100 rpm) over night. Undissolved tissue was removed by centrifugation at 14000 rpm for 5 min. The supernatant was transferred to a new 1.5 ml reaction tube and DNA was precipitated with 0.5 ml 100% Isopropanol and pelleted by centrifugation at 14000 rpm for 10 min. After removing the residual supernatant, the pellet was air- dried at room temperature for at least 30 min. DNA pellets were dissolved in 200 µl 10 mM Tris buffer (pH 8) in a thermomixer at 55°C and 100 rpm.

Primers for PCR reactions are listed in table 10 and PCR compositions as well as PCR conditions are listed in Tables 10 and 11.

Table 10 | Genotyping PCR compostion

Name	Buffer A	$MgCl_2$ (25mM)	Q- Solution	primers	dNTPs (10 mM)	Taq	H_2O
Aldh1l1-Cre	2.5 µl	2.5 µl	5 µl	0.5 µl	0.5 µl	0.5 µl	11 µl
dCas9- VPR	2.5 µl	2.5 µl	5 µl	0.5 µl	0.5 µl	0.5 µl	11 µl

Table 11 | Genotyping PCR conditions

Name	Aldh1l1- Cre		dCas9- VPR	
1.Initial Denaturation	95°C	2 min	95°C	2 min
2. Denaturation	95°C	30 s	95°C	30 s
3. Annealing	58°C	30 s	58 °C	30 s
4. Elongation	72°C	2.5 min to 2. 35x	72°C	2.5 min to 2. 35x
5.Final Elongation	72°C	5 min	72°C	5 min
Fragment size	420 bp		2.2 kb	

5.3 Stereotactic operations

5.3.1 Anesthesia

Mice were anaesthetized with an intraperitoneal injection of a mix of Fentanyl (0.05 mg/kg bodyweight), Midazolam (5 mg/kg bodyweight) and Medetomidine (0.5 mg/kg bodyweight) dissolved in a 0.9% NaCl (a solution called “Sleep”). After surgery the mice were recovered from anesthesia with a mix of Buprenorphine (0.1 mg/kg bodyweight), Atipamezol (2.5 mg/kg bodyweight) and Flumazenil (0.5 mg/kg bodyweight) in 0.9% NaCl.

5.3.2 Stab wound injury

After verification of successful anesthesia, the fur on top of the skull was shaved using an electric razor. Mice were immobilized in a sterotactic apparatus and the skull was exposed with a cut of the integument. The skull was opened with a dental drill, above the somatosensory cortex and the right cortical hemisphere was subjected to a 0.5 mm deep and 1mm long stab wound injury using a microblade. The wound was closed using a mono-filament and three stitches.

5.3.3 Injection

Three days post injury the mice were anaesthetized and immobilized as described above. Viral particles (300µl total volume) were injected into the center of the injury side (0.5 mm deep) using a pulled glass pipette and a positive displacement pump. Particles were injected with 30 nl/min in short start/stop intervals (5s injection – 5s pause). Subsequently the wound was closed using a mono- filament and three stitches.

5.3.4 Perfusion and Fixation

Animals were anaesthetized by injection of Ketamin and transcardially perfused with PBS followed by 4% paraformaldehyde. Brains were then isolated and fixed in 4% PFA at 4°C overnight, washed with and then stored in PBS.

5.3.5 Preparation of brain slices

To prevent ice crystals from breaking cell membranes, brains were cryoprotected. Brains were transferred to 15 ml tubes with 30% (w/v) sucrose in PBS and incubated at 4°C until the tissue sinks.

Brains were then cut into 70 µm floating sections at the cryostat with a chamber temperature of 4°C, an object head temperature of -35°C and -10°C while cutting. Sliced were stored in storing solution at -20°C.

References

Acloque, H. et al. 2009. “Epithelial-Mesenchymal Transitions: The Importance of Changing Cell State in Development and Disease.” *J Clin Invest* 119(6): 1438–49.

Adli, Mazhar. 2018. “The CRISPR Tool Kit for Genome Editing and Beyond.” *Nature Communications* 9(1): 1–13.

Alcamo, Elizabeth A. et al. 2008. “Satb2 Regulates Callosal Projection Neuron Identity in the Developing Cerebral Cortex.” *Neuron* 57(3): 364–77.

Amabile, A. et al. 2016. “Inheritable Silencing of Endogenous Genes by Hit-and-Run Targeted Epigenetic Editing.” *Cell* 167(1): 219-232.e14.

Ammal Kaidery, Navneet, Shaista Tarannum, and Bobby Thomas. 2013. “Epigenetic Landscape of Parkinson’s Disease: Emerging Role in Disease Mechanisms and Therapeutic Modalities.” *Neurotherapeutics: The Journal of the American Society for Experimental NeuroTherapeutics* 10(4): 698–708.

Anders, C., O. Niewoehner, A. Duerst, and M. Jinek. 2014. “Structural Basis of PAM-Dependent Target DNA Recognition by the Cas9 Endonuclease.” *Nature* 513(7519): 569–73.

Anton, T., and S. Bultmann. 2017. “Site-Specific Recruitment of Epigenetic Factors with a Modular CRISPR/Cas System.” *Nucleus* 8(3): 279–86.

Arimbasseri, Aneeshkumar G., Keshab Rijal, and Richard J. Maraia. 2013. “Transcription Termination by the Eukaryotic RNA Polymerase III.” *Biochimica et biophysica acta* 1829(3–4): 318–30.

Arita, Kyohei et al. 2008. “Recognition of Hemi-Methylated DNA by the SRA Protein UHRF1 by a Base-Flipping Mechanism.” *Nature* 455(7214): 818–21.

Arlotta, Paola et al. 2005. “Neuronal Subtype-Specific Genes That Control Corticospinal Motor Neuron Development in Vivo.” *Neuron* 45(2): 207–21.

Bae, Sangsu, Jiyeon Kweon, Heon Seok Kim, and Jin-Soo Kim. 2014. “Microhomology-Based Choice of Cas9 Nuclease Target Sites.” *Nature Methods* 11(7): 705–6.

Bahar Halpern, Keren, Tal Vana, and Michael D. Walker. 2014. “Paradoxical Role of DNA Methylation in Activation of FoxA2 Gene Expression during Endoderm Development.” *The Journal of Biological Chemistry* 289(34): 23882–92.

Balboa, D. et al. 2015. “Conditionally Stabilized DCas9 Activator for Controlling Gene Expression in Human Cell Reprogramming and Differentiation.” *Stem Cell Reports* 5(3): 448–59.

Baranek, Constanze et al. 2012. “Protooncogene Ski Cooperates with the Chromatin-Remodeling Factor Satb2 in Specifying Callosal Neurons.” *Proceedings of the National Academy of Sciences of the United States of America* 109(9): 3546–51.

Barbosa, Joana S. et al. 2015. “Neurodevelopment. Live Imaging of Adult Neural Stem Cell Behavior in the Intact and Injured Zebrafish Brain.” *Science (New York, N.Y.)* 348(6236): 789–93.

Barbosa, Joana S., Rossella Di Giaimo, Magdalena Götz, and Jovica Ninkovic. 2016. “Single-Cell in Vivo Imaging of Adult Neural Stem Cells in the Zebrafish Telencephalon.” *Nature Protocols* 11(8): 1360–70.

Barski, Artem et al. 2007. “High-Resolution Profiling of Histone Methylations in the Human Genome.” *Cell* 129(4): 823–37.

Baumann, Valentin et al. 2019. “Targeted Removal of Epigenetic Barriers during Transcriptional Reprogramming.” *Nature Communications* 10(1): 2119.

Berninger, Benedikt et al. 2007. “Functional Properties of Neurons Derived from In Vitro Reprogrammed Postnatal Astroglia.” *The Journal of Neuroscience* 27(32): 8654–64.

Bernstein, Bradley E. et al. 2005. “Genomic Maps and Comparative Analysis of Histone Modifications in Human and Mouse.” *Cell* 120(2): 169–81.

Bianconi, E. et al. 2013. “An Estimation of the Number of Cells in the Human Body.” *Ann Hum Biol* 40(6): 463–71.

Black, Brian L., Keith L. Ligon, Yuan Zhang, and Eric N. Olson. 1996. “Cooperative Transcriptional Activation by the Neurogenic Basic Helix-Loop-Helix Protein MASH1 and Members of the Myocyte Enhancer Factor-2 (MEF2) Family.” *Journal of Biological Chemistry* 271(43): 26659–63.

Black, Joshua B. et al. 2016. “Targeted Epigenetic Remodeling of Endogenous Loci by CRISPR/Cas9-Based Transcriptional Activators Directly Converts Fibroblasts to Neuronal Cells.” *Cell Stem Cell* 19(3): 406–14.

de Boni, Laura et al. 2018. “DNA Methylation Alterations in IPSC- and HESC-Derived Neurons: Potential Implications for Neurological Disease Modeling.” *Clinical Epigenetics* 10(1): 13.

Boonsanay, Verawan et al. 2016. “Regulation of Skeletal Muscle Stem Cell Quiescence by Suv4-20h1-Dependent Facultative Heterochromatin Formation.” *Cell Stem Cell* 18(2): 229–42.

Booth, Michael J., Eun-Ang Raiber, and Shankar Balasubramanian. 2015. “Chemical Methods for Decoding Cytosine Modifications in DNA.” *Chemical Reviews* 115(6): 2240–54.

Boyer, Laurie A. et al. 2006. “Polycomb Complexes Repress Developmental Regulators in Murine Embryonic Stem Cells.” *Nature* 441(7091): 349–53.

Breunig, C. T. et al. 2018a. “One Step Generation of Customizable GRNA Vectors for Multiplex CRISPR Approaches through String Assembly GRNA Cloning (STAgR).” *PLoS One* 13(4): e0196015.

Breunig, Christopher T. et al. 2018. “A Customizable Protocol for String Assembly GRNA Cloning (STAgR).” *JoVE (Journal of Visualized Experiments)* (142): e58556.

Britanova, Olga et al. 2008. “Satb2 Is a Postmitotic Determinant for Upper-Layer Neuron Specification in the Neocortex.” *Neuron* 57(3): 378–92.

Buckley, R. H. 2004. “Molecular Defects in Human Severe Combined Immunodeficiency and Approaches to Immune Reconstitution.” *Annu Rev Immunol* 22: 625–55.

Buckley, Rebecca H. 2004. “The Multiple Causes of Human SCID.” *Journal of Clinical Investigation* 114(10): 1409–11.

Bultmann, Sebastian, and Stefan H. Stricker. 2018. “Entering the Post-Epigenomic Age: Back to Epigenetics.” *Open Biology* 8(3): 180013.

Buryanov, Yaroslav, and Taras Shevchuk. 2005. “The Use of Prokaryotic DNA Methyltransferases as Experimental and Analytical Tools in Modern Biology.” *Analytical Biochemistry* 338(1): 1–11.

Cano-Rodriguez, D. et al. 2016. “Writing of H3K4Me3 Overcomes Epigenetic Silencing in a Sustained but Context-Dependent Manner.” *Nat Commun* 7: 12284.

Caviness, V. S., and T. Takahashi. 1995. “Proliferative Events in the Cerebral Ventricular Zone.” *Brain & Development* 17(3): 159–63.

Cedar, Howard, and Yehudit Bergman. 2009. “Linking DNA Methylation and Histone Modification: Patterns and Paradigms.” *Nature Reviews. Genetics* 10(5): 295–304.

Chakraborty, S. et al. 2014. “A CRISPR/Cas9-Based System for Reprogramming Cell Lineage Specification.” *Stem Cell Reports* 3(6): 940–47.

Chavez, Alejandro et al. 2015. “Highly Efficient Cas9-Mediated Transcriptional Programming.” *Nature Methods* 12(4): 326–28.

Chavez, Alejandro et al. 2016. “Comparison of Cas9 Activators in Multiple Species.” *Nature Methods* 13(7): 563–67.

Chen, Renchao, Xiaoji Wu, Lan Jiang, and Yi Zhang. 2017. “Single-Cell RNA-Seq Reveals Hypothalamic Cell Diversity.” *Cell reports* 18(13): 3227–41.

Cheng, A. W. et al. 2013. “Multiplexed Activation of Endogenous Genes by CRISPR-on, an RNA-Guided Transcriptional Activator System.” *Cell Res* 23(10): 1163–71.

Chou, Shen-Ju, and Dennis D. M. O’Leary. 2013. “Role for Lhx2 in Corticogenesis through Regulation of Progenitor Differentiation.” *Molecular and Cellular Neuroscience* 56: 1–9.

Choudhury, S. R. et al. 2016. “CRISPR-DCas9 Mediated TET1 Targeting for Selective DNA Demethylation at BRCA1 Promoter.” *Oncotarget* 7(29): 46545–56.

Chouliaras, Leonidas et al. 2013. “Consistent Decrease in Global DNA Methylation and Hydroxymethylation in the Hippocampus of Alzheimer’s Disease Patients.” *Neurobiology of Aging* 34(9): 2091–99.

Condliffe, Daniel et al. 2014. “Cross-Region Reduction in 5-Hydroxymethylcytosine in Alzheimer’s Disease Brain.” *Neurobiology of Aging* 35(8): 1850–54.

Coppieters, Natacha et al. 2014. “Global Changes in DNA Methylation and Hydroxymethylation in Alzheimer’s Disease Human Brain.” *Neurobiology of Aging* 35(6): 1334–44.

Corish, Pete, and Chris Tyler-Smith. 1999. “Attenuation of Green Fluorescent Protein Half-Life in Mammalian Cells.” *Protein Engineering, Design and Selection* 12(12): 1035–40.

Coutts, Margaret, and Hans S. Keirstead. 2008. “Stem Cells for the Treatment of Spinal Cord Injury.” *Experimental Neurology* 209(2): 368–77.

Cubelos, Beatriz et al. 2010. “Cux1 and Cux2 Regulate Dendritic Branching, Spine Morphology, and Synapses of the Upper Layer Neurons of the Cortex.” *Neuron* 66(4): 523–35.

Darst, Russell P. et al. 2010. “Bisulfite Sequencing of DNA.” *Current protocols in molecular biology / edited by Frederick M. Ausubel ... [et al.]* CHAPTER: Unit-7.917.

Davis, R. L., H. Weintraub, and A. B. Lassar. 1987. “Expression of a Single Transfected CDNA Converts Fibroblasts to Myoblasts.” *Cell* 51(6): 987–1000.

De Jager, Philip L et al. 2014. “Alzheimer’s Disease: Early Alterations in Brain DNA Methylation at ANK1, BIN1, RHBDF2 and Other Loci.” *Nature Neuroscience* 17(9): 1156–63.

Delile, Julien et al. 2019. “Single Cell Transcriptomics Reveals Spatial and Temporal Dynamics of Gene Expression in the Developing Mouse Spinal Cord.” *Development* 146(12): dev173807.

Diniz, Luan Pereira et al. 2017. “Astrocyte Transforming Growth Factor Beta 1 Protects Synapses against Aβ Oligomers in Alzheimer’s Disease Model.” *The Journal of Neuroscience: The Official Journal of the Society for Neuroscience* 37(28): 6797–6809.

Doench, J. G. et al. 2014. “Rational Design of Highly Active SgRNAs for CRISPR-Cas9-Mediated Gene Inactivation.” *Nat Biotechnol* 32(12): 1262–67.

Doench, John G. et al. 2016. “Optimized SgRNA Design to Maximize Activity and Minimize Off-Target Effects of CRISPR-Cas9.” *Nature biotechnology* 34(2): 184–91.

Dow, L. E. et al. 2015. “Inducible in Vivo Genome Editing with CRISPR-Cas9.” *Nat Biotechnol* 33(4): 390–94.

Duncan, Christopher G. et al. 2018. “Dosage Compensation and DNA Methylation Landscape of the X Chromosome in Mouse Liver.” *Scientific Reports* 8(1): 1–17.

Durovic, Tamara, and Jovica Ninkovic. 2019. “Electroporation Method for In Vivo Delivery of Plasmid DNA in the Adult Zebrafish Telencephalon.” *JoVE (Journal of Visualized Experiments)* (151): e60066.

Engler, Carola, Romy Kandzia, and Sylvestre Marillonnet. 2008. “A One Pot, One Step, Precision Cloning Method with High Throughput Capability.” *PLoS ONE* 3(11). https://www.ncbi.nlm.nih.gov/pmc/articles/PMC2574415/ (November 4, 2019).

Ertekin-Taner, Nilüfer. 2010. “Genetics of Alzheimer Disease in the Pre- and Post-GWAS Era.” *Alzheimer’s Research & Therapy* 2(1): 3.

Fame, Ryann M., Jessica L. MacDonald, and Jeffrey D. Macklis. 2011. “Development, Specification, and Diversity of Callosal Projection Neurons.” *Trends in Neurosciences* 34(1): 41–50.

Fang, Jian et al. 2016. “Hemi-Methylated DNA Opens a Closed Conformation of UHRF1 to Facilitate Its Histone Recognition.” *Nature Communications* 7: 11197.

Foraker, Jessica et al. 2015. “The APOE Gene Is Differentially Methylated in Alzheimer’s Disease.” *Journal of Alzheimer’s disease: JAD* 48(3): 745–55.

Frauer, Carina et al. 2011. “Recognition of 5-Hydroxymethylcytosine by the Uhrf1 SRA Domain.” *PloS One* 6(6): e21306.

Funato, Kosuke et al. 2014. “Use of Human Embryonic Stem Cells to Model Pediatric Gliomas with H3.3K27M Histone Mutation.” *Science (New York, N.Y.)* 346(6216): 1529–33.

Gao, X. et al. 2014. “Comparison of TALE Designer Transcription Factors and the CRISPR/DCas9 in Regulation of Gene Expression by Targeting Enhancers.” *Nucleic Acids Res* 42(20): e155.

Gascón, Sergio et al. 2015. “Identification and Successful Negotiation of a Metabolic Checkpoint in Direct Neuronal Reprogramming.” *Cell Stem Cell*.

Gasiunas, Giedrius, Rodolphe Barrangou, Philippe Horvath, and Virginijus Siksnys. 2012. “Cas9-CrRNA Ribonucleoprotein Complex Mediates Specific DNA Cleavage for Adaptive Immunity in Bacteria.” *Proceedings of the National Academy of Sciences of the United States of America* 109(39): E2579-2586.

Gibson, Daniel G et al. 2009a. “Enzymatic Assembly of DNA Molecules up to Several Hundred Kilobases.” *Nature Methods* 6(5): 343–45.

Gilbert, Luke A. et al. 2013. “CRISPR-Mediated Modular RNA-Guided Regulation of Transcription in Eukaryotes.” *Cell* 154(2): 442–51.

Goate, A. et al. 1991. “Segregation of a Missense Mutation in the Amyloid Precursor Protein Gene with Familial Alzheimer’s Disease.” *Nature* 349(6311): 704–6.

Gohlke, Julia M. et al. 2008. “Characterization of the Proneural Gene Regulatory Network during Mouse Telencephalon Development.” *BMC Biology* 6: 15.

Guo, Ziyuan et al. 2014. “In Vivo Direct Reprogramming of Reactive Glial Cells into Functional Neurons after Brain Injury and in an Alzheimer’s Disease Model.” *Cell Stem Cell* 14(2): 188–202.

Haeussler, Maximilian et al. 2016. “Evaluation of Off-Target and on-Target Scoring Algorithms and Integration into the Guide RNA Selection Tool CRISPOR.” *Genome Biology* 17(1): 148.

Hardwick, J. M. et al. 1992. “The Epstein-Barr Virus R Transactivator (Rta) Contains a Complex, Potent Activation Domain with Properties Different from Those of VP16.” *J Virol* 66(9): 5500–5508.

Harris, Henry. 1999. *The Birth of the Cell*. New Haven, Conn. ; London: Yale University Press.

He, Y. F. et al. 2011. “Tet-Mediated Formation of 5-Carboxylcytosine and Its Excision by TDG in Mammalian DNA.” *Science* 333(6047): 1303–7.

Heidenreich, Kim A., and Daniel A. Linseman. 2004. “Myocyte Enhancer Factor-2 Transcription Factors in Neuronal Differentiation and Survival.” *Molecular Neurobiology* 29(2): 155–65.

Heinrich, Christophe et al. 2010. “Directing Astroglia from the Cerebral Cortex into Subtype Specific Functional Neurons.” *PLoS biology* 8(5): e1000373.

Heinrich, Christophe, Francesca M. Spagnoli, and Benedikt Berninger. 2015. “In Vivo Reprogramming for Tissue Repair.” *Nature Cell Biology* 17(3): 204–11.

Heins, Nico et al. 2002. “Glial Cells Generate Neurons: The Role of the Transcription Factor Pax6.” *Nature Neuroscience* 5(4): 308–15.

Heintzman, Nathaniel D. et al. 2007. “Distinct and Predictive Chromatin Signatures of Transcriptional Promoters and Enhancers in the Human Genome.” *Nature Genetics* 39(3): 311–18.

Heintzman, Nathaniel D et al. 2009. “Histone Modifications at Human Enhancers Reflect Global Cell-Type-Specific Gene Expression.” *Nature* 459(7243): 108–12.

Henderson, Ian R. et al. 2010. “The de Novo Cytosine Methyltransferase DRM2 Requires Intact UBA Domains and a Catalytically Mutated Paralog DRM3 during RNA-Directed DNA Methylation in Arabidopsis Thaliana.” *PLoS genetics* 6(10): e1001182.

Hermann, Mario et al. 2014. “Binary Recombinase Systems for High-Resolution Conditional Mutagenesis.” *Nucleic Acids Research* 42(6): 3894–3907.

Hilton, I. B. et al. 2015. “Epigenome Editing by a CRISPR-Cas9-Based Acetyltransferase Activates Genes from Promoters and Enhancers.” *Nat Biotechnol* 33(5): 510–17.

Holliday, R., and J. E. Pugh. 1975. “DNA Modification Mechanisms and Gene Activity during Development.” *Science (New York, N.Y.)* 187(4173): 226–32.

Hotchkiss, R. D. 1948. “The Quantitative Separation of Purines, Pyrimidines, and Nucleosides by Paper Chromatography.” *J Biol Chem* 175(1): 315–32.

Huang, Y. H. et al. 2017. “DNA Epigenome Editing Using CRISPR-Cas SunTag-Directed DNMT3A.” *Genome Biol* 18(1): 176.

Ieda, M. et al. 2010. “Direct Reprogramming of Fibroblasts into Functional Cardiomyocytes by Defined Factors.” *Cell* 142(3): 375–86.

Ishino, Y. et al. 1987. “Nucleotide Sequence of the Iap Gene, Responsible for Alkaline Phosphatase Isozyme Conversion in Escherichia Coli, and Identification of the Gene Product.” *Journal of Bacteriology* 169(12): 5429–33.

Ito, S. et al. 2011. “Tet Proteins Can Convert 5-Methylcytosine to 5-Formylcytosine and 5-Carboxylcytosine.” *Science* 333(6047): 1300–1303.

Iurlaro, Mario et al. 2013. “A Screen for Hydroxymethylcytosine and Formylcytosine Binding Proteins Suggests Functions in Transcription and Chromatin Regulation.” *Genome Biology* 14(10): R119.

Jabaudon, Denis. 2017. “Fate and Freedom in Developing Neocortical Circuits.” *Nature Communications* 8(1): 1–9.

Jaenisch, Rudolf, and Adrian Bird. 2003. “Epigenetic Regulation of Gene Expression: How the Genome Integrates Intrinsic and Environmental Signals.” *Nature Genetics* 33 Suppl: 245–54.

Jinek, Martin et al. 2012. “A Programmable Dual-RNA-Guided DNA Endonuclease in Adaptive Bacterial Immunity.” *Science (New York, N.Y.)* 337(6096): 816–21.

Joshi, Pushkar S. et al. 2008. “Bhlhb5 Regulates the Post-Mitotic Acquisition of Area Identities in Layers II–V of the Developing Neocortex.” *Neuron* 60(2): 258–72.

Jurkowski, Tomasz P., Mirunalini Ravichandran, and Peter Stepper. 2015. “Synthetic Epigenetics-towards Intelligent Control of Epigenetic States and Cell Identity.” *Clinical Epigenetics* 7: 18.

Kabadi, A. M., D. G. Ousterout, I. B. Hilton, and C. A. Gersbach. 2014. “Multiplex CRISPR/Cas9-Based Genome Engineering from a Single Lentiviral Vector.” *Nucleic Acids Res* 42(19): e147.

Kadkhodaei, Banafsheh et al. 2009. “Nurr1 Is Required for Maintenance of Maturing and Adult Midbrain Dopamine Neurons.” *The Journal of Neuroscience* 29(50): 15923–32.

Kadkhodaei, Banafshe et al. 2013. “Transcription Factor Nurr1 Maintains Fiber Integrity and Nuclear-Encoded Mitochondrial Gene Expression in Dopamine Neurons.” *Proceedings of the National Academy of Sciences of the United States of America* 110(6): 2360–65.

Kantor, B. et al. 2018. “Downregulation of SNCA Expression by Targeted Editing of DNA Methylation: A Potential Strategy for Precision Therapy in PD.” *Mol Ther* 26(11): 2638–49.

Kearns, N. A. et al. 2015. “Functional Annotation of Native Enhancers with a Cas9-Histone Demethylase Fusion.” *Nat Methods* 12(5): 401–3.

Kelsey, Gavin, Oliver Stegle, and Wolf Reik. 2017. “Single-Cell Epigenomics: Recording the Past and Predicting the Future.” *Science (New York, N.Y.)* 358(6359): 69–75.

Kim, Tae Hoon et al. 2005. “A High-Resolution Map of Active Promoters in the Human Genome.” *Nature* 436(7052): 876–80.

Koerner, Martha V. et al. 2012. “A Downstream CpG Island Controls Transcript Initiation and Elongation and the Methylation State of the Imprinted Airn Macro NcRNA Promoter.” *PLoS Genetics* 8(3). https://www.ncbi.nlm.nih.gov/pmc/articles/PMC3291542/ (September 15, 2019).

Konermann, S. et al. 2014a. “Genome-Scale Transcriptional Activation by an Engineered CRISPR-Cas9 Complex.” *Nature*. http://www.ncbi.nlm.nih.gov/pubmed/25494202.

Kriks, Sonja et al. 2011. “Dopamine Neurons Derived from Human ES Cells Efficiently Engraft in Animal Models of Parkinson’s Disease.” *Nature* 480(7378): 547–51.

Kumar, M., B. Keller, N. Makalou, and R. E. Sutton. 2001. “Systematic Determination of the Packaging Limit of Lentiviral Vectors.” *Human Gene Therapy* 12(15): 1893–1905.

Lambert, J. C. et al. 2013. “Meta-Analysis of 74,046 Individuals Identifies 11 New Susceptibility Loci for Alzheimer’s Disease.” *Nature Genetics* 45(12): 1452–58.

Latos, Paulina A. et al. 2009. “An in Vitro ES Cell Imprinting Model Shows That Imprinted Expression of the Igf2r Gene Arises from an Allele-Specific Expression Bias.” *Development (Cambridge, England)* 136(3): 437–48.

Lei, Yong et al. 2017a. “Targeted DNA Methylation in Vivo Using an Engineered DCas9-MQ1 Fusion Protein.” *Nature Communications* 8(1): 16026.

Leifer, D et al. 1993. “MEF2C, a MADS/MEF2-Family Transcription Factor Expressed in a Laminar Distribution in Cerebral Cortex.” *Proceedings of the National Academy of Sciences of the United States of America* 90(4): 1546–50.

Li, E., T. H. Bestor, and R. Jaenisch. 1992. “Targeted Mutation of the DNA Methyltransferase Gene Results in Embryonic Lethality.” *Cell* 69(6): 915–26.

Li, J. F. et al. 2013. “Multiplex and Homologous Recombination-Mediated Genome Editing in Arabidopsis and Nicotiana Benthamiana Using Guide RNA and Cas9.” *Nat Biotechnol* 31(8): 688–91.

Lin, Lin et al. 2018. “Genome-Wide Determination of on-Target and off-Target Characteristics for RNA-Guided DNA Methylation by DCas9 Methyltransferases.” *GigaScience* 7(3): 1–19.

Lister, Ryan et al. 2009. “Human DNA Methylomes at Base Resolution Show Widespread Epigenomic Differences.” *Nature* 462(7271): 315–22.

Liu, P. et al. 2018. “CRISPR-Based Chromatin Remodeling of the Endogenous Oct4 or Sox2 Locus Enables Reprogramming to Pluripotency.” *Cell Stem Cell* 22(2): 252-261.e4.

Liu, X. S. et al. 2016a. “Editing DNA Methylation in the Mammalian Genome.” *Cell* 167(1): 233-247.e17.

Liu, X. Shawn et al. 2018. “Rescue of Fragile X Syndrome Neurons by DNA Methylation Editing of the FMR1 Gene.” *Cell* 172(5): 979-992.e6.

Liu, Y. et al. 1999. “Crystal Structure of the Conserved Core of the Herpes Simplex Virus Transcriptional Regulatory Protein VP16.” *Genes Dev* 13(13): 1692–1703.

Lock, L. F., D. W. Melton, C. T. Caskey, and G. R. Martin. 1986. “Methylation of the Mouse Hprt Gene Differs on the Active and Inactive X Chromosomes.” *Molecular and Cellular Biology* 6(3): 914–24.

Lodato, Simona, Ashwin S. Shetty, and Paola Arlotta. 2015. “Cerebral Cortex Assembly: Generating and Reprogramming Projection Neuron Diversity.” *Trends in neurosciences* 38(2): 117–25.

Loo, Lipin et al. 2019. “Single-Cell Transcriptomic Analysis of Mouse Neocortical Development.” *Nature Communications* 10(1): 1–11.

Lord, Jenny, and Carlos Cruchaga. 2014. “The Epigenetic Landscape of Alzheimer’s Disease.” *Nature Neuroscience* 17(9): 1138–40.

Lowder, Levi G. et al. 2015. “A CRISPR/Cas9 Toolbox for Multiplexed Plant Genome Editing and Transcriptional Regulation.” *Plant Physiology* 169(2): 971–85.

Lu, Jianfeng, Robert A. Bradley, and Su-Chun Zhang. 2014. “Turning Reactive Glia into Functional Neurons in the Brain.” *Cell stem cell* 14(2): 133–34.

Lunnon, Katie et al. 2014. “Methylomic Profiling Implicates Cortical Deregulation of ANK1 in Alzheimer’s Disease.” *Nature Neuroscience* 17(9): 1164–70.

Luz-Madrigal, Agustín et al. 2019. “DNA Demethylation Is a Driver for Chick Retina Regeneration.” *bioRxiv*: 804161.

MacDonough, Tracy Marie. 2016. “Transcriptional Regulation Of Subcerebral Cortical Projection Neurons At Multiple Steps Of Mammalian Cortical Development.” UC Santa Cruz. https://escholarship.org/uc/item/3qp6h6zs (October 4, 2019).

Maeder, Morgan L. et al. 2013. “CRISPR RNA-Guided Activation of Endogenous Human Genes.” *Nature Methods* 10(10): 977–79.

Makarova, Kira S. et al. 2006. “A Putative RNA-Interference-Based Immune System in Prokaryotes: Computational Analysis of the Predicted Enzymatic Machinery, Functional Analogies with Eukaryotic RNAi, and Hypothetical Mechanisms of Action.” *Biology Direct* 1: 7.

Mali, Prashant et al. 2013. “CAS9 Transcriptional Activators for Target Specificity Screening and Paired Nickases for Cooperative Genome Engineering.” *Nature Biotechnology* 31(9): 833–38.

Mano, Tatsuo et al. 2017. “Neuron-Specific Methylome Analysis Reveals Epigenetic Regulation and Tau-Related Dysfunction of BRCA1 in Alzheimer’s Disease.” *Proceedings of the National Academy of Sciences of the United States of America* 114(45): E9645–54.

Mao, Zixu, and Bernardo Nadal-Ginard. 1996. “Functional and Physical Interactions between Mammalian Achaete-Scute Homolog 1 and Myocyte Enhancer Factor 2A.” *Journal of Biological Chemistry* 271(24): 14371–75.

Masserdotti, G., S. Gascon, and M. Gotz. 2016. “Direct Neuronal Reprogramming: Learning from and for Development.” *Development* 143(14): 2494–2510.

Masserdotti, Giacomo et al. 2015. “Transcriptional Mechanisms of Proneural Factors and REST in Regulating Neuronal Reprogramming of Astrocytes.” *Cell Stem Cell* 17(1): 74–88.

Mastroeni, Diego et al. 2010. “Epigenetic Changes in Alzheimer’s Disease: Decrements in DNA Methylation.” *Neurobiology of Aging* 31(12): 2025–37.

Daniilidou, M et al. 2011. “Epigenetic Mechanisms in Alzheimer’s Disease.” *Neurobiology of Aging* 32(7): 1161–80.

Mathys, Hansruedi et al. 2019. “Single-Cell Transcriptomic Analysis of Alzheimer’s Disease.” *Nature* 570(7761): 332–37.

Mattugini, Nicola et al. 2019. “Inducing Different Neuronal Subtypes from Astrocytes in the Injured Mouse Cerebral Cortex.” *Neuron* 103(6): 1086-1095.e5.

McEvilly, Robert J. et al. 2002. “Transcriptional Regulation of Cortical Neuron Migration by POU Domain Factors.” *Science (New York, N.Y.)* 295(5559): 1528–32.

Meissner, Alexander et al. 2008. “Genome-Scale DNA Methylation Maps of Pluripotent and Differentiated Cells.” *Nature* 454(7205): 766–70.

Mendenhall, Eric M. et al. 2013. “Locus-Specific Editing of Histone Modifications at Endogenous Enhancers.” *Nature Biotechnology* 31(12): 1133–36.

Mercorio, Roberta et al. 2018. “PICALM Gene Methylation in Blood of Alzheimer’s Disease Patients Is Associated with Cognitive Decline.” *Journal of Alzheimer’s disease: JAD* 65(1): 283–92.

Miller, Jeffrey C. et al. 2011. “A TALE Nuclease Architecture for Efficient Genome Editing.” *Nature Biotechnology* 29(2): 143–48.

Mitalipov, S., and D. Wolf. 2009. “Totipotency, Pluripotency and Nuclear Reprogramming.” *Adv Biochem Eng Biotechnol* 114: 185–99.

Molyneaux, Bradley J., Paola Arlotta, Joao R. L. Menezes, and Jeffrey D. Macklis. 2007. “Neuronal Subtype Specification in the Cerebral Cortex.” *Nature Reviews Neuroscience* 8(6): 427–37.

Moreno-Mateos, Miguel A. et al. 2015. “CRISPRscan: Designing Highly Efficient SgRNAs for CRISPR-Cas9 Targeting in Vivo.” *Nature Methods* 12(10): 982–88.

Morita, S. et al. 2016. “Targeted DNA Demethylation in Vivo Using DCas9-Peptide Repeat and ScFv-TET1 Catalytic Domain Fusions.” *Nat Biotechnol* 34(10): 1060–65.

Morris, S. A., and G. Q. Daley. 2013. “A Blueprint for Engineering Cell Fate: Current Technologies to Reprogram Cell Identity.” *Cell Res* 23(1): 33–48.

Moscou, Matthew J., and Adam J. Bogdanove. 2009. “A Simple Cipher Governs DNA Recognition by TAL Effectors.” *Science (New York, N.Y.)* 326(5959): 1501.

Naumann, Ulf et al. 2011. "Genetic Evidence That DNA Methyltransferase DRM2 Has a Direct Catalytic Role in RNA-Directed DNA Methylation in Arabidopsis Thaliana." *Genetics* 187(3): 977–79.

Nieto, Marta et al. 2004. "Expression of Cux-1 and Cux-2 in the Subventricular Zone and Upper Layers II–IV of the Cerebral Cortex." *Journal of Comparative Neurology* 479(2): 168–80.

Nishimasu, Hiroshi et al. 2014. "Crystal Structure of Cas9 in Complex with Guide RNA and Target DNA." *Cell* 156(5): 935–49.

Okada, M. et al. 2017. "Stabilization of Foxp3 Expression by CRISPR-DCas9-Based Epigenome Editing in Mouse Primary T Cells." *Epigenetics Chromatin* 10: 24.

Okano, M., D. W. Bell, D. A. Haber, and E. Li. 1999. "DNA Methyltransferases Dnmt3a and Dnmt3b Are Essential for de Novo Methylation and Mammalian Development." *Cell* 99(3): 247–57.

Paquet, Dominik et al. 2016. "Efficient Introduction of Specific Homozygous and Heterozygous Mutations Using CRISPR/Cas9." *Nature* 533(7601): 125–29.

Pelletier, J., and N. Sonenberg. 1988. "Internal Initiation of Translation of Eukaryotic MRNA Directed by a Sequence Derived from Poliovirus RNA." *Nature* 334(6180): 320–25.

Peters, Alan, and Edward G. Jones. 1984. *Cellular Components of the Cerebral Cortex*. Plenum Press.

Peterson, B. A. et al. 2016. "Genome-Wide Assessment of Efficiency and Specificity in CRISPR/Cas9 Mediated Multiple Site Targeting in Arabidopsis." *PLoS One* 11(9): e0162169.

Pflueger, Christian et al. 2018. "A Modular DCas9-SunTag DNMT3A Epigenome Editing System Overcomes Pervasive off-Target Activity of Direct Fusion DCas9-DNMT3A Constructs." *Genome Research*. http://genome.cshlp.org/content/early/2018/06/27/gr.233049.117 (August 24, 2019).

Qi, L. S. et al. 2013. "Repurposing CRISPR as an RNA-Guided Platform for Sequence-Specific Control of Gene Expression." *Cell* 152(5): 1173–83.

Ramesh, Vidya et al. 2016. "Loss of Uhrf1 in Neural Stem Cells Leads to Activation of Retroviral Elements and Delayed Neurodegeneration." *Genes & Development* 30(19): 2199–2212.

Renbaum, P et al. 1990. "Cloning, Characterization, and Expression in Escherichia Coli of the Gene Coding for the CpG DNA Methylase from Spiroplasma Sp. Strain MQ1(M.SssI)." *Nucleic Acids Research* 18(5): 1145–52.

Richmond, Timothy J., and Curt A. Davey. 2003. "The Structure of DNA in the Nucleosome Core." *Nature* 423(6936): 145–50.

Riggs, A. D. 1975. "X Inactivation, Differentiation, and DNA Methylation." *Cytogenetics and Cell Genetics* 14(1): 9–25.

Roth, Martin et al. 2010. “FoxG1 and TLE2 Act Cooperatively to Regulate Ventral Telencephalon Formation.” *Development* 137(9): 1553–62.

Roubroeks, Janou A. Y., Rebecca G. Smith, Daniel L. A. van den Hove, and Katie Lunnon. 2017. “Epigenetics and DNA Methylomic Profiling in Alzheimer’s Disease and Other Neurodegenerative Diseases.” *Journal of Neurochemistry* 143(2): 158–70.

Sadakierska-Chudy, Anna, Richard M. Kostrzewa, and Małgorzata Filip. 2015. “A Comprehensive View of the Epigenetic Landscape Part I: DNA Methylation, Passive and Active DNA Demethylation Pathways and Histone Variants.” *Neurotoxicity Research* 27(1): 84–97.

Sadowski, I., J. Ma, S. Triezenberg, and M. Ptashne. 1988. “GAL4-VP16 Is an Unusually Potent Transcriptional Activator.” *Nature* 335(6190): 563–64.

Sakuma, Tetsushi et al. 2015a. “Multiplex Genome Engineering in Human Cells Using All-in-One CRISPR/Cas9 Vector System.” *Scientific Reports* 4(1): 5400.

Santos-Rosa, Helena et al. 2002. “Active Genes Are Tri-Methylated at K4 of Histone H3.” *Nature* 419(6905): 407–11.

Saunderson, E. A. et al. 2017. “Hit-and-Run Epigenetic Editing Prevents Senescence Entry in Primary Breast Cells from Healthy Donors.” *Nat Commun* 8(1): 1450.

Seipel, K., O. Georgiev, and W. Schaffner. 1992. “Different Activation Domains Stimulate Transcription from Remote ('enhancer’) and Proximal ('promoter’) Positions.” *EMBO J* 11(13): 4961–68.

Selkoe, Dennis J. 2012. “Preventing Alzheimer’s Disease.” *Science (New York, N.Y.)* 337(6101): 1488–92.

Sharif, Jafar, and Haruhiko Koseki. 2018. “Hemimethylation: DNA’s Lasting Odd Couple.” *Science* 359(6380): 1102–3.

Sherrington, R. et al. 1995. “Cloning of a Gene Bearing Missense Mutations in Early-Onset Familial Alzheimer’s Disease.” *Nature* 375(6534): 754–60.

Sherrington, R et al. 1996. “Alzheimer’s Disease Associated with Mutations in Presenilin 2 Is Rare and Variably Penetrant.” *Human Molecular Genetics* 5(7): 985–88.

Simon, Christiane, Magdalena Götz, and Leda Dimou. 2011. “Progenitors in the Adult Cerebral Cortex: Cell Cycle Properties and Regulation by Physiological Stimuli and Injury.” *Glia* 59(6): 869–81.

Singer-Sam, J. et al. 1990. “Use of a HpaII-Polymerase Chain Reaction Assay to Study DNA Methylation in the Pgk-1 CpG Island of Mouse Embryos at the Time of X-Chromosome Inactivation.” *Molecular and Cellular Biology* 10(9): 4987–89.

Spitz, F., and E. E. Furlong. 2012. “Transcription Factors: From Enhancer Binding to Developmental Control.” *Nat Rev Genet* 13(9): 613–26.

Spruijt, Cornelia G. et al. 2013. “Dynamic Readers for 5-(Hydroxy)Methylcytosine and Its Oxidized Derivatives.” *Cell* 152(5): 1146–59.

St George-Hyslop, P. et al. 1992. “Genetic Evidence for a Novel Familial Alzheimer’s Disease Locus on Chromosome 14.” *Nature Genetics* 2(4): 330–34.

St George-Hyslop, P. H. et al. 1987. “The Genetic Defect Causing Familial Alzheimer’s Disease Maps on Chromosome 21.” *Science (New York, N.Y.)* 235(4791): 885–90.

Stepper, P. et al. 2017a. “Efficient Targeted DNA Methylation with Chimeric DCas9-Dnmt3a-Dnmt3L Methyltransferase.” *Nucleic Acids Res* 45(4): 1703–13.

Sternberg, S. H. et al. 2014. “DNA Interrogation by the CRISPR RNA-Guided Endonuclease Cas9.” *Nature* 507(7490): 62–67.

Strahl, B. D., and C. D. Allis. 2000. “The Language of Covalent Histone Modifications.” *Nature* 403(6765): 41–45.

Stricker, S. H., and M. Götz. 2018. “DNA-Methylation: Master or Slave of Neural Fate Decisions?” *Front Neurosci* 12: 5.

Stricker, Stefan H et al. 2008. “Silencing and Transcriptional Properties of the Imprinted Airn NcRNA Are Independent of the Endogenous Promoter.” *The EMBO Journal* 27(23): 3116–28.

Sugitani, Yoshinobu et al. 2002. “Brn-1 and Brn-2 Share Crucial Roles in the Production and Positioning of Mouse Neocortical Neurons.” *Genes & Development* 16(14): 1760–65.

Sun, Yirui et al. 2008. “Long-Term Tripotent Differentiation Capacity of Human Neural Stem (NS) Cells in Adherent Culture.” *Molecular and Cellular Neurosciences* 38(2): 245–58.

Takahashi, K., and S. Yamanaka. 2006. “Induction of Pluripotent Stem Cells from Mouse Embryonic and Adult Fibroblast Cultures by Defined Factors.” *Cell* 126(4): 663–76.

Tan, M. et al. 2011. “Identification of 67 Histone Marks and Histone Lysine Crotonylation as a New Type of Histone Modification.” *Cell* 146(6): 1016–28.

Tanenbaum, M. E. et al. 2014. “A Protein-Tagging System for Signal Amplification in Gene Expression and Fluorescence Imaging.” *Cell* 159(3): 635–46.

Tarabykin, V., A. Stoykova, N. Usman, and P. Gruss. 2001. “Cortical Upper Layer Neurons Derive from the Subventricular Zone as Indicated by Svet1 Gene Expression.” *Development (Cambridge, England)* 128(11): 1983–93.

Teerawanichpan, Prapapan et al. 2004. “Characterization of Two Rice DNA Methyltransferase Genes and RNAi-Mediated Reactivation of a Silenced Transgene in Rice Callus.” *Planta* 218(3): 337–49.

Telley, Ludovic et al. 2016. “Sequential Transcriptional Waves Direct the Differentiation of Newborn Neurons in the Mouse Neocortex.” *Science* 351(6280): 1443–46.

Tessarz, P., and T. Kouzarides. 2014. “Histone Core Modifications Regulating Nucleosome Structure and Dynamics.” *Nat Rev Mol Cell Biol* 15(11): 703–8.

Tohgi, H., K. Utsugisawa, Y. Nagane, M. Yoshimura, Y. Genda, et al. 1999. “Reduction with Age in Methylcytosine in the Promoter Region -224 Approximately -101 of the Amyloid Precursor Protein Gene in Autopsy Human Cortex.” *Brain Research. Molecular Brain Research* 70(2): 288–92.

Tohgi, H., K. Utsugisawa, Y. Nagane, M. Yoshimura, M. Ukitsu, et al. 1999. “The Methylation Status of Cytosines in a Tau Gene Promoter Region Alters with Age to Downregulate Transcriptional Activity in Human Cerebral Cortex.” *Neuroscience Letters* 275(2): 89–92.

Tulloch, Jessica et al. 2018. “Glia-Specific APOE Epigenetic Changes in the Alzheimer’s Disease Brain.” *Brain Research* 1698: 179–86.

Urdinguio, Rocio G., Jose V. Sanchez-Mut, and Manel Esteller. 2009. “Epigenetic Mechanisms in Neurological Diseases: Genes, Syndromes, and Therapies.” *The Lancet. Neurology* 8(11): 1056–72.

Urnov, Fyodor D. et al. 2005. “Highly Efficient Endogenous Human Gene Correction Using Designed Zinc-Finger Nucleases.” *Nature* 435(7042): 646–51.

Vad-Nielsen, J., K. R. Gammelgaard, T. F. Daugaard, and A. L. Nielsen. 2019. “Cause-and-Effect Relationship between FGFR1 Expression and Epithelial-Mesenchymal Transition in EGFR-Mutated Non-Small Cell Lung Cancer Cells.” *Lung Cancer* 132: 132–40.

Van Broeckhoven, C. et al. 1992. “Mapping of a Gene Predisposing to Early-Onset Alzheimer’s Disease to Chromosome 14q24.3.” *Nature Genetics* 2(4): 335–39.

Van Cauwenberghe, Caroline, Christine Van Broeckhoven, and Kristel Sleegers. 2016. “The Genetic Landscape of Alzheimer Disease: Clinical Implications and Perspectives.” *Genetics in Medicine: Official Journal of the American College of Medical Genetics* 18(5): 421–30.

Vaquerizas, J. M., S. K. Kummerfeld, S. A. Teichmann, and N. M. Luscombe. 2009. “A Census of Human Transcription Factors: Function, Expression and Evolution.” *Nat Rev Genet* 10(4): 252–63.

Vazquez-Vilar, M. et al. 2016. “A Modular Toolbox for GRNA-Cas9 Genome Engineering in Plants Based on the GoldenBraid Standard.” *Plant Methods* 12: 10.

Vickaryous, M. K., and B. K. Hall. 2006. “Human Cell Type Diversity, Evolution, Development, and Classification with Special Reference to Cells Derived from the Neural Crest.” *Biol Rev Camb Philos Soc* 81(3): 425–55.

Vierbuchen, Thomas et al. 2010. “Direct Conversion of Fibroblasts to Functional Neurons by Defined Factors.” *Nature* 463(7284): 1035–41.

Vojta, A. et al. 2016a. “Repurposing the CRISPR-Cas9 System for Targeted DNA Methylation.” *Nucleic Acids Res* 44(12): 5615–28.

Waddington, C. H. 1957. *The Strategy of the Genes; a Discussion of Some Aspects of Theoretical Biology*. London,: Allen & Unwin.

Waddington, CH. 2012. “The Epigenotype. 1942.” *Int J Epidemiol* 41(1): 10–13.

Wang, C. et al. 2015. “A Simple CRISPR/Cas9 System for Multiplex Genome Editing in Rice.” *J Genet Genomics* 42(12): 703–6.

Wang, H., M. La Russa, and L. S. Qi. 2016. “CRISPR/Cas9 in Genome Editing and Beyond.” *Annu Rev Biochem* 85: 227–64.

Whyte, W. A. et al. 2013. “Master Transcription Factors and Mediator Establish Super-Enhancers at Key Cell Identity Genes.” *Cell* 153(2): 307–19.

Woltjen, K. et al. 2009. “PiggyBac Transposition Reprograms Fibroblasts to Induced Pluripotent Stem Cells.” *Nature* 458(7239): 766–70.

Wu, Tao P. et al. 2016. “DNA Methylation on N(6)-Adenine in Mammalian Embryonic Stem Cells.” *Nature* 532(7599): 329–33.

Wu, X. et al. 2014. “Genome-Wide Binding of the CRISPR Endonuclease Cas9 in Mammalian Cells.” *Nat Biotechnol* 32(7): 670–76.

Xie, C. et al. 2017. “SgRNA Expression of CRIPSR-Cas9 System Based on MiRNA Polycistrons as a Versatile Tool to Manipulate Multiple and Tissue-Specific Genome Editing.” *Sci Rep* 7(1): 5795.

Xie, K., B. Minkenberg, and Y. Yang. 2015. “Boosting CRISPR/Cas9 Multiplex Editing Capability with the Endogenous TRNA-Processing System.” *Proc Natl Acad Sci U S A* 112(11): 3570–75.

Xu, X. et al. 2016. “A CRISPR-Based Approach for Targeted DNA Demethylation.” *Cell Discov* 2: 16009.

Yamauchi, Takaki et al. 2014. “The MET1b Gene Encoding a Maintenance DNA Methyltransferase Is Indispensable for Normal Development in Rice.” *Plant Molecular Biology* 85(3): 219–32.

Yan, Q. et al. 2016. “Multiplex CRISPR/Cas9-Based Genome Engineering Enhanced by Drosha-Mediated SgRNA-ShRNA Structure.” *Sci Rep* 6: 38970.

Yu, Huimei et al. 2015. “Tet3 Regulates Synaptic Transmission and Homeostatic Plasticity via DNA Oxidation and Repair.” *Nature Neuroscience* 18(6): 836–43.

Zalatan, J. G. et al. 2015. “Engineering Complex Synthetic Transcriptional Programs with CRISPR RNA Scaffolds.” *Cell* 160(1–2): 339–50.

Zeisel, Amit et al. 2015. “Cell Types in the Mouse Cortex and Hippocampus Revealed by Single-Cell RNA-Seq.” *Science* 347(6226): 1138–42.

Zetche, Bernd, Sara E. Volz, and Feng Zhang. 2015. “A Split Cas9 Architecture for Inducible Genome Editing and Transcription Modulation.” *Nature biotechnology* 33(2): 139–42.

Zhang, Feng et al. 2011. “Programmable Sequence-Specific Transcriptional Regulation of Mammalian Genome Using Designer TAL Effectors.” *Nature biotechnology* 29(2): 149–53.

Zhang, Guoqiang et al. 2015. “N6-Methyladenine DNA Modification in Drosophila.” *Cell* 161(4): 893–906.

Zhao, Lei et al. 2014. “The Dynamics of DNA Methylation Fidelity during Mouse Embryonic Stem Cell Self-Renewal and Differentiation.” *Genome Research* 24(8): 1296–1307.

Zhao, Ruohe et al. 2017. “Microglia Limit the Expansion of β-Amyloid Plaques in a Mouse Model of Alzheimer’s Disease.” *Molecular Neurodegeneration* 12(1): 47.

Zhou, H. et al. 2018. “In Vivo Simultaneous Transcriptional Activation of Multiple Genes in the Brain Using CRISPR-DCas9-Activator Transgenic Mice.” *Nat Neurosci* 21(3): 440–46.

Zhou, Q. et al. 2008. “In Vivo Reprogramming of Adult Pancreatic Exocrine Cells to Beta-Cells.” *Nature* 455(7213): 627–32.

Zhou, Yang et al. 2014. “Unstable Expression of Transgene Is Associated with the Methylation of CAG Promoter in the Offspring from the Same Litter of Homozygous Transgenic Mice.” *Molecular Biology Reports* 41(8): 5177–86.

Ziller, M. J. et al. 2018. “Dissecting the Functional Consequences of De Novo DNA Methylation Dynamics in Human Motor Neuron Differentiation and Physiology.” *Cell Stem Cell* 22(4): 559-574.e9.

Zuckermann, Marc et al. 2018. “A Novel Cloning Strategy for One-Step Assembly of Multiplex CRISPR Vectors.” *Scientific Reports* 8(1): 1–8.

Abbreviations

5caC	C5-carboxylcytosine
5fC	C5-formylcytosine
5hmC	C5- hydroxymethylcytosine
3mC	N3- methylcytosine
5mC	5- methylcytosine
AA	amino acid
Ab	antibody
bp	basepair
C- terminal	carboxy- terminal
CRISPR	clustered regularly interspaced short palindromic repeat
dCas9	deadCas9
DMSO	dimethylsulfoxide
DNA	desoxy- ribonucleic acid
DTT	dithiothreitol
FACS	fluorescence activated cell sorting
Fig	Figure
E. coli	*Escherichia coli*
g	gram
gRNA	guideRNA
h	hour or human
HBS	HEPES buffered saline
HEPES	4- (2- hydroxyethyl)-1-piperazineethanesulfonic acid

kb	kilobases
L2K	Lipofectamin 2000
l	liter
LB	lysogeny broth
µ	micro-
m	milli-
min	minute
MOI	multiplicity of infection
n	nano
NGS	normal goat serum or Next Generation Sequencing
N- terminal	amino- terminal
OD	optical density
PAM	protospacer adjacent motif
PBS	phosphate buffered saline
s	second
TBS	Tris- buffered saline
TBS- T	TBS + Tween
TSS	Transcription Start Site
Tris	2- Amino- 2- hydroxymethyl- propane- 1, 3- diol
U	units
V	Volt
v/v	volume per volume
w/v	weight per volume

List of Figures

List of Publications

Köferle A, Worf K, **Breunig C**, Baumann V, Herrero J, Wiesbeck M, Hutter LH, Götz M, Fuchs C, Beck S, Stricker SH: "**CORALINA: a universal method for the generation of gRNA libraries for CRISPR-based screening".** *BMC Genomics*, doi: 10.1186/s12864-016-3268-z

Breunig CT, Durovic T, Neuner AM, Baumann V, Wiesbeck MF, Köferle A, Götz M, Ninkovic J, Stricker SH: **"One step generation of customizable gRNA vectors for multiplex CRISPR approaches through string assembly gRNA cloning (STAgR)"**. *PLoS One* 13, doi: 10.1371 (2018).

Breunig CT, Neuner AM, Giehrl-Schwab J, Wurst W, Götz M, Stricker SH: "**A Customizable Protocol for String Assembly gRNA Cloning (STAgR)"** *J Vis Exp* (142), doi:10.3791/58556 (2018).

Di Giaimo R, Durovic T, Barquin P, Kociaj A, Lepko T, Aschenbroich S, **Breunig CT**, Irmler M, Cernilogar FM, Schotta G, Barbosa JS, Trümbach D, Baumgart EV, Neuner AM, Beckers J, Wurst W, Stricker SH, Ninkovic J: "**The Aryl Hydrocarbon Receptor Pathway Defines the Time Frame for Restorative Neurogenesis".** *Cell Rep,* doi: 10.1016/j.celrep.2018.11.055 (2018).

Baumann V, Wiesbeck M, **Breunig CT**, Braun JM, Köferle A, Ninkovic J, Götz M, Stricker SH: "**Targeted removal of epigenetic barriers during transcriptional reprogramming"**. *Nat Commun*, doi: 10.1038/s41467-019-10146-8 (2019).

Lepko T, Pusch M, Müller T, Schulte D, Ehses J, Kiebler M, Hasler J, Huttner HB, Vandenbroucke RE, Vandendriessche C, Modic M, Martin-Villalba A, Zhao S, LLorens-Bobadilla E, Schneider A, Fischer A, **Breunig CT**, Stricker SH, Götz M, Ninkovic J: "**Choroid plexus-derived miR-204 regulates the number of quiescent neural stem cells in the adult brain".** *Embo J,* doi: 10.15252/embj.2018100481 (2019).

Acknowledgements

I want to thank Stefan Stricker, who gave me the opportunity to work in his lab. Stefan, thanks for all the thrilling discussions, sharing your experience and for your contagious passion for science.

Magdalena, I never met someone who is so passionate about what they are doing and is so full of knowledge, like you are. Thank you for all the discussions, the advice, and the nice working atmosphere.

I would also like to thank my other two TAC members. Peter and Christina, thank you very much for accompanying me during this thesis.

Valentin, I consider us as the founding member of this lab and I think we did a good job. Thanks for not only becoming my colleague but also for becoming my friend.

Many thanks to Maxi, who also became a dearest friend. I appreciate all the moments of laughter and good food, playing Magic and having a Spezi. I don't know what I would have done without you guys.

Andrea, you were the best master student I ever had. I hope you understand how much you helped me during a hard time of my PhD.

Anna, thanks for being this angry Austrian woman. I am glad you joined the lab and grateful for all the nice Türkitches we shared at the Isar. Thanks also for proof-reading!!

Tobi, Luis, Julia, you were awesome students. The time you were part of this lab, was just the best time ever.

Edina, thank you for helping me so much during this last year.

Thanks to all of the other people in the Götz lab, especially Bob, Miriam, Sonia and Kalina. It was such a nice time to get to know you all and to have fun together.

Thanks also to Manja, Tatiana, Andrea, Flo, and Ines for all the technical support.

Thank you, Tobias Straub for analyzing the bisulfite sequencing data.

I want to thank a few people alongside the road. Olaf and Susi, who have been my supervisors during my master's thesis. Without you guys, I would have never continued in science. You

showed me what passion for science means and how not to forget to have fun during all the hard times. Thanks for this. Mar has been my supervisor during my stay in Scotland. Mar I want to thank you for all the things I could learn from you. You contributed a lot to the scientist I am today.

I also want to thank my family. I am so grateful for all the support throughout the years. I am such a lucky guy, to have so many special people in my life.

Speaking of a special person, I want to thank you, Kathi. You are my heart and my anchor, you kept me grounded for all these years. I am beyond grateful for everything you have done for me. I cannot grasp how unbelievable lucky I am to have you beside me. Thanks, my love.

Eidesstattliche Versicherung

Breunig, Christopher Thomas

Name, Vorname

Ich erkläre hiermit, an Eides statt,

dass ich die vorliegende Dissertation mit dem Thema

„Using gRNA Multiplexing for Epigenetic and Transcriptional Engineering“ selbständig verfasst, mich außer der angegebenen keiner weiteren Hilfsmittel bedient und alle Erkenntnisse, die aus dem Schrifttum ganz oder annährend übernommen sind, als solche kenntlich gemacht und nach ihrer Herkunft unter Bezeichnung der Fundstelle einzeln nachgewiesen habe.

Ich erkläre des Weiteren, dass die hier vorgelegte Dissertation nicht in gleicher oder in ähnlicher Form bei einer anderen Stelle zur Erlangung eines akademischen Grades eingereicht wurde.

München, 20.06.2020 _____

Ort, Datum

Unterschrift Christopher Breunig